



**THE STUDY OF HEP88 MAB MEDIATED PROGRAM CELL
DEATH THROUGH PARAPTOSIS-LIKE AND/OR
APOPTOSIS IN HEPG2 CELL LINE**

BY

MISS THANTIP MITUPATUM

**A DISSERTATION SUBMITTED IN PARTIAL FULFILLMENT OF
THE REQUIREMENTS FOR THE DEGREE OF
THE DOCTOR OF PHILOSOPHY IN
BIOCHEMISTRY AND MOLECULAR BIOLOGY
FACULTY OF MEDICINE
THAMMASAT UNIVERSITY
ACADEMIC YEAR 2014
COPYRIGHT OF THAMMASAT UNIVERSITY**

**THE STUDY OF HEP88 MAB MEDIATED PROGRAM CELL
DEATH THROUGH PARAPTOSIS-LIKE AND/OR
APOPTOSIS IN HEPG2 CELL LINE**

BY

MISS THANTIP MITUPATUM



**A DISSERTATION SUBMITTED IN PARTIAL FULFILLMENT OF
THE REQUIREMENTS FOR THE DEGREE OF
DOCTOR OF PHILOSOPHY IN
BIOCHEMISTRY AND MOLECULAR BIOLOGY
FACULTY OF MEDICINE
THAMMASAT UNIVERSITY
ACADEMIC YEAR 2014
COPYRIGHT OF THAMMASAT UNIVERSITY**



THAMMASAT UNIVERSITY
FACULTY OF MEDICINE

DISSERTATION

BY
MISS THANTIP MITUPATUM

ENTITLED
THE STUDY OF HEP88 MAB MEDIATED PROGRAM CELL DEATH
THROUGH PARAPTOSIS-LIKE AND/OR APOPTOSIS
IN HEPG2 CELL LINE

was approved as partial fulfillment of the requirements for the degree of
Doctor of Philosophy

on July 10, 2015

Chairman



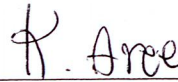
(Sittiruk Roytrakul, Ph.D.)

Member and Advisor



(Associate Professor Panadda Rojpibulstit)

Member and Co-advisor



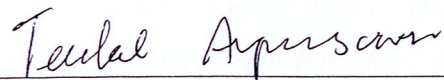
(Assistant Professor Kalaya Aree, Ph.D.)

Member and Co-advisor



(Associate Professor Sasichai Kangsadalampai, Ph.D.)

Member



(Assistant Professor Teerakul Arpornsuwan, Ph.D.)

Dean



(Associate Professor Preecha Wanichsetakul, M.D.)

Dissertation Title	THE STUDY OF HEP88 MAB MEDIATED PROGRAM CELL DEATH THROUGH PARAPTOSIS-LIKE AND/OR APOPTOSIS IN HEPG2 CELL LINE
Author	Miss Thantip Mitupatum
Degree	Doctor of Philosophy in Biochemistry and Molecular Biology
Faculty	Faculty of Medicine
University	Thammasat University
Dissertation Advisor	Associate Professor Panadda Rojpibulstit
Dissertation Co-Advisor	Assistant Professor Kalaya Aree, Ph.D. Associate Professor Sasichai Kangsadalampai, Ph.D.
Academic Years	2014

ABSTRACT

The hepatocellular carcinoma (HCC) is the most common cancer worldwide, which is high incidence and high mortality rate. HCC becomes a crucial cancer because it is low detected at the early diagnosis and the remedies are still not specific to late stage of HCC. Interestingly, the targeted therapy via monoclonal antibodies (mAbs) specific to tumor-associated antigen is continuously developed in treatment and diagnosis of the disease. After establishing and consequently explored, it was found that Hep88 mAb has been shown anticancer effects against a HepG2 cell line. In this study, the gene expression at mRNA level of *caspase-3*, *caspase-8* and *caspase-9*, the caspases enzyme activities in IC50 dose of Hep88 mAb-treated HepG2 cells and IC50 dose of doxorubicin-treated HepG2 cells were investigated to compare ability of them. After that, the concentration of Hep88 mAb treatment was increased to cytotoxic dose to detect the hallmarks of apoptosis by flow cytometry. Hep88 mAb-treated HepG2 cells were stained with different methods to examine the apoptotic cell population, the cell cycle progression and active caspase-3 determination. Afterwards, the mechanisms of program cell death (PCD) of IC50 and cytotoxic dose of Hep88 mAb were determined through the gene expression at mRNA level of *Bax*, *Bcl-2*, *p53*, *cathepsin B*, *caspase-3* and *caspase-9*. Finally, the proteomic analysis of proteins

involved in the anticancer activities of Hep88 mAb in HepG2 cells were explored by GeLC-MS/MS. The results were demonstrated that Hep88 mAb induced HepG2 cell line by the activation and expression of caspase-3, caspase-8 and caspase-9 in 24 hours of treatment. When compare with doxorubicin, Hep88 mAb treated cells were revealed higher enzyme activation and higher gene expression. Moreover, the increasing of G2/M phase cell cycle arrest, subsequent increasing of apoptotic cells population and more active caspase-3 detection were found in cytotoxic dose of Hep88 mAb-treated HepG2 cells in time- and dose-dependent manner. The expression of *Bax*, *Bcl-2*, *p53*, *cathepsin B*, *caspase-3* and *caspase-9* were used to evaluate the paraptosis and apoptosis PCD. Up-regulation of *Bax*, *p53*, *caspase-3* and *caspase-9* as well as the down-regulation of *Bcl-2* could be responsible for the apoptotic effects of Hep88 mAb observed in this study. While, up-regulation of *cathepsin B* (CTSB) might contribute to paraptosis effects. Both paraptosis and apoptosis were occurred after treated with IC50 and cytotoxic dose of Hep88 mAb, which were depended on the strongest expression. Furthermore, the protein profile of Hep88 mAb-treated HepG2 cells had shown 323 differentially expressed proteins. From all of differentially expressed proteins, 29 proteins were found after Hep88 mAb. Two of these proteins were only found in IC50 dose of treatment, they were spindlin-1 (SPIN1) and ankyrin repeat domain (CLIP4). Spindlin-1 might contribute to paraptosis effects and ankyrin repeat domain might relate to the inhibitory effects on apoptosis cell death of Hep88 mAb. While, the apoptosis induction in this study might associated with 29 proteins that involved apoptotic process and apoptotic signaling pathway. These findings represent new insights into the molecular mechanisms underlying the anticancer properties of Hep88 mAb in liver cancer cells.

Keywords: Hepatocellular carcinoma, Monoclonal antibody, Caspase, Apoptosis, Paraptosis, Bax, Bcl-2, p53 and Cathepsin B

หัวข้อคุณสมบัติ	การศึกษากลไกการออกฤทธิ์ของโมโนโคลนอลแอนติบอดีเฮป 88 ที่ทำให้เกิดการตายผ่านทางพาราพโตซิส และ/หรืออะพอพโตซิสในเซลล์มะเร็งตับชนิดเฮปจี 2
ชื่อผู้เขียน	น.ส. ชารทิพย์ มิตรอุปถัมภ์
ชื่อปริญญา	ปรัชญาดุษฎีบัณฑิต
สาขาวิชา	ชีวเคมีและชีววิทยาโมเลกุล
คณะ	คณะแพทยศาสตร์
มหาวิทยาลัย	มหาวิทยาลัยธรรมศาสตร์
อาจารย์ที่ปรึกษาหลัก	รองศาสตราจารย์ ปนัดดา โรจนพิบูลสถิตย์
อาจารย์ที่ปรึกษาร่วม	ผู้ช่วยศาสตราจารย์ ดร.กัลยา อารีย์ รองศาสตราจารย์ ดร. ศศิชัย กังสดาลอำไพ
ปีการศึกษา	2557

บทคัดย่อ

โรคมะเร็งตับจัดเป็นมะเร็งที่พบเป็นอันดับต้นๆของโลก โดยมะเร็งตับนั้นมีบทบาทสำคัญเนื่องจากเป็นมะเร็งที่มีผลทำให้เกิดการตายสูง เนื่องมาจากวิธีการตรวจวินิจฉัยและการรักษายังไม่จำเพาะ อันเป็นที่น่าสนใจว่าการรักษาด้วยโมโนโคลนอลแอนติบอดีที่จำเพาะกับแอนติเจนของมะเร็งนั้นยังคงถูกพัฒนาอยู่ตลอดเวลาเพื่อที่จะนำมาใช้ในการรักษาและวินิจฉัยโรคมะเร็งทั้งหลาย ซึ่งหลังจากที่ได้มีการค้นพบว่าเฮป 88 โมโนโคลนอลแอนติบอดี (Hep88 monoclonal antibody) มีฤทธิ์ในการยับยั้งเซลล์มะเร็งตับเฮปจี 2 (HepG2) แล้วนั้น การศึกษาในครั้งนี้จึงได้ทำการทดลองเกี่ยวกับการแสดงออกของยีน คาสเปส-3 (*caspase-3*), คาสเปส-8 (*caspase-8*) และคาสเปส-9 (*caspase-9*) ที่ระดับเอ็มอาร์เอ็นเอ (gene expression at mRNA level) และกิจกรรมของเอนไซม์คาสเปส ในเซลล์มะเร็งตับเฮปจี 2 ที่ถูกกระตุ้นด้วยเฮป 88 โมโนโคลนอลแอนติบอดี และเซลล์มะเร็งตับเฮปจี 2 ที่ถูกกระตุ้นด้วยยาโดxorubicin (doxorubicin) ที่ระดับความเข้มข้นที่สามารถยับยั้งเซลล์มะเร็งให้ลดลงครึ่งหนึ่ง (half-inhibitory concentration, IC50 dose) เพื่อเปรียบเทียบกับยารักษามะเร็งตับที่ใช้ในปัจจุบัน หลังจากนั้นทำการเพิ่มความเข้มข้นของเฮป 88 โมโนโคลนอลแอนติบอดี จนกระทั่งอยู่ในระดับที่ทำให้เซลล์มะเร็งตายได้ (cytotoxic dose) เพื่อตรวจสอบเอกลักษณ์ของการเกิดอะพอพโตซิส (hallmarks of apoptosis) จากเทคนิคโฟลไซโตเมทรี (flow cytometry) เซลล์มะเร็งตับเฮปจี 2 ที่ถูกกระตุ้นด้วยเฮป 88 โมโนโคลนอลแอนติบอดีจะถูกย้อมเซลล์ด้วยวิธีแบบ

ต่างๆ ซึ่งจะทำให้ทราบถึง ประชากรเซลล์ที่เกิดอะพอพโตซิส (apoptotic cells population) ลักษณะของวัฏจักรเซลล์ (cell cycle progression) และปริมาณของเอนไซม์คาสเปส-3 ที่ทำงานได้ (active caspase-3) หลังจากนั้นยังได้ทำการศึกษาการตายของเซลล์มะเร็งระดับหลังจากถูกกระตุ้นด้วยเฮป 88 โมโนโคลนอลแอนติบอดีที่ความเข้มข้นระดับที่ยับยั้งเซลล์มะเร็งลงครึ่งหนึ่ง (IC50 dose) และระดับที่ทำให้เซลล์มะเร็งตาย (cytotoxic dose) ผ่านการพิจารณาการแสดงออกของ ยีน แบกซ์ (Bax), บีซีแอล-2 (Bcl-2), พี53 (p53), คาธเปซิน บี (cathepsin B), คาสเปส-3 (caspase-3) และ คาสเปส-9 (caspase-9) ที่ระดับเอ็มอาร์เอ็นเอ สูดท้ายทำการวิเคราะห์ข้อมูล โปรตีนที่เกี่ยวข้องกับความสามารถในการยับยั้งมะเร็ง (anticancer activities) ของเฮป 88 โมโนโคลนอลแอนติบอดีต่อเซลล์มะเร็งระดับเฮปจี 2 ถูกสำรวจโดยเทคนิคเจล-แอลซี-เอ็มเอส/เอ็มเอส (GeLC-MS/MS) ซึ่งผลการทดลองแสดงให้เห็นว่าเฮป 88 โมโนโคลนอลแอนติบอดีกระตุ้นเซลล์มะเร็งระดับเฮปจี 2 ด้วยการกระตุ้นการทำงานของเอนไซม์และการแสดงออกของคาสเปส ที่เวลา 24 ชั่วโมง เมื่อเปรียบเทียบกับยาโดโซรูบิซินยังพบว่าเซลล์มะเร็งระดับหลังที่ถูกกระตุ้นด้วยเฮป 88 โมโนโคลนอลแอนติบอดีมีการแสดงออกของยีนและกิจกรรมของเอนไซม์ของคาสเปส-3, คาสเปส-8 และ คาสเปส-9 ที่เพิ่มมากขึ้นนอกจากนี้การเพิ่มขึ้นของการยับยั้งการเข้าสู่วัฏจักรเซลล์ในระยะก่อนการแบ่งเซลล์ (G2/M phase arrest), ส่งผลให้มีการเพิ่มขึ้นของประชากรเซลล์ที่เกิดอะพอพโตซิส (apoptotic cells population) และการเพิ่มขึ้นของปริมาณของเอนไซม์คาสเปส-3 ที่ทำงานได้ (active caspase-3) ถูกพบในการทดลองเพิ่มความเข้มข้นที่ใช้ในการกระตุ้นเซลล์มะเร็งจนกระทั่งอยู่ในระดับที่ทำให้เซลล์มะเร็งตายได้ (cytotoxic dose) โดยพบว่าลักษณะต่างๆ ล้วนเพิ่มขึ้นตามสัดส่วนของความเข้มข้นและเวลาที่ใช้ในการกระตุ้น ส่วนการแสดงออกของยีนแบกซ์ (Bax), บีซีแอล-2 (Bcl-2), พี53 (p53), คาธเปซิน บี (cathepsin B), คาสเปส-3 (caspase-3) และ คาสเปส-9 (caspase-9) ถูกใช้เพื่อประเมินผลการตายของเซลล์แบบอะพอพโตซิส และพาแรพโตซิส การเพิ่มขึ้นของการแสดงออกของแบกซ์ (Bax), พี53 (p53), คาสเปส-3 (caspase-3) และ คาสเปส-9 (caspase-9) และการลดลงของการแสดงออกของบีซีแอล-2 (Bcl-2) สามารถอ้างได้ถึงผลของการเกิดอะพอพโตซิสจากเฮป 88 โมโนโคลนอลแอนติบอดี ขณะที่การเพิ่มขึ้นของการแสดงออกของคาธเปซิน บี (cathepsin B) เกี่ยวข้องกับผลของการเกิดพาแรพโตซิส โดยทั้งการเกิดอะพอพโตซิส และพาแรพโตซิสถูกทำให้เกิดขึ้นหลังจากกระตุ้นด้วยระดับความเข้มข้นของเฮป 88 โมโนโคลนอลแอนติบอดีที่ยับยั้งเซลล์มะเร็งให้ลดลงครึ่งหนึ่ง (IC50 dose) และระดับความเข้มข้นที่ทำให้เกิดการตายของเซลล์มะเร็ง (cytotoxic dose) โดยที่ลักษณะการตายของเซลล์นั้นก็ขึ้นกับการแสดงออกที่เด่นชัดที่สุด นอกจากนี้ข้อมูลโปรตีนของเซลล์มะเร็งระดับหลังจากการกระตุ้นด้วยเฮป 88 โมโนโคลนอลแอนติบอดีพบว่ามีทั้งหมด 323 ชนิด และมีโปรตีนเพียง 29 ชนิดที่จะพบได้ในเซลล์มะเร็งระดับหลังจากการกระตุ้นด้วยเฮป 88 โมโนโคลนอลแอนติบอดี โดยโปรตีน 2 ชนิด คือ สเปนดลิน-1

(spindlin-1) และแอนคิรินรีพีทโดเมน (ankyrin repeat domain) เป็นโปรตีนที่สามารถพบได้ในเซลล์มะเร็งระดับที่ถูกกระตุ้นด้วยโมโนโคลนอลแอนติบอดีเฮป 88 ที่มีความเข้มข้นในระดับที่ยับยั้งมะเร็งลดลงครึ่งหนึ่งเท่านั้น (IC50 dose) โดยที่สปีนดลิน-1 เป็นโปรตีนที่เกี่ยวข้องกับกระบวนการตายแบบพาแรพโตซิส และแอนคิรินรีพีทโดเมนเป็นโปรตีนที่เกี่ยวข้องกับกลไกการยับยั้งการเกิดอะพอพโตซิสของเฮป 88 โมโนโคลนอลแอนติบอดี ขณะที่โปรตีนที่เกี่ยวข้องกับกระบวนการเกิดอะพอพโตซิสอยู่ 29 ชนิด ซึ่งมีความเกี่ยวข้องกับกระบวนการเกิดอะพอพโตซิส (apoptotic process) และกระบวนการส่งสัญญาณให้เกิดอะพอพโตซิส (apoptotic signaling pathway) อยู่ทั้งหมด 29 ชนิด ข้อมูลทั้งหมดที่ได้ทำการศึกษาในครั้งนี้จึงสามารถทำให้เกิดมุมมองใหม่ของกลไกการยับยั้งและกลไกการตายของเซลล์มะเร็งระดับหลังจากการถูกกระตุ้นด้วยเฮป 88 โมโนโคลนอลแอนติบอดี

คำสำคัญ: มะเร็งตับ, โมโนโคลนอลแอนติบอดี, คาสเปส, อะพอพโตซิส, พาแรพโตซิส, แบกซ์, บีซีแอล-2, พี53 และ คาแรปซิน บี

ACKNOWLEDGEMENTS

My name may be on the cover, but putting together a complete this research requires many helping from many people. This thesis will never be successful without the valuable helps from these people.

Firstly, I wish to thank you my advisor. Associate Professor Panadda Rojpibulstit, who provided the great opportunity to study in this field, give me many valuable advice and push me forward to successful in Ph.D. study. Next, I would like to thank you my co-advisors, Associate Professor Sasichai Kangsadalampai and Assistant Professor Dr. Kalaya Aree who provided the very good advice and made a recommendation about my work, in addition, all consultants, chairman, committee in this thesis. I deeply appreciated to Faculty of Medicine, Thammasat University, Thailand and all staffs for bearing laboratory and all facilities to done this thesis.

Besides above, I grateful acknowledge to Dr.Sittiruk Roytrakul, Khun Suthathip Kittisenachai and Khun Atchara Paemane at Genome Institute, National Center for Genetic Engineering and Biotechnology (BIOTEC), National Science and Technology Development Agency (NSTDA), Thailand for many helping with advice in the part of real-time PCR and proteomics.

I thankful appreciate to Khun Songchan Puthong and Khun Anumart Buakeaw at Antibody Production Research Unit, The Institute of Biotechnology and Genetic Engineering (IBGE), Chulalongkorn University, Thailand for all helping with advice in the part of cell culture and monoclonal antibody preparation.

I would like to thank the Thammasat University Ph.D. Program scholarship for the financial support.

Along my study life, I must thank you all teachers who improved my skill and knowledge since I was child until today. I would like to thanks all friends that help and take care during my study.

Most of all, I would like to express my deepest appreciate feeling to my beloved family for all their supports in my life.

Ms.Thantip Mitupatum

TABLE OF CONTENTS

	Page
ABSTRACT	(1)
ABSTRACT (THAI)	(3)
ACKNOWLEDGEMENTS	(6)
LIST OF TABLES	(13)
LIST OF FIGURES	(14)
LIST OF ABBREVIATIONS	(17)
CHAPTER 1 INTRODUCTION	1
1.1 Introduction	1
1.2 Objectives	4
1.3 Beneficiaries	4
CHAPTER 2 REVIEW OF LITERATURE	6
2.1 Hepatocellular carcinoma (HCC)	6
2.1.1 Pathogenesis of HCC	6
2.1.2 The cause of HCC	7
2.1.2.1 Hepatitis B Virus (HBV) infection	7
2.1.2.2 Hepatitis C Virus (HCV) infection	7
2.1.2.3 Aflatoxins consumption	8
2.1.3 Treatment in HCC	9

2.1.3.1 Liver transplantation	9
2.1.3.2 Surgical resection	9
2.1.3.3 Percutaneous ethanol injection	9
2.1.3.4 Transcatheter arterial chemoembolization	10
2.1.3.5 Radiofrequency ablation	10
2.1.3.6 Immunotherapy	10
2.2 Monoclonal antibody	11
2.2.1 The death mechanism of cancer via monoclonal antibody treatment	12
2.2.2 The anti-HCC monoclonal antibodies production	12
2.2.3 Hep88 monoclonal antibody	13
2.3. Program cell death (PCD)	13
2.3.1 Caspase-dependent PCD	14
2.3.2 Caspase-independent PCD	15
2.4. Caspases	18
2.4.1 Caspase-8	20
2.4.2 Caspase-9	20
2.4.3 Caspase-3	21
2.5 Cathepsins	21
2.6 Bax	22
2.7 Bcl-2	23
2.8 p53	23
2.9 Polymerase chain reaction (PCR)	24

2.10 Real-time PCR	26
2.10.1 Types of real-time quantification	27
2.10.1.1 Absolute Quantitation	27
2.10.1.2 Relative Quantitation	27
2.10.1.3 Standard curve method	28
2.10.1.4 Comparative Ct method ($2^{-\Delta\Delta Ct}$)	28
2.10.1.5 Pfaffl model.	29
2.10.2 Normalization	29
2.10.3 Calculated Variation	30
2.11 Flow cytometry	30
2.11.1 Fluorophores	31
2.11.2 Cells sample preparation	31
2.11.2.1 Cell fixation	31
(1) Methanol/ethanol fixation	31
(2) PFA/Saponin fixation and permeabilization	32
2.12 Proteomics	32
2.13 Mass spectrometry	33
2.13.1 Vacuum system	33
2.13.2 Sample inlet	33
2.13.3 Ion sources	33
2.13.4 Mass Analyzers	34
2.13.4.1 Types of mass analyzers	34
(1) Time-of-flight (TOF) analyzer	34
(2) Quadrupole mass analyzer	34
(3) Quadrupole-ion trap mass analyzer	34
2.13.5 Detectors	35

CHAPTER 3 RESEARCH METHODOLOGY	36
3.1 Cell culture and Cytotoxicity effect of Hep88 mAb	37
3.2 Real-time PCR	37
3.2.1 The apoptotic mechanism of Hep88 mAb treated-HepG2 cell	37
3.2.2 The early mechanism of PCD in HepG2 cell after treated with Hep88 mAb	37
3.2.3 Validating the amplified PCR product	38
3.2.3.1 Primer design	38
3.2.3.2 PCR Amplification	38
3.2.3.3 Gene cloning	38
3.2.3.4 Screening of gene recombinant plasmid	38
3.2.3.5 Plasmid extraction	38
3.2.3.6 Sequence analysis	39
3.2.4 Generating standard curve of interesting gene	39
3.2.4 .1 Copy number calculation	39
3.2.5 Total RNA extraction	40
3.2.6 Reverse transcription	40
3.2.7 Quantitative real-time PCR analysis	40
3.3 Enzyme Colorimetric assay	43
3.3.1 Protein extraction	43
3.3.2 Caspase-3/ CPP32 Colorimetric assay	43
3.3.3 FLICE/Caspase-8 Colorimetric assay	44
3.3.4 Caspase-9 Colorimetric assay	44
3.4 Flow cytometry	44
3.4.1 Detecting apoptosis	45
3.4.2 Detecting cell cycle	45
3.4.3 Active caspase-3	46

3.5 Proteomics	46
3.5.1 Total protein extraction	46
3.5.2 Protein concentration determination by Lowry method	46
3.5.3 Denaturing gel electrophoresis (SDS-PAGE)	47
3.5.4 Silver staining	47
3.5.5 In-gel digestion	47
3.5.6 Nano LC-MS/MS analysis	48
3.5.7 Protein identification and Gene ontology categories	49
3.5.8 Gene ontology annotation and mapping of protein networks	50
3.5.9 Quantification of the changes in protein analysis	50
 CHAPTER 4 RESULTS AND DISCUSSION	 51
4.1 The expression of mRNA involving the mechanism of apoptosis and paraptosis	51
4.1.1 Plasmids construction and copy-number determination	51
4.1.2 The mRNA expression of caspase-3, caspase-8 and caspase-9 at 24, 48 and 72 hours	54
4.1.3 The pathway determination through <i>Bax</i> , <i>Bcl-2</i> , <i>p53</i> , <i>cathepsin B</i> , <i>caspase-9</i> and <i>caspase-3</i> mRNA expression at 3, 6, 9, 12, 18 and 24 hours	55
4.1.3.1 The mRNA expression of <i>Bax</i> , <i>Bcl-2</i> , <i>p53</i> , <i>cathepsin B</i> , <i>caspase-9</i> and <i>caspase-3</i>	55
(1) IC50 dose of Hep88 mAb treatment	57
(2) Cytotoxic dose of Hep88 mAb treatment	62
4.2 Enzyme activity involving in the apoptotic mechanism	67
4.2.1 Caspase-3, -8 and -9 activities	67
4.3 Flow cytometry	69
4.3.1 Hep88 mAb induced apoptotic cell death in HepG2 cells	69
4.3.2 Hep88 mAb induced cell cycle progression in HepG2 cells	72

	(12)
4.3.3 Effect of Hep88 mAb on an active caspase-3 expression	74
4.4 GeLC-MS/MS	75
4.4.1 The differentially expressed proteins in Hep88 mAb-treated HepG2 cells from GeLC-MS/MS analysis	75
4.4.2 Mapping proteins network from the GeLC-MS/MS data	78
CHAPTER 5 CONCLUSIONS AND RECOMMENDATIONS	92
REFERENCES	107
APPENDICES	121
APPENDIX A	122
APPENDIX B	128
APPENDIX C	129
BIOGRAPHY	133

LIST OF TABLES

Tables	Page
Table 2.1 Ultrastructural features of apoptosis and paraptosis	16
Table 3.1 Primer PCR for Real-time PCR	41
Table 3.2 Primer PCR for Real-time PCR	42
Table 4.1 The fold change of the expression of early apoptotic mechanism involving genes in IC50 of Hep88 mAb treatment	61
Table 4.2 The fold change of the expression of early apoptotic mechanism involving genes in cytotoxic dose of Hep88 mAb treatment	61
Table 4.3 Effect of Hep88 monoclonal antibody on active caspase-3 expression in HepG2	75
Table 4.4 Apoptotic proteins altered after Hep88 monoclonal antibody treatment	81
Table 4.5 The expressed proteins altered after Hep88 monoclonal antibody treatment	86

LIST OF FIGURES

Figures	Page
Figure 1.1 A conceptual framework of this study	5
Figure 2.1 Apoptosis pathway	17
Figure 2.2 The structure of caspases and its active form	18
Figure 2.3 The different structure of prodomain on the initiator and the effector of apoptotic caspases	19
Figure 2.4 The steps in PCR	25
Figure 2.5 Basic components of mass spectrometers	33
Figure 3.1 A conceptual framework of this study	36
Figure 4.1 Standard curve for caspase-3, -8, -9 and EF-2 gene	52
Figure 4.2 Standard curve for Bax, Bcl-2, p53, cathepsin B (CTSB), caspase-9, caspase-3, and EF-2 gene	53
Figure 4.3 Effects on caspase expression of doxorubicin and Hep88 monoclonal antibody-treated HepG2 cells	56
Figure 4.4 Real-time PCR analysis for <i>Bax</i> , <i>Bcl-2</i> , <i>p53</i> , <i>cathepsin B</i> , <i>caspase-3</i> and <i>caspase-9</i> expression in IC50 dose of Hep88 mAb treatment at 12, 18 and 24 hours.	58
Figure 4.5 Real-time PCR analysis for <i>Bax</i> , <i>Bcl-2</i> , <i>p53</i> , <i>cathepsin B</i> , <i>caspase-3</i> and <i>caspase-9</i> expression in IC50 dose of Hep88 mAb treatment at 3, 6 and 9 hours.	59
Figure 4.6 Real-time PCR analysis for <i>Bcl-2</i> expression, <i>Bax</i> expression and the ratio of <i>Bcl-2/Bax</i> in IC50 dose and cytotoxic dose of Hep88 mAb treatment at 12, 18 and 24 hours.	60
Figure 4.7 Real-time PCR analysis for <i>Bax</i> , <i>Bcl-2</i> , <i>p53</i> , <i>cathepsin B</i> , <i>caspase-3</i> and <i>caspase-9</i> expression in IC50 dose of Hep88 mAb treatment at 12, 18 and 24 hours.	65
Figure 4.8 Real-time PCR analysis for <i>Bax</i> , <i>Bcl-2</i> , <i>p53</i> , <i>cathepsin B</i> , <i>caspase-3</i> and <i>caspase-9</i> expression in IC50 dose of Hep88 mAb treatment at 3, 6 and 9 hours.	66

Figure 4.9 Effects on caspase activities of doxorubicin and Hep88 mAb -treated HepG2 cells.	68
Figure 4.10 Flow cytometry analysis of apoptotic cell death in Hep88 mAb -treated HepG2 cells.	70
Figure 4.11 Changes in the percentage of early apoptotic and viable HepG2 cells induced by Hep88 mAb.	71
Figure 4.12 Effects on varying doses and times of Hep88 mAb incubation on cell cycle progression in HepG2 cells	73
Figure 4.13 Effect of Hep88 monoclonal antibody on active caspase-3 in HepG2.	74
Figure 4.14 The Venn diagram comparison of the differentially expressed proteins from the Hep88 mAb-treated HepG2 cells	76
Figure 4.15 The functional distribution of proteins significantly differentially expressed in Hep88 mAb-treated HepG2 cells.	80
Figure 4.16 The cellular component distribution of proteins significantly differentially expressed in Hep88 mAb-treated HepG2 cells.	80
Figure 4.17 The quantification of the change of 29 apoptotic proteins differentially expressed in Hep88 mAb-treated HepG2 cells.	85
Figure 4.18 The quantification of the change of 29 proteins differentially expressed in Hep88 mAb-treated HepG2 cells.	89
Figure 4.19 The 29 apoptotic proteins of 323 differentially expressed proteins in Hep88 mAb-treated HepG2 cells	90
Figure 4.20 The 29 apoptotic proteins of 323 differentially expressed proteins in Hep88 mAb-treated HepG2 cells with its functional partners' proteins.	91
Figure 5.1 The proposed mechanism of cytotoxic dose of Hep88 mAb-treated HepG2 cell at 3 hours.	95
Figure 5.2 The proposed mechanism of cytotoxic dose of Hep88 mAb-treated HepG2 cell at 6 hours.	96
Figure 5.3 The proposed mechanism of cytotoxic dose of Hep88 mAb-treated HepG2 cell at 9 hours.	97
Figure 5.4 The proposed mechanism of cytotoxic dose of Hep88 mAb-treated	98

HepG2 cell at 12 hours.	
Figure 5.5 The proposed mechanism of cytotoxic dose of Hep88 mAb-treated HepG2 cell at 18 hours.	99
Figure 5.6 The proposed mechanism of cytotoxic dose of Hep88 mAb-treated HepG2 cell at 24 hours.	100
Figure 5.7 The proposed mechanism of IC50 dose of Hep88 mAb-treated HepG2 cell at 3 hours.	101
Figure 5.8 The proposed mechanism of IC50 dose of Hep88 mAb-treated HepG2 cell at 6 hours.	102
Figure 5.9 The proposed mechanism of IC50 dose of Hep88 mAb-treated HepG2 cell at 9 hours.	103
Figure 5.10 The proposed mechanism of IC50 dose of Hep88 mAb-treated HepG2 cell at 12 hours.	104
Figure 5.11 The proposed mechanism of IC50 dose of Hep88 mAb-treated HepG2 cell at 18 hours.	105
Figure 5.12 The proposed mechanism of IC50 dose of Hep88 mAb-treated HepG2 cell at 24 hours.	106

LIST OF ABBREVIATIONS

Symbols/Abbreviations	Terms
°C	Degree Celsius
ACN	Acetonitrile
ADCC	Antibody dependent cell mediated cytotoxicity
AIFs	Apoptosis inducing factors
Ag	Antigen
Apaf-1	Apoptosis protease activating factor-1
ATP	Adenosine triphosphate
Bak	Bcl- 2 antagonist killer
Bcl-2	Bcl-2 homologous antagonist killer
Bax	Bcl-2 associated X protein
BCA	Bicinchoninic acid BCIP/NBT 5-bromo-4-chloro-3'-indolyphosphate/ nitro-blue tetrazolium
Bcl-2	B-cell lymphoma 2
BH3	Bcl-2 homology region 3
Bid	BH3 interacting-domain death agonist
BLAST	Basic local alignment search tool
bp	Base pair
CAD	Caspase-activated domain
CARD	Caspase-activating recruitment domain
CDC	Complementary-dependent cytotoxicity
cDNA	Complementary deoxyribonucleic acid
Ct	Threshold cycle
CTSB	Cathepsin B
Cyt c	Cytochrome c
dATP	Di adenosine triphosphate
DED	Death effector domain
DEPC	Diethylpyrocarbonate

DISC	Death inducing signal complex
DNA	Deoxyribonucleic acid
DTT	Dithiothreitol
EF-2	Elongation factor-2
ESI	Electrospray ionization
FACS	Fluorescence-activated cell sorter
FADD	Fas-associated death domain
Fas L	Fas ligand
FITC	Fluorescein isothiocyanate
G0	Gap0 period
G1	Gap1 period
G2	Gap2 period
HCC	Hepatocellular carcinoma
HNF1A	Hepatocyte nuclear factor 1 alpha
Hsp	Heat shock protein
IAA	Iodoacetamide
IAPs	Inhibitor of apoptosis proteins
IC50	Half maximal inhibitory concentration
kb	Kilobase
kDa	Kilo Dalton
LC	Liquid chromatography
LMP	Lysosomal membrane permeabilization
M phase	Mitotic period
mAb	Monoclonal Antibody
Mev	Multiexperiment viewer
mg	Milligram
ml	Millilitre
mM	Millimolar
MOMP	Mitochondria outer membrane permeabilization
mRNA	Messenger ribonucleic acid
MS	Mass spectrometry

MTT	3-(4,5-dimethylthiazol-2-yl)-2,5-diphenyltetrazolium bromide
PAGE	Poly acrylamide gel electrophoresis
PBS	Phosphate-buffered saline
PCD	Programmed cell death
PCR	Polymerase chain reaction
PEI	Percutaneous ethanol injection
pH	Power of Hydrogen ion concentration
PI	Propidium iodide
pNA	Para-nitroanillide
QUAD	Quadrapole
RPMI	Roswell Park Memorial Institute
RNA	Ribonucleic acid
rRNA	Ribosomal ribonucleic acid
S phase	Synthesis period
SDS	Sodium dodecyl sulfate
Smac/Diablo	Second mitochondria derived activator of caspase/ Direct IAP-binding protein with low pH
STRING	Search tool for retrieval of interacting genes
tBid	Truncated BH3 interacting-domain death agonist
TNF- α	Tumor necrosis factor-alpha
TOF	Time of flight
TRADD	TNFR1-associated death domain protein
TRAIL-R1	TNF-related apoptosis inducing ligand receptor-1
TRAIL-R2	TNF-related apoptosis inducing ligand receptor-2
μg	Microgram
μl	Microlitre

CHAPTER 1

INTRODUCTION

1.1 Introduction

Nowadays, the leading causes of death in the world were changed from accidental or infectious diseases to cancer. Cancer causes worldwide death accounted for 7.6 million deaths (around 13% of all deaths) in 2008 (Ferlay et al., 2010). In Thailand, cancer is also becoming a significant health problem. Hepatocellular carcinoma (HCC) is the leading cause of death in Thailand (Somboon, Siramolpiwat, & Vilaichone, 2014; Vatanasapt, Sriamporn, & Vatanasapt, 2002). While, HCC is the fifth most common cancer worldwide (Jemal et al., 2008). Its prevalence and mortality rate is varied from region to region, the lower is noticed in most developed area (5-10 per 100,000) but, the higher is gradually detected in developing country (>20 per 100,000) including in the South-East Asian countries. In Thailand, HCC is the most common cancer in men (37.4 per 100,000) and the third most common in women (16.3 per 100,000). The main etiology for HCC in Thailand is hepatitis B virus (HBV) infection, while for worldwide are the chronic infection of hepatitis B virus (HBV), hepatitis C virus (HCV), and alcohol and aflatoxin ingestion. These agents alter the function of groups of genes involved in the control of cell growth, apoptosis and DNA repair. The liver cell destruction, regeneration and the microenvironment alteration are occurred. The result of those events contributed to the multistep causation of HCC. Although, the technologies in HCC treatment and diagnosis have been continuously developed; the incidence and the mortality rate of HCC patient are still increased in every year. This trend is result from the defects in sensitivity and specificity during early detection, as well as less effective treatment in eliminating any remaining cancer cells.

Along with other traditional HCC treatment modalities such as; surgical (hepatic resection), non-surgical management including percutaneous ethanol injection; PEI, transcatheter arterial chemoembolization; TACE, radiofrequency ablation; RFA, the survival rates depend on many factors but, especially on tumor size and staging (Osaki & Nishikawa, 2014). Alternatively, the immunotherapy via monoclonal

antibodies (mAbs) is a targeted therapy that specific to tumor-associated antigen. This remedy is also a target specific HCC cells that is expected to lead to the eradication of tumors and the diminishing of their progression, while also reducing toxicity to normal cells. The assassinate mechanism of cancer cell by monoclonal antibodies may be caused by its binding to 1) a cancer protein surface resulting in an immune-response (antibody-dependent cell-mediated cytotoxicity; ADCC or complement-dependent cytotoxicity; CDC), or 2) a growth-factor receptor that blocks the cell's signaling capacity for cell growth.

The advantages of monoclonal antibodies that described above leading to developed and produced monoclonal antibodies for treated any cancer in more widespread. Among these, Hep88 monoclonal antibody that specific to hepatocellular carcinoma was produced by Laohathai and Bhamarapravati (Laohathai & Bhamarapravati, 1985). The preliminary study was found that Hep88 mAb affects to destroy the hepatocellular carcinoma (Puthong, Rojpibulstit, & Buakeaw, 2009). Moreover, Hep88 mAb's specific antigens, mortalin (HSPA9) and alpha-enolase, as well as the ultracellular structures in hepatocellular carcinoma after treated with Hep88 mAb were previously studied (Manochantr et al., 2011; Rojpibulstit et al., 2014). The hepatocellular carcinoma alteration appearance was massive vacuolization of the cytoplasm and mitochondrial swelling, but absence of chromatin condensation. These imply the death of HCC induced by Hep88 mAb via apoptosis-like PCD (paraptosis). Though the characteristic to define as paraptosis were that of lacking of apoptotic morphology and might not respond through caspases cascade pathway. But so many reports up to date pointed out that various type of cell death could be mutually stimulated on the detected cells whereas the morphological change might be detected by the predominant one (Guo, Chen, Wang, & Chen, 2010). For example, it has been reported that the contribution to be apoptosis- or paraptosis-PCD in colorectal cancer cells after treated with Ginsenoside Rh2 activated were not accounted only as caspase- or non-caspase dependent (B. Li et al., 2011). But, instead it was controlled through any other pathway which trigger cascade reaction via several kinds of protease activation including caspase, cathepsin etc. This means that whilst the overlapping of various death routes was ongoing developed, more than one mechanism may be

activated at the same time. It was, however, resulting in turning up only dominant ultrastructural change as was subsequently detected by electron micrograph.

Therefore, in this present study, to verify what apoptotic mechanisms, caspase- or non-caspase dependent, are induced by Hep88 monoclonal antibody on HepG2 cell line. The investigation was hence on the expression and activity of caspase-3, caspase-8 and caspase-9 in HCC treated cells using real-time PCR technique and colorimetric assay, respectively. The *Bax*, *Bcl-2*, *p53* and *Cathepsin B* expression in this study were also detected using real-time PCR technique as well. The active caspase-3 induction, cell cycle progression and apoptosis induction were investigated by flow cytometry. Moreover, the protein profile was determined by GeLC-MS/MS proteomics. Therefore, rather than the mechanism involving by Hep88 mAb induction cell death was determined, the overall of results from this study might be useful to get the propose mechanism that necessary to develop new drugs for the HCC treatment in the near future.

1.2 Objectives

The objectives of this study are to study apoptosis and paraptosis mechanisms in hepatocellular carcinoma (HepG2) treated with Hep88 mAb compare with the untreated cell line, i.e.:

1.2.1 To study the apoptosis mechanism after Hep88 mAb induction through the expression in mRNA level of *caspase-3*, *caspase-8*, *caspase-9* and the enzymes activities of caspase-3, caspase-8 and caspase-9 at 24, 48 and 72 hours compare with doxorubicin.

1.2.2 To monitor the cell cycle, the apoptosis induction and the active-caspase-3 determination after treatment with increased the concentration of Hep88 mAb.

1.2.3 To investigate the mechanism of program cell death in IC50 and cytotoxic dose of Hep88 mAb-treated cells through the expression in mRNA level of *Bax*, *Bcl-2*, *p53*, *cathepsin B*, *caspase-9* and *caspase-3* at 3, 6, 9, 12, 18, 24 hours.

1.2.4 To explore the protein profile of the Hep88 mAb-treated HepG2 cells.

1.3 Beneficiaries

This is the first study about gene expression at the mRNA level (*caspase-3*, *caspase-8*, *caspase-9*, *Bax*, *Bcl-2*, *p53*, *Cathepsin B*), enzymes activities (caspase-3, caspase-8 and caspase-9), active caspase-3 detection, cell cycle progression, apoptosis induction and protein profile regarding the effect of Hep88 monoclonal antibody in hepatocellular carcinoma cell line. The results obtain from this study may provide information to understand the effect of Hep88 monoclonal antibody against hepatocellular carcinoma (HepG2).

Conceptual Framework

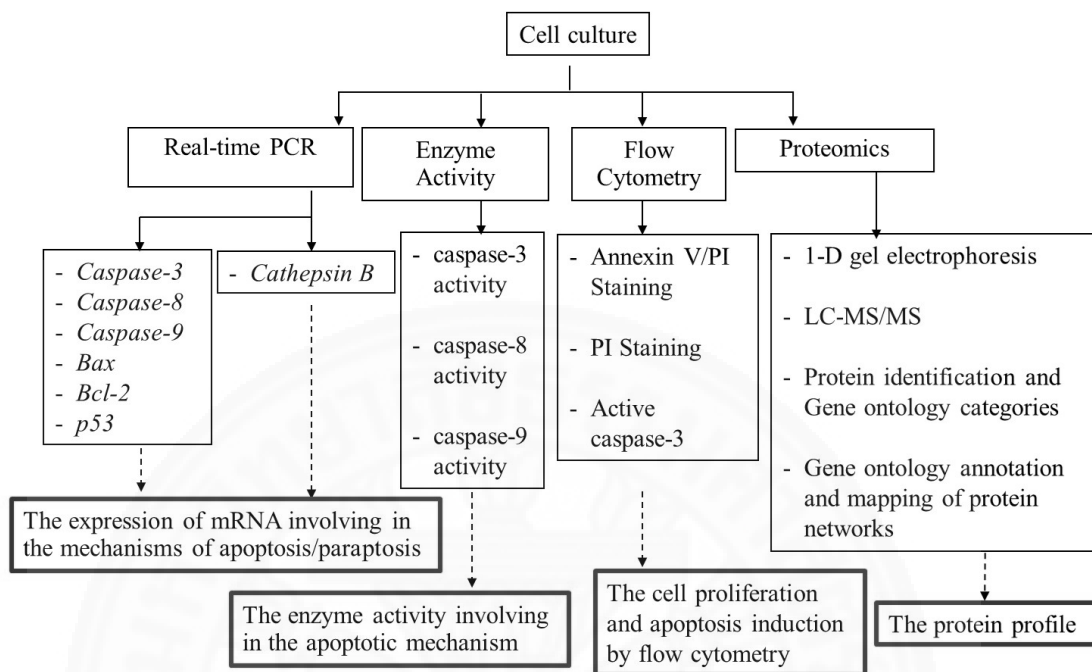


Figure 1.1 A conceptual framework of this study

CHAPTER 2

REVIEW OF LITERATURE

2.1 Hepatocellular carcinoma (HCC)

Hepatocellular carcinoma (HCC) is the most common and aggressive cancer in the world. It is recorded as the fifth most common cancer and the third most common cause of cancer death (El-Serag, 2012). It causes over 700,000 deaths worldwide annually (J. D. Yang & Roberts, 2010). Over the last decade, two main epidemiology patterns were exhibited. The high prevalence is in Asia while the relative low is in Europe and North America. However, up to date, the incidence has increased significantly in United Kingdom and United State of America. It has been reported that approximately 20,000 newly diagnostic cases in the USA each year (Altekruse, McGlynn, & Reichman, 2009). In Thailand, it ranks the first leading cancer in males and third in females since the mid-2000s (National Cancer Institute of Thailand, 2011). The male: female ratio for HCC differs from 3-4:1 in the Northern part of Thailand to 5-6:1 in the Central and Southern part of Thailand (Srivatanakul, Sriplung, & Deerasmee, 2004). An estimated 63,740 new cases (ASR= 38.6 per 100,000 population in males, ASR= 14.6 per 100,000 population in females) were found in 2011 (National Cancer Institute of Thailand, 2011). Unfortunately, the prognosis is very poor due to the late presentation, the difficulty of surgical approach and the lacking of an effective treatment to cure any remaining cancer cells.

2.1.1 Pathogenesis of HCC

All etiological factors associated with HCC are causes of chronic liver disease. Thus, cirrhosis is the true risk factor for cancer development. Nearly 80% of patients with HCC pass through the stage of cirrhosis before the stage of cancer developing (Minguez, Tovar, Chiang, Villanueva, & Llovet, 2009). The mechanisms that etiological factors lead to cirrhosis and development of HCC may involve chronic inflammation, which has been progressively recognized as a pro-carcinogenic condition.

However, there are several factors contribute to the pathogenesis of hepatocellular carcinoma (HCC). The number of HCC worldwide more than 80% caused by hepatitis B virus, hepatitis C virus and aflatoxin. In brief, the mechanism that these agents can alter the function of genes involved in the cell growth, apoptosis and DNA repair. The chronic hepatic inflammatory response that induced by HBV, HCV and aflatoxin are not only increase liver cell destruction and regeneration but also stimulate hepatic cell growth until it turns to be cancer.

2.1.2 The cause of HCC

From the majority of hepatocellular carcinomas (HCC) risk factor, it has been identified based on epidemiological studies i.e. chronic HBV and HCV infection and aflatoxin consumption.

2.1.2.1 Hepatitis B Virus (HBV) infection

HBV is a small DNA virus that is classified as *Hepadnavirus* family (Liang, 2009). The chronic HBV infection increases the risk of HCC. The host immune responses are triggered by the recognition of viral antigen that presented on infected cell (Tseng et al., 2012). Presently, there are several mechanisms that HBV induces the normal liver cells to the pathogenesis and going to HCC. HBV serves directed genetic contribution to HCC by integrates part of its viral DNA genome at several locations into or close to cellular genes that control cell growth and apoptosis in the normal liver cells (Murakami et al., 2005). It causes the mutation and the malfunction in cell growth and apoptosis. On the other hand, it serves indirected genetic contribution by a small regulatory protein HBx, which implicate in signal transduction and transcription activation. HBx protein is binding with p53 (Kordestani, Mirshafiee, Hosseini, & Sharifi, 2014), thus p53 is inactivated their functions and then cancer is developed.

2.1.2.2 Hepatitis C Virus (HCV) infection

HCV is a RNA virus that classified as *Hepacivirus* genus. It consists of a single-stranded plus sense RNA molecule and surrounds with nucleocapsid and envelope (Chevaliez & Pawlotsky, 2006). After entry into cells, it is replicated,

released and transmitted to new infect. As a results, HCV infection is found in a variable proportion of HCC cases (El-Serag, 2012). The percentage of chronic infection development between HCV and HBV individual infection were found that HCV individual infection was higher HBV individual infection (approximately 75% of HCV and 10% of HBV). Chronic HCV infection is related to many factors that contribute to evasion of host immune response by the virus. The most frequent factor is the mutation of the viral genome that makes several quasispecies (Lauring & Andino, 2010).

The major role of HCV in carcinogenesis is likely to be indirect. The infected cell is responded to inflammation and lead to cell destruction, regeneration and fibrosis. However, the HCV also play a direct role to hepatocytes by HCV core protein that has been suggested to affect the regulation of genes expression in cell cycle and apoptosis (Chevaliez & Pawlotsky, 2006).

2.1.2.3 Aflatoxins consumption

Aflatoxin B1 is one of the most potent hepatocarcinogens, it is identified as a class I carcinogen in USA and Europe. It is a contaminant toxin in many food products. The contaminant toxin consumption is mostly found in the developing countries, it leads the normal liver cell to HCC. Furthermore, it remains a serious cause of HCC in China and Sub-Saharan Africa, especially when coupled with HBV infection (Lv, Yu, Li, Luo, & Wang, 2014).

Aflatoxin B1 is metabolized by the liver detoxifying enzyme cytochrome p450 into exo-8, 9 epoxide (Kew, 2013). Aflatoxin B1 epoxide form adducts with DNA, and activates DNA mutations. The favorite site for aflatoxin induced DNA adducts is in the p53 gene. This leads to GC-TA transversion on p53 gene, and resulting in p53 protein alteration by Arg (R) changes to Ser (S). This mutation can be detected in the half of HCC from highly aflatoxin contamination area (Smela, Currier, Bailey, & Essigmann, 2001). Based on the fact that p53 is a tumor suppressor gene which regulates the cell cycle by acting as transcription activator. It also plays a role in apoptosis and DNA repair. Hence, p53 inactivation or mutation are a common pathway for the HCC causation.

2.1.3 Treatment in HCC

Nowadays, the numerous clinical management for HCC such as surgery, ablative therapies, regional therapies, radiation therapy and systemic therapies are widely used. Nevertheless, the results of treatment is depended on the size and stage of tumor. The early-stage can be managed successfully in curative treatments with transplantation, resection, and percutaneous ethanol injection (PEI) (Pang & Lam, 2015) while a small percentage of late stage patient will achieve long-term survival after treatment with the same. The late stage of HCC is needed more specific because of the advanced nature of these HCC. It will be rapid recurrence, even the successfully in resection can be done. Many treatment options exist for management of HCC, each has its own limitation. It is clearly expressed as the following.

2.1.3.1 Liver transplantation

Liver transplantation is the replacement of HCC or diseased liver with a liver donor graft. However, the liver transplantation has many limitations. Liver from the donor must be compatible with the recipient (Bruix & Sherman, 2005). The chance of survival will be decreased, when the liver tumor has metastasized or the immunosuppressant drug is applied for the patient (Byam, Renz, & Millis, 2013).

2.1.3.2 Surgical resection

Surgical resection is operated to remove a tumor with surrounding normal liver tissue. However, the resection has to preserve the adequate part of liver remnant for normal body function. This remedy suggests for the patient who has well prognosis. Unfortunately, it is only a small number of patient who has a suitable liver function for surgical resection (Llovet, Schwartz, & Mazzaferro, 2005).

2.1.3.3 Percutaneous ethanol injection

The percutaneous ethanol (alcohol) injection (PEI) therapy has been widely used in Japan and accepted as an attractive alternative treatment in patients with a small size of hepatocellular carcinoma (HCC). The effects of ethanol are toxic at the cellular level. Ethanol diffuses into the cell and causes the protein denaturation and the cellular dehydration that lead to coagulation and necrosis. After that HCC

subsequently changes to fibrosis and small vessel thrombosis. Finally, it also contribute to cellular death. However, this therapy can achieve a 5-year survival rate of around 60% for patients with small size of HCC (Yamamoto et al., 2001)

2.1.3.4 Transcatheter arterial chemoembolization

Transcatheter arterial chemoembolization (TACE) is usually performed for unresectable cancers as a temporary treatment for the patient who waiting for the liver transplant. TACE is done by injecting an antineoplastic drug (e.g. cisplatin) mixed with a radio opaque contrast and an embolic agent into the right or left hepatic artery via the groin artery (Sergio et al., 2008). The multiple trials show objective tumor responses and slowed tumor progression (Sergio et al., 2008). However, TACE is not suitable for patients with poor liver function and large tumors size.

2.1.3.5 Radiofrequency ablation

Radiofrequency ablation (RFA) uses high frequency radio-waves to destroy tumor by local heating. The electrodes are inserted into the liver tumor under ultrasound image guidance. It is suitable for small tumors (Bruix & Sherman, 2005).

2.1.3.6 Immunotherapy

Cancer immunotherapy is a medical term which is defined as the use of immune system to eliminate the cancer cell. The main types of cancer immunotherapy now being used, are included monoclonal antibodies (antibody-based therapy), cancer vaccines (cell-based therapy) and non-specific immunotherapies (Topalian, Weiner, & Pardoll, 2011). In the last few decades, antibody-based therapy for cancer has become established and achieved the successfully in recent years.

Nowadays, the monoclonal antibodies are produced for cancer immunotherapy usage. It is designed to recognize and find specific proteins on cancer cells. So, it can be called targeted immunotherapy because of monoclonal antibodies are made to target to cancer cells. Monoclonal antibody has become critical for the successful treatment and it has been proved to increase survival rate of cancerous

patients in clinics. For examples; Bevacizumab, an anti-vascular endothelial growth factor (anti-VEGF) antibody that has been approved by the FDA and becomes widely used with many cancers (Pavlidis & Pavlidis, 2013).

2.2 Monoclonal antibody

A monoclonal antibody (mAb) is a produced-molecule that constructed to recognize only one specific antigen on the interested cells (Kohler & Milstein, 1975). It is classified to be mono-specific antibodies because they are all clones from a unique parent cell.

In cancer immunotherapy, the effective therapeutic monoclonal antibodies are focused on mAbs-induced apoptosis cancer cells death (Crescence et al., 2012; de Weers et al., 2011). The novel mAbs that bind their targets and possess a novel mechanism. The multiple mechanisms have been proposed to explain the anti-cancer activity of unconjugated tumor antigen-specific monoclonal antibodies. Because of most mAbs do not directly induce cell death. It has to rely on immune effector mechanism.

However, most of cancers have already developed a variety of mechanisms to escape the immune attack. Hence, several type of synthetic monoclonal antibodies can induce cell death without the need for immune effector mechanisms. It may be very important tool in the cancer treatment that have involved complex mechanisms to protect themselves from complement-dependent cytotoxicity (CDC) or antibody-dependent cellular cytotoxicity (ADCC). For example: Cetuximab can directly inhibit cell proliferation, angiogenesis and survival by blocking epidermal growth factor receptor (EGFR) binding (Martinelli, De Palma, Orditura, De Vita, & Ciardiello, 2009).

Moreover, mAbs can be conjugated to deliver the chemotherapeutic agents, radioactive agents and target signaling molecules for cancer treatment.

2.2.1 The death mechanism of cancer via monoclonal antibody treatment

Monoclonal antibodies (mAbs)-mediated cell death can be classified by the appearance of mAbs. Two main type of mAb appearance are the conjugated mAbs and the naked mAbs. The conjugated mAbs are tagged with toxin, radioactive, or cytokine. They induces cell death through the co-function between monoclonal antibody and tagged molecules. The mAbs carry the tagged molecule to target cell, then the tagged molecule induces cell death. While, the naked mAbs might be directly binding with the specific protein on cell which mediate cancer cell death through antibody-dependent cellular cytotoxicity (ADCC), complement-dependent cytotoxicity CDC, or inducing program cell death.

2.2.2 The anti-HCC monoclonal antibodies production

Laohathai and Bhamarapravati produced anti-HCC mAbs by mice immunization (Laohathai & Bhamarapravati, 1985). An albino Balb/c mice were immunized by injection with the suspension of S102 HCC cell line into the peritoneum. At day 20 after the first immunized, Booster injections were given. After boosting for 2 weeks, the mice were bled to collect antisera for the approximation of antibody against HCC antigen by using an indirect ELISA testing. Prior the fusion step between mouse spleen B-cell of immunized mice and myeloma cell for 3 days, the suspension of S102 was intravenous injected to be an antigen for final booster. The antibody producing B-cells from immunized mice were collected then fused with myeloma cell line (NS-1) to be anti-HCC-producing hybridoma cell. After that, the hybridoma cells were cultured for 10–14 days before collected the culture supernatants to screen the specific antibody production by using an indirect ELISA test (the plate was coated with the S102 HCC cell line).

The anti-HCC-producing hybridoma cells were subcloned, and then frozen in liquid nitrogen until use. Monoclonal antibodies (mAbs) were produced in vitro by collecting high concentrated supernatants from the anti-HCC-producing clone. The mAbs from each positive clones were further purified from the supernatant using a purified protein column. The purified-mAbs from different hybridoma clones were

evaluated for their cytotoxic activity via the MTT colorimetric assay to screening for the effective anti-cancer hybridoma clone.

2.2.3 Hep88 monoclonal antibody

Hep88 monoclonal antibody (mAb) was generated by immunization of mice with the suspension of an established human hepatocellular carcinoma cell line from a Thai patient (S102) as mention earlier. This monoclonal antibody is able to either kill HepG2 cell line (ATCC strain HB 8065) or inhibit the proliferation of hepatocellular carcinoma cell lines: S102, R12 (established Thai patient's hepatocellular carcinoma cell lines) but had no effect on the normal liver cell line: Chang liver (ATCC strain CCL 13). Moreover, preliminary results showed that this monoclonal antibody induced the cellular component of HepG2 cell line alteration as paraptosis morphology that showed cytoplasmic vacuolization, mitochondria and endoplasmic reticulum (ER) slightly swelling (Manochantr et al., 2011). The heat shock protein mortalin (HSP9A) is highlighted as a specific antigen of Hep88 mAb (Rojpibulstit et al., 2014).

2.3. Program cell death (PCD)

Program cell death (PCD) is an essential process for the regulation of developed and homeostatic cell during an organism's life cycle. It is characterized by a series of biochemical event that lead to morphological changes. The program cell death has been often mentioned as "apoptosis". The most defining features of apoptosis are involved in the activation of caspases, chromatin condensation, cell shrinkage, plasma membrane blebbing and DNA fragmentation (Elmore, 2007). However, the recent findings has shown the alternative PCD pathways (B. Li et al., 2011; Rojpibulstit et al., 2014; Zhou et al., 2014).

Apoptosis-like PCD is also displayed as one of that alternative PCD (B. Li et al., 2011; Zhou et al., 2014). The features of apoptosis-like PCD has been shown the morphological of less compact chromatin condensation, cytoplasmic vacuolization and

independent of caspase activation and inhibition (Broker, Kruyt, & Giaccone, 2005). Thus, it can be defined as caspase-independent PCD.

2.3.1 Caspase-dependent PCD

Caspase-dependent PCD is mainly mention to apoptosis. It is characterized by the sequential activation of a series of caspases. Moreover, it is also defined by the morphological changes such as chromatin condenses, phosphatidylserine exposure, cytoplasmic shrinkage, membrane blebbing and formation of apoptotic bodies.

The mechanisms of caspase-dependent PCD are highly complicated. Nowadays, there are two main pathway including the extrinsic or death receptor pathway and intrinsic or mitochondrial pathway.

The extrinsic pathway initiate cell death through transmembrane receptor-mediated interactions. It plays a critical role in transmitting from the cell surface to the intracellular signaling pathways. The sequence of extrinsic events are occurred by the binding between the receptors and the homologous trimeric ligand. After that, the cytoplasmic adapter proteins are recruited which exhibit corresponding death domains that bind with the receptors. For example; the binding of Fas ligand to Fas receptor results in the assembly of the adapter protein Fas-associated death domain (FADD), and the binding of TNF ligand to TNF receptor results in the assembly of the adapter protein TNF receptor associated-protein with death domain (TRADD) and it links the activation to FADD (Elmore, 2007; Park, 2012). FADD then associates with procaspase-8 via dimerization of the death effector domain and forms a death-inducing signaling complex (DISC) (Kischkel et al., 1995). It is resulting in the auto-catalytic activation of procaspase-8. Once caspase-8 is activated, the apoptosis PCD is triggered (Kruidering & Evan, 2000) as shown in the Figure 2.1.

While, the intrinsic pathways initiate cell death through the intracellular signals that act directly on targets within the cell. Those signals cause the mitochondrial outer membrane permeabilization (MOMP), the release of cytochrome c and the clustering of procaspase-9 are both leading to caspase-9 activation (S. Yuan et al., 2010).

The important regulators of both extrinsic and intrinsic pathway are associated with mitochondria. The mitochondrial-mediated caspase activation is controlled by Bcl-2 family proteins. Pro-apoptotic proteins in Bcl-2 family for example, Bax, Bak, Bad, Bid, etc. are proved to be the bridging signaling generating mitochondrial outer membrane permeabilization (MOMP). Pro-apoptotic proteins, Bid is undergone a conformational change to truncated Bid (tBid) to facilitate Bax insertion by translocation from cytosol to the outer mitochondrial membrane in early step of intrinsic pathway resulting in the releasing of multiple factor molecules from mitochondria including cytochrome c (Du, Fang, Li, Li, & Wang, 2000; Wei et al., 2000; Yamaguchi, Bhalla, & Wang, 2003). Cytochrome c was subsequently adapted with another molecules to form apoptosome and then activated caspase-9 and caspase-3 (Estaquier, Vallette, Vayssiere, & Mignotte, 2012; S. Yuan et al., 2010). However, these events can be inhibited by the sequestration of anti-apoptotic Bcl-2 and pro-apoptotic Bax proteins (Buron et al., 2010).

2.3.2 Caspase-independent PCD

Caspase-independent PCD differs from caspase-dependent PCD. The differences between them are involved several molecular mediators in mitochondria and lysosome. When the mitochondria is induced to form MOMP, it is able to release multiple factors that may trigger a caspase-independent cell death such as apoptosis-inducing factor (AIF), Endo G and Omi/HtrA2 (Broker et al., 2005; Chipuk & Green, 2005; Kook et al., 2007; Ruchalski et al., 2006; Zhou et al., 2014). While, cathepsins and multi-proteases can be released from lysosome by lysosomal membrane permeabilization (LMP) (Boya & Kroemer, 2008; Johansson et al., 2010; Tardy, Codogno, Autefage, Levade, & Andrieu-Abadie, 2006). The mitochondrial and lysosomal proteins releasing are caused by MOMP and LMP, which controlled by Bcl-2 family proteins. (Szegezdi, Macdonald, Ni Chonghaile, Gupta, & Samali, 2009). The scientific data of caspase-independent PCD demonstrated that involved in cathepsins activation and not responded to caspase inhibitors and caspases activation (Broker et al., 2005; Joy et al., 2010; Malhi, Guicciardi, & Gores, 2010; Sperandio et al., 2004). The proteolytic enzymes cathepsins are also released to degrade intracellular proteins or activate caspases as well as other enzyme to induce cell death (Bhoopathi et al., 2010;

Johansson et al., 2010; Oberle et al., 2010). It is now recognized this type of PCD as apoptosis-like PCD or paraptosis by morphological characterization different from apoptosis, i.e. numerous vacuolization without apoptotic body or membrane blebbing (Chipuk & Green, 2005).

Table 2.1

Ultrastructural features of apoptosis and paraptosis (Danaila et al., 2013).

Morphology	Apoptosis	Paraptosis
Cell body	Shrinkage	Sometimes enlarged
Cell membrane	Intact, blebbing	Intact
Cytoskeleton	Collape before death	Collape before death
Lysosomes	Intact	Intact
Endoplasmic reticulum	Dilated, loss of libosomes from external membranes	Sometimes dilated
Mitochondria	Intact with cytochrome c release and ATP synthesis	Late swollen, without ATP synthesis
Cytoplasm	Compact and condensed, with intact organelles	Vacuolised, with numerous vacuoles
Nucleus	Shrinkage and fragmented, disintegrating nucleolus	Without fragmentation
Chromatin	Condensation and internucleosomal DNA fragmentation	With or without condensation
Apoptotic bodies and their removal	Common heterophagy (rapid) by other cells	Absent

Note. Adapted from “Apoptosis, paraptosis, necrosis, and cell regeneration in posttraumatic cerebral arteries,” by L. Danaila, I. Popescu, V. Pais, D. Riga, S. Riga, and E. Pais, 2013, *Chirurgia (Bucur)*, 108(3), p. 319-324.

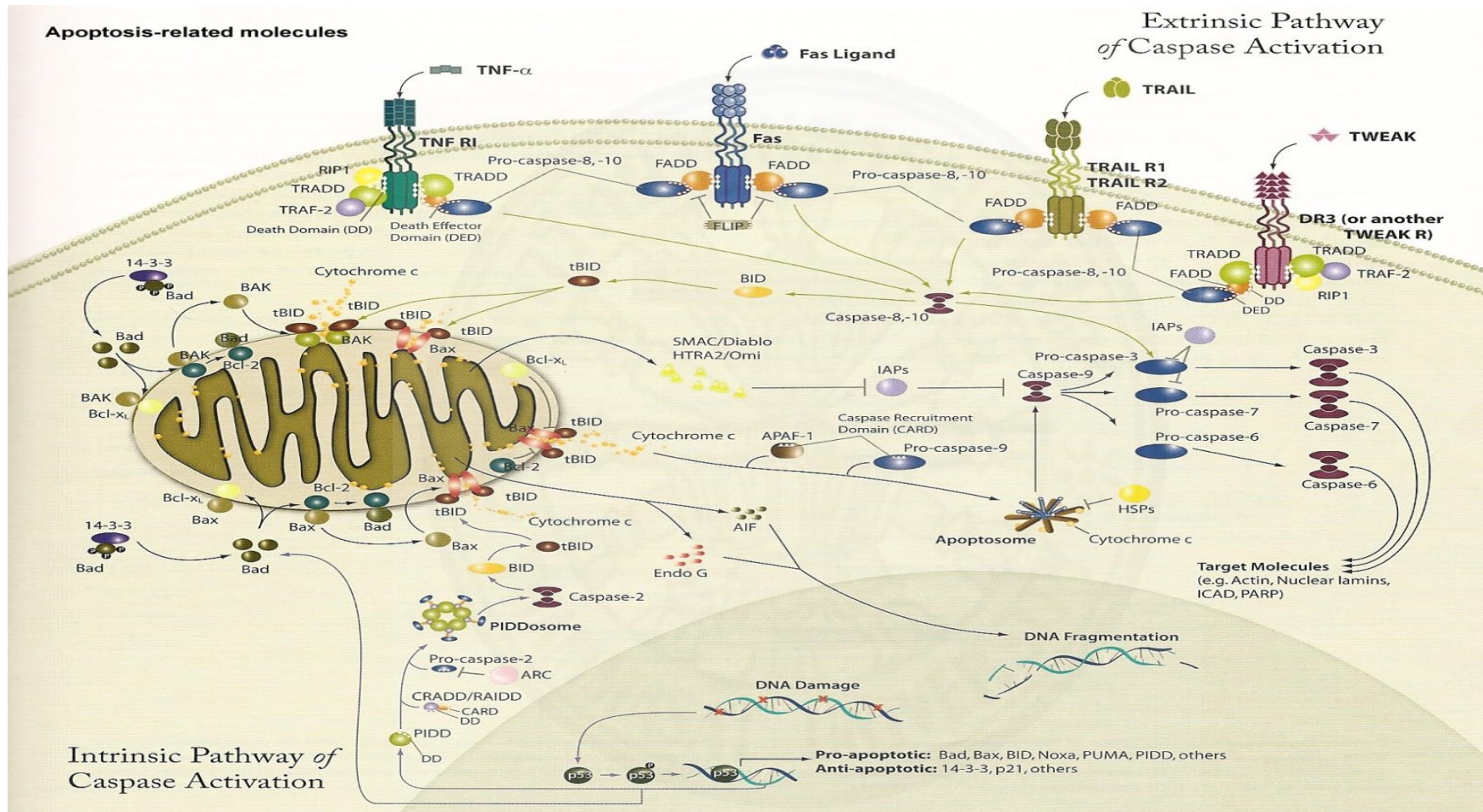


Figure 2.1 Apoptosis pathway

Note Retrieved from <http://www.hixonparvo.info/apoptosis.jpg>

2.4 Caspases

Normally, caspases are synthesized as inactive proenzyme, which are known as procaspases. The structure of caspases are organized into a prodomain region, a large subunit and a small subunit (Park, 2012). Upon activation, the large and small subunits of caspase are released from prodomain and then separated as a subunit as shown in the Figure 2.2. The active caspases are often contained with two large and two small subunits as the tetramer, so it possess two active sites (Salvesen & Riedl, 2008). Caspases cleave peptide bond on carboxyl site of aspartic acid residues. Therefore, it can be called aspartate-specific cysteine proteases.

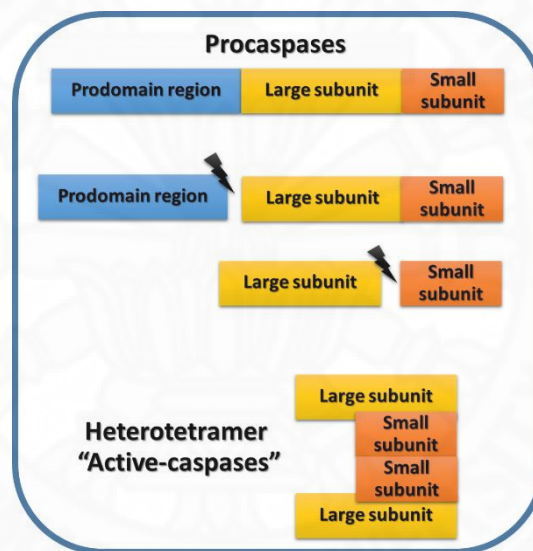


Figure 2.2 The structure of caspases and its active form.

Caspases can be divided into 2 families, which are play a role in apoptosis (caspase-2, -3, -6, -7, -8, -9, -10 and -12) and cytokine processing (caspase-1, -4, -5 and -11). The apoptotic caspases can be subdivided into initiator caspases and effector caspases based on their prodomain as shown in the Figure 2.3. The caspase-2, -8, -9 and -10 are the long-prodomain initiator caspases, it can be recruited to caspase-activating molecule (FADD or Apaf-1) through caspase recruitment domain (CARD) and death effector domain (DED) (S. Yuan et al., 2010). The short prodomain is the effector caspases that contain caspase -3, -6 and -7. However, caspases are divided into three subfamilies when based on their homology in amino acid sequences. Three

caspases subfamily members include apoptosis activator (caspase-2, caspase-8, caspase-9 and caspase-10), apoptosis executioner (caspase-3, caspase-6 and caspase-7) and inflammatory mediator (caspase-1, caspase-4, caspase-5, caspase-11, caspase-12, caspase-13 and caspase-14).

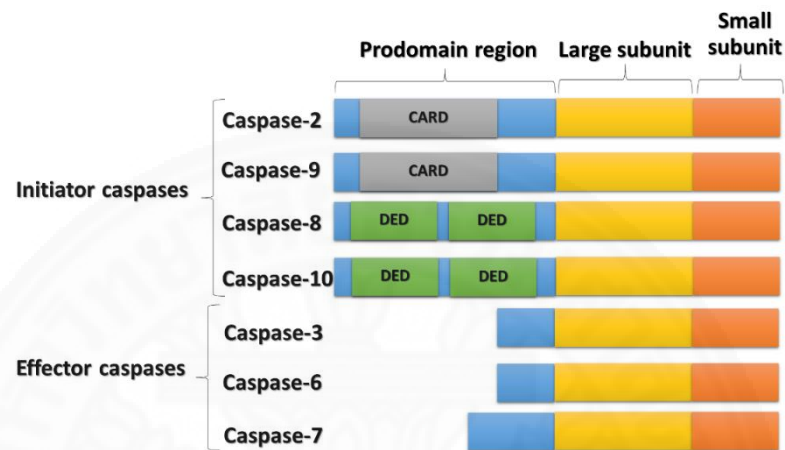


Figure 2.3 The different structure of prodomain on the initiator and the effector of apoptotic caspases.

The activation of caspases is induced by two main pathways. The death receptor induction via death signaling is apoptotic extrinsic pathway, and the mitochondria induction is apoptotic intrinsic pathway.

The Fas ligand (FasL) and tumor necrosis factor (TNF)-2 are the death signals that can be specifically recognized with their corresponding death receptors, such as Fas (FasR) or TNF receptor (TNFR-1). The binding between the signal and death receptor causes FADD aggregation, which is interacted with death effector domains (DEDs) in the prodomain of procaspase-8. These interaction induce the oligomerization of procaspase-8, then form into the molecule complex named death-inducing signaling complex (DISC). After that, two procaspase-8 attach to each other and activate themselves to be caspase-8. It is vigorously activated and can directly activate the downstream procaspases (e.g. procaspase-3). Moreover, it can activate the mitochondria-mediated pathway by truncating Bid (a pro-apoptotic Bcl-2 family protein).

The mitochondria can be mediated procaspase-activation by induced mitochondria outer membrane permeability (MOMP). A truncating Bid dislocates from cytosol to attach to pro-apoptotic protein Bax/Bak on the mitochondrial membrane and let them oligomerization to channel form. As a result, the molecules such as cytochrome c, apoptosis-inducing factor (AIF) and other molecules are released from mitochondria and brought to program cell death. When cytochrome c in mitochondria was released to the cytosol, the apoptotic protease activation factor-1 (Apaf-1) is oligomerized together with procaspase-9, dATP and cytochrome c. It is resulting in a complex formation known as apoptosome that can activate caspase-9. Active form of caspase-9 can activate apoptosis executioner caspases (procaspase-3 and procaspase-7) and lead to apoptosis in the cell.

2.4.1 Caspase-8

Caspase-8 is a member of the cysteine proteases, which is the critical protein in the extrinsic apoptotic pathway. Like all caspases, caspase-8 is synthesized as an inactive procaspase in the cytosol, and it is activated through the ligation of death receptor with cytosolic adapter protein that recruited to form the death-inducing signaling complex (DISC). Activated caspase-8 directly cleaves and initiates a cascade of downstream effector caspases.

Furthermore, the linkage between caspase-8 and mitochondria is found. When Bid is cleaved by caspase-8, Bid can translocates to the mitochondria. It induces pro-apoptotic mitochondrial changes and lead to cytochrome c release as described earlier (Kruidering & Evan, 2000).

2.4.2 Caspase-9

Caspase 9 is the initiator caspase of the intrinsic apoptosis pathway. The procaspase-9 structure mainly consisting of prodomain (CARD domain), large subunit and small subunit. CARD domain is found in both N-terminal of Apaf-1 and the prodomain of procaspase-9. As a results, they interact with each other by CARD domains and form a complex. When, procaspase-9 in a multimeric complex with dATP and Apaf-1 is called apoptosome. It has an effect on procaspase-9, procaspase-9 is

cleaved to generate the large and small subunits. The subunits then dimerized to form an activated caspase 9, and it subsequently activated downstream caspases 3.

2.4.3 Caspase-3

Caspase-3 is the effector caspase (a key factor in apoptosis execution), which is activated by other protease. Two copies of each large and small subunit are generated to form an active heterotetramer that cleaves the specific protein substrates within the cell. However, the active form of caspase-3 is highly labile and is rapidly turn to inactivated form (Tawa et al., 2004).

The hallmark of apoptotic morphology such as DNA fragmentation, phosphatidylserine exposure on cell outer membrane and apoptotic body formation are caused by the function of caspase-3. Active caspase-3 cleaves the inhibitor of caspase-activated DNase (ICAD) to release caspase-activated DNase (CAD) (Wolf, Schuler, Echeverri, & Green, 1999). Then, CAD promotes the DNA fragmentation in apoptotic cells. In addition, the phosphatidylserine exposure on cell outer membrane is caused from the inhibition of flippase activity by caspase-3 activation. The apoptotic body formation is caused from the cleavage of actin-myosin filaments by active caspase-3.

2.5 Cathepsins

Cathepsins are a class of globular proteases, it includes cathepsin A, B, C, D, E, F, G, H, L, K, O, S, V and W (Gondi & Rao, 2013; Tan, Peng, Lu, & Tang, 2013). Cathepsins are synthesized as inactive proenzymes and processed to become the active enzymes.

Cathepsin B is a lysosomal cysteine protease that functions as an endopeptidase and an exopeptidase (Turk et al., 2012). Especially, the endopeptidases activities of cathepsins are auto-activated at acidic pH in the lysosomes (Turk, Turk, & Turk, 2001). It functions in intracellular protein catabolism, and be involved in other physiological processes such as caspase-dependent PCD (apoptosis) and caspase-independent PCD (paraptosis). However, cathepsin B is also known to be settled in the mitochondria (Muntener, Zwicky, Csucs, Rohrer, & Baici, 2004) where it is associated

to initiate cell death. While, it is also known to be lived in the nucleus (Riccio et al., 2001) where it is involved to the nuclear scaffold.

Many evidences indicated that cathepsin B is also involved in downstream apoptosis regulation of mitochondria. The mechanisms are occurred when the lysosome is destabilization by stress induction. The active cysteine cathepsins are released in cytosol, where they process Bid to active and/or degrade pro-apoptotic Bcl-2 homologues, by which free the pro-apoptotic activity of Bak and Bax. This is then followed by mitochondrial outer membrane permeabilization (MOMP) and subsequent cytochrome c release, which leads to caspase activation and execution of cell death program (Stoka, Turk, & Turk, 2005).

Another way, cathepsin B may also stimulate cell death through caspase-independent PCD by randomly cleave the intracellular proteins.

2.6 Bax

The Bax also known as Bcl-2-like protein 4, which is encoded by the *Bax* gene. The *Bax* gene was the first identified as pro-apoptotic member of the Bcl-2 protein family, it contains BH1, BH2 and BH3 domains. Bcl-2 family is group of genes that share some characteristic domains of Bcl-2 homology (BH) domains (BH1, BH2, BH3 and BH4). As a result, these proteins can form heterodimers or homodimers to each other, they act as anti-apoptotic or pro-apoptotic regulators that are involved in a wide variety of cellular activities (Kelekar & Thompson, 1998).

Bax is a key regulator that promotes apoptosis through the mitochondria. Bax is usually found in the cytosol, but upon initiation of apoptotic signaling, Bax undergoes a conformational change. It becomes organelle membrane-associated, especially mitochondrial membrane associated. On the mitochondrial membrane, Bax interact with the voltage-dependent anion channel (VDAC) and form an oligomeric pore in the outer membrane. As a results cytochrome c and other pro-apoptotic factors from the mitochondria is released, and leading to activation of caspases (Keinan, Tyomkin, & Shoshan-Barmatz, 2010). In addition, there are many research that reveal the upregulated expression of Bax by the tumor suppressor protein p53. Bax has been

shown to be involved in p53-mediated apoptosis (W. Li et al., 2015; Munagala, Kausar, Munjal, & Gupta, 2011).

2.7 Bcl-2

The Bcl-2 family comprises a group of structurally related proteins and are grouped into three main groups: the anti-apoptotic proteins group (Bcl-2, Bcl-xL, Bcl-w, Mcl-1, Bcl-10, and Bcl-2 related protein A1); the pro-apoptotic proteins group (Bak, Bax, Bcl-rambo, Bcl-xs, Bok/Mtd); and the pro-apoptotic BH3-only proteins group (Bad, Bid, Bik/Nbk, Bim, Blk, Bmf, Hrk/DP5). The balance between pro-apoptotic protein and anti-apoptotic protein is used to determine apoptotic cell death.

Bcl-2 (B-cell lymphoma-2) protein, encoded by the *Bcl-2* gene, is specifically considered as an important anti-apoptotic protein. The Bcl-2 protein contain BH1, BH2, BH3 and BH4 domain. The mitochondrial-mediated cell death is regulated by Bcl-2 that controls the mitochondrial membrane permeability. Bcl-2 inhibits MOMP formation by binding to the pro-apoptotic protein Bax. Similarly in the report that demonstrated that an overexpression of Bcl-2 leading to preventing the release of cytochrome c from the mitochondria (Kelekar & Thompson, 1998).

2.8 p53

Thirty years ago, the 53 kDa protein was discovered in human and mouse cells. A variety of the 53 kDa protein (p53) studies, indicated that it was an oncogene. Oncogenes were thought to be the key to understanding cancer. In contrast, the existence of tumor suppressor genes was totally anticipant, and there was little reason to believe differently in the mid of 1980s until 4-5 years later (in 1989) the turning point in p53 research occurred. In the presently, the study about p53 has revealed many of the principles involving human tumorigenesis. The p53 acts as a tumor suppressor in many tumor types; induces growth arrest or apoptosis depending on the physiological condition and cell type.

Under normal conditions, p53 is inactive in the cytoplasm. When stress conditions, p53 level is increased and accumulated in nucleus (Solozobova, Rolletschek, & Blattner, 2009). The activation of p53 can cause cell cycle arrest through the transactivation of the cell division process required genes (Vousden & Lu, 2002).

Moreover, the p53 also involved in apoptosis induction by mediated either stimulation of Bax expression, or repression of Bcl-2 expression (Handayani, Sakinah, Nallappan, & Pihie, 2007). During apoptosis, Bax protein level increases and translocates from cytoplasm to mitochondria (Keinan et al., 2010).

2.9 Polymerase chain reaction (PCR)

The PCR is an amplification of short DNA sequences method, which was developed by Kary Mullis in 1983. In the reaction use a pair of primers, that are complementary to a defined sequence on the DNA. These primers are extended by an enzyme *Taq* polymerase (a thermo-stable DNA polymerase that was isolated from *Thermus aquaticus*, a bacterium that grows in hot spring water) so that a copy of the target sequence is made by a series of repeated temperature changes (called cycles).

The PCR cycles contain three important steps to amplify target sequence as shown in the Figure 2.4. First, regular cycling event is denaturation step, consists of heating the reaction to 95°C to melting the DNA template by disrupting the hydrogen bonds between complementary bases, yielding single-stranded DNA molecules. Second, annealing step is lowered reaction temperature about 50–65 °C, allow annealing of the primers to the single-stranded DNA template. Stable DNA–DNA hydrogen bonds are only formed when the primer sequence very closely matches the template sequence. The polymerase binds to the primer-template hybrid and begins DNA formation. Third, extension or elongation step is the optimum temperature (72 °C) of DNA polymerase used. The DNA polymerase synthesizes a new complementary DNA strand to the DNA template strand in 5' to 3' direction by adding deoxynucleotide triphosphates (dNTPs). After amplification, the target PCR product is abundant to be detected and analyzed on an agarose gel by staining with an ethidium bromide.

In addition, the PCR also had an impact on the RNA analysis when it was developed technique by using enzyme reverse transcriptase. RNA is isolated and synthesized to cDNA by that enzyme activity. The cDNA is then used in a conventional PCR and this is called reverse transcriptase-PCR (RT-PCR). The advantage of this improvement technique is the ability to identify the targeted gene that rare or low levels of expressed mRNA.

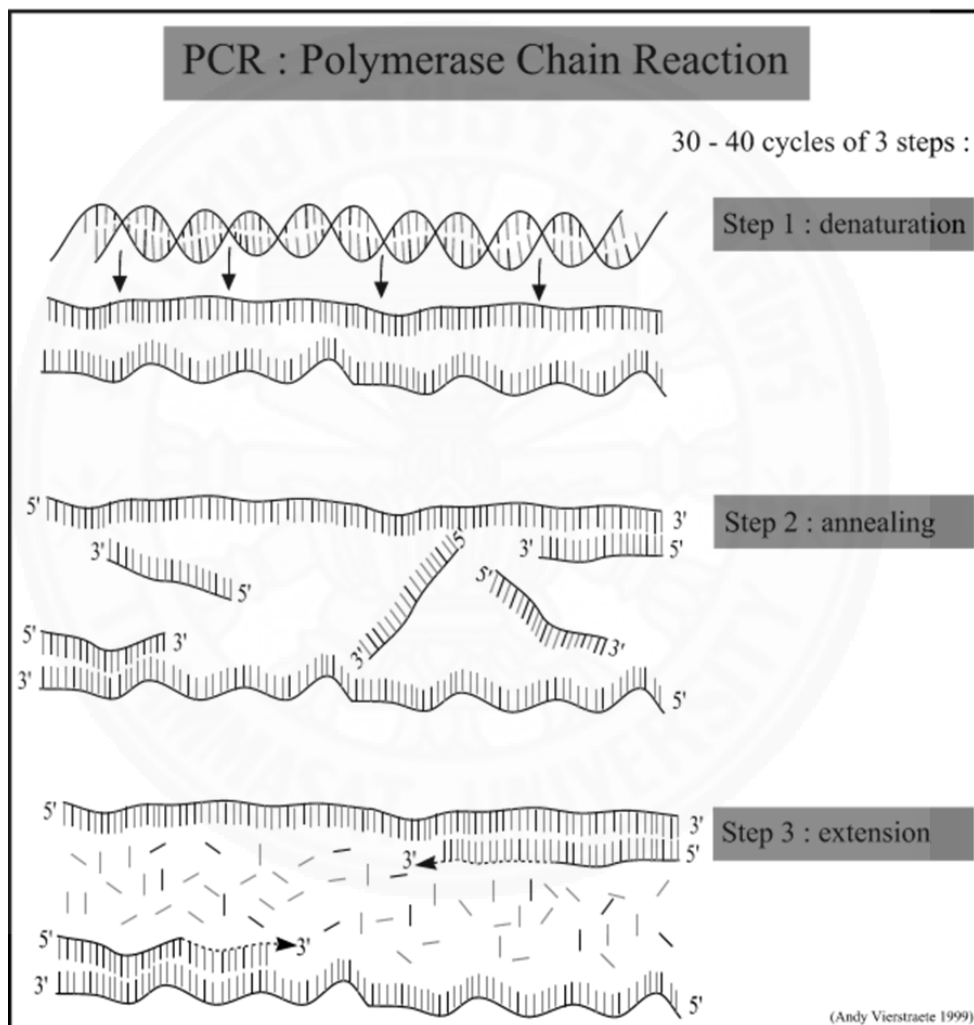


Figure 2.4 The steps in PCR

Note. Adapted from Vierstraete, A. (Producer). (1999). *The steps in PCR* [picture].\

Retrieved from <http://users.ugent.be/~avierstr/principles/pcr.html>

2.10 Real-time PCR

A large number of techniques have been developed to analyze and determine amount of mRNA in the gene expression. The real-time PCR is currently being employed for high throughput analysis. This is not only important for the gene expression studies, but also important in screening a marker for certain clinical disorders.

The real-time PCR is also called quantitative PCR or qPCR. It is a molecular biological technique based-on the polymerase chain reaction (PCR), which is detected and quantified the target amplified PCR products at a while the PCR progression by fluorescent signal detection. The reactions of real-time PCR are quantified at each time point of PCR cycle. This value is usually referred to threshold cycle (Ct) where the amplification is first detected.

The Ct is a relative measure of the concentration of target in the PCR reaction, which is generated from the intersection between an amplification curve and a threshold line. The threshold line is a level of the changed reaction that used for the determination of the threshold cycle (Ct) in real-time. The level of threshold is set above the baseline (It is the initial cycles of PCR, there is little change in fluorescence signal), but sufficiently low to be within the exponential growth region of the amplification curve.

The real-time PCR can identify between mRNAs with the most resembled-sequences. This method requires small amount of template to analyze the gene expression. It can be operated to quantify the mRNA as either a one-step reaction, where the entire reaction from cDNA synthesis to PCR amplification is performed in a single tube, or as a two-step reaction, where reverse transcription and PCR amplification occur in separate tubes.

The one-step real-time PCR is both reverse transcriptase and DNA polymerase reactions that occurs in a same tube. The starting template in this method is an RNA, which is rapidly degraded if not handled properly.

The two-step real-time PCR is a method that separates the reverse transcription reaction from the real-time PCR reaction. The process of reverse transcription generate cDNA template and then, the cDNA template was diluted in the

same amount before using in the real-time PCR. This two-step method is often performed when using a non-specific DNA binding dye (such as SYBR Green I) because it is easier to eliminate primer-dimers through the manipulation of melting temperatures (T_m).

2.10.1 Types of real-time quantification

2.10.1.1 Absolute Quantitation

The absolute quantitation uses the serial dilutions of known concentration standards to generate a standard curve. The standard curve produces a linear relationship between C_t and initial amounts of cDNA or mRNA (compare with plasmid DNA as copy number). The copy number of unknown samples are determined by compare C_t values with the standard curve. The amplification efficiencies are assumed equal in all of standards and samples. Furthermore, the concentration of standard serial dilutions have to quantification in the precise range and in the specific detectable levels.

The standard for real-time PCR can be a fragment of double-stranded DNA (dsDNA), single-stranded DNA (ssDNA), or plasmid-cloned DNA. The methods for constructing a DNA standard for two-step real-time PCR are cloning target gene sequence into a plasmid, purifying a conventional PCR product, or directly synthesizing the target nucleic acid.

2.10.1.2 Relative Quantitation

The relative quantitation is determined by the changes of sample gene expression compare with a reference sample. The results of relative quantitation are usually expressed as a target/reference ratio.

Presently, there are many mathematical models available to calculate the gene expression from relative quantitation. However, this method depends on the yield different results. Thus, the amplification efficiency of the reaction is the most important consideration to get the accurate measurement when perform relative quantitation. The amplification efficiency is calculated by using the data from a standard curve with the following formula:

$$\text{Exponential amplification} = 10^{(-1/\text{slope})}$$

$$\text{Efficiency} = [10^{(-1/\text{slope})}] - 1$$

2.10.1.3 Standard curve method

The quantity of each experimental sample is determined using a standard curve and then expressed relative to a housekeeping gene sample. The housekeeping gene is used as a calibrator which is designated as 1-fold. The standard curve method is usually applied in the unequal amplification efficiencies of target gene and housekeeping gene. This method does not require to prepare the exogenous standards and quantify the calibrator samples. Moreover, the complex mathematics are not needed for this method. However, the results from this standard curve method must be normalized with an endogenous gene (usually a housekeeping gene).

2.10.1.4 Comparative Ct method (2- $\Delta\Delta$ Ct)

The comparative Ct method is a mathematical model that calculates the changes in gene expression as a relative fold difference between an experimental and calibrator sample. While this method includes a correction for non-ideal amplification efficiencies (not equal to 1), the kinetics of the target gene and housekeeping gene amplification must be equal.

A validation in this method must be performed by the serial dilutions of the target gene and housekeeping gene. The data are plotted between the log scale of concentration and the difference of Ct value in each dilution. The slope of linear equation is used to determine the suitability of this method. If the value of slope is less than 0.1, the comparative Ct method can be used.

In this real-time PCR method, the PCR product size should not be larger than 200 bp. The comparative Ct method does not require a standard curve, it should be strictly optimized before the experimental operation.

2.10.1.5 Pfaffl method

Michael Pfaffl proposed the quantification method that combines the gene quantification and the normalization into a single calculation. The amplification efficiencies of the target and housekeeping genes are used to correct the differences in this method. The relative expression software tool (REST[®]), which runs in Microsoft[®] Excel, is operated to analyzed this method. The Pairwise Fixed Reallocation Randomization Test[®] is used to calculate the significance of result. The significance of result indicates that the reference gene is suitable for normalization.

Among these methods described earlier, the absolute quantitation is more efficient than relative quantitation because it has reliable standards for quantitation in every PCR amplification. On the other hand, the relative quantitation data (comparative Ct) are only suitable to run the samples within the same real-time PCR reaction. The control gene is used in every time of real-time PCR reaction to confirm the reliability of data analysis between two real-time PCR reactions. If the real-time PCR quantification is not performed on the same times or in same laboratories, the constant results from absolute quantification are more suitable. Nevertheless, both of absolute and relative quantitation methods produce comparable results in the term of fold-change of gene expression data.

2.10.2 Normalization

The normalization of gene expression data is used to correct the variation between samples from different individuals starting material. The variation usually occurs in the cell number or tissue mass, the integrity or quantity of RNA, or the process of experimental treatment. In the idealistic conditions, cell number is used to standardize the mRNA levels. Despite, whole tissue is unable to normalize the expression data. For these reason, the control gene (housekeeping gene) is used to normalize the expression data. The idealistic property of control gene for real-time PCR is an unchanging fashion although the expression is performed in any cell types, any stage of development, or any kind of treatment. Moreover, a control gene also acts as a positive control for the reaction.

2.10.3 Calculated Variation

In the real-time PCR experiment, the intra- and inter-assay variation might be occurred. It can be calculated to validate the assay results. However, the Ct values cannot used to interpret the variation because they are the logarithm unit. Hence, the variation is calculated from the copy number to get the accuracy in the measurement. The amount of error on an intra-assay variation within a single assay quantification is observed when the same template is run multiple times on the same plate with the same reagents. The real-time PCR experiments are usually performed in triplicate, it can be calculated for an intra-assay variation. The high variation might be caused from the low concentration of template and the low specification of primer. While, the amount of error on an inter-assay variation within two separate assays quantification is observed when the same template is run on either the same or different days. The inter-assay variation is often calculated from a standard sample data that performed as a positive control in all plates.

2.11 Flow cytometry

Flow cytometry is a laser-based technology which is employed in cell counting, cell sorting and biomarker detection. The performed cells in this technique have been labelled with fluorophore before passed in a stream of fluid through the laser beams and detected by an electronic detection apparatus. The signals are collected to give an information in multiple parameters of many thousands of cells/particles per second. The forward light scatter data is related to the cell size while, the amount of side scatter data is related to the presence of intracellular granules. A flow cytometry machine sorts and counts the cells that have been labelled by using fluorescent dyes. The labels that are used depend on the laser that is used in the analyzer. The laser excites the fluorochromes which emitted light are detected by the device.

2.11.1 Fluorophores

There are several fluorophores that are used in flow cytometry. These fluorophores are generally attached to a molecule or an antibody that recognizes a target feature either displayed on the cell membrane or the intracellular component. Each of the fluorophores has a unique excited-peak and a unique emission wavelength. For example: The blue argon laser (488 nm) is an air-cooled laser, is easier to set up. It is used in single laser machines. Some of the labels using with the blue argon laser (488 nm) including in the green channel on FL1 (Alexa Fluor 488, GFP, FITC, CFSE, DyLight 488 or CFDA-SE), orange channel on FL2 (PE or PI) and red channel on FL3 (PE-Alexa Fluor 700, PerCP-Cy5.5, PerCP, PE-Cy5.5 or PE-Cy5).

2.11.2 Cells sample preparation

For flow cytometry, the cells must be suspended as single cells at a density of 10^5 – 10^7 cells/ml to prevent the narrow bores of the flow cytometer and its tubing from clogging up. However, the cells from solid tissues e.g. liver or tumors were produced single cells by mechanically or enzymatically method before analyzed. The cells staining for flow cytometry might be perform in fix cells or live cells, depend on the part of interesting on the cellular components.

2.11.2.1 Cell fixation

The fix cells were performed when study intracellular components by flow cytometry. The plasma membrane of the cell must be permeabilized to allow dyes or antibody molecules through while retaining the cell's overall integrity. There are two most common ways to fixation and permeabilization. They are a one-step fix/perm protocol (ethanol/methanol) or a two-step fix/perm protocol (most often paraformaldehyde; PFA/Saponin).

(1) Methanol/ethanol fixation

Methanol/ethanol fixation is very quick, fixes and permeabilizes at the same time and is very inexpensive. However, alcohols can lead to lipid extraction and removal of some protein and generally does not preserve intracellular structures.

(2) PFA/Saponin fixation and permeabilization

PFA/Saponin fixation and permeabilization is milder in this regard and tends to preserve epitopes and more “loosely” membrane-bound proteins. This process requires that saponin is in all wash steps. Saponin pores are transient and are needed to wash unbound antibody out of the permeabilized cell. In this case, the experiment need an appropriate negative control. Because the permeabilized cell has more surfaces for non-specific binding and can passively trap unbound antibody inside.

2.12 Proteomics

Because of the proteins are the parts of living lives. The emerging exploration of proteomes from the overall level of intracellular protein composition, structure, and activity patterns leading to illustrated an important component of functional genomics. For this reason, a mixture word of protein and genome which is the groups of proteins produced or modified by an organism called “proteome”. The proteomics is the large-scale study of proteins, especially their structures and functions. It is generally refers to the large-scale experimental analysis of proteins, which is often specifically used for protein purification and mass spectrometry.

The polyacrylamide gel electrophoresis (SDS-PAGE) is a widespread method that uses to separate proteins from the samples. The proteins in SDS-PAGE gel are stained and followed by section and digestion the band of proteins to identify the differentially expressed proteins by mass spectrometry. This method is called the shotgun proteomics (GeLC-MS) which used in identifying whole proteins in complex mixtures by using a combination of high performance liquid chromatography combined with mass spectrometry. The shotgun proteomics method starts with the proteins in the mixture being separated on denaturing polyacrylamide gel (SDS-PAGE), cut into a range of protein size, digested with enzymatically and the resulting peptides. The peptides are separated by liquid chromatography. Finally, the mass spectrometry is used to identify the peptides.

2.13 Mass spectrometry

Mass spectrometry (MS) is an extremely valuable analytical technique which is the most common technologies for proteomics. The principles of mass spectrometer helps to identify the amount and type of the presence of molecules in a sample by measuring the mass-to-charge ratio (m/z) and a large quantities of gas-phase ions.

All type of mass spectrometers are basically similar. They consists of five essential components i.e. a vacuum system, a sample inlet, an ion source, a mass analyzer, and a detector as shown in Figure 2.5.

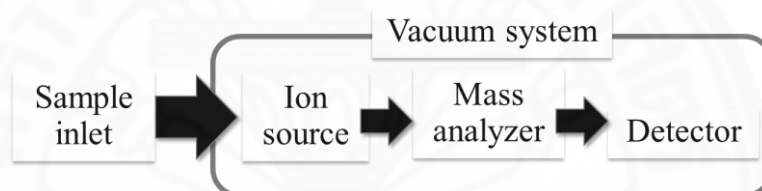


Figure 2.5 Basic components of mass spectrometers.

2.13.1 Vacuum system

Mass spectrometer operate under the vacuum to minimize collision between air molecules and ions. The vacuum system is generated by the pumps includes thurbomolecular pump, diffusion pump and rotary vane pump.

2.13.2 Sample inlet

The sample inlet can be a high performance liquid chromatography (HPLC), gas chromatography (GC), or capillary electrophoresis system.

2.13.3 Ion sources

The ion source in a mass spectrometer converts a part of the sample into ions by solid, liquid or gas phase ionization techniques. The ionization techniques have been a key to determine what types of samples can be analyzed by mass spectrometry. The electron ionization and chemical ionization are used for gases and vapors. The techniques often used with liquid and solid biological samples include electrospray ionization (ESI) and matrix-assisted laser desorption/ionization (MALDI). The ions are then transported by an electric and magnetic fields to the mass analyzer.

2.13.4 Mass Analyzers

A mass analyzer uses an electric and magnetic field to affect the path and velocity of the ionized molecules. The differences in masses of the fragments allows the mass analyzer to sort the ions. The ions move through the mass analyzer, which they depend on the mass-to-charge (m/z) ratios. In another word, more charged molecules are faster-moving than less charged molecules.

2.13.4.1 Types of mass analyzers

There are several types of mass analyzers that used for mass spectrometry. They are in the following:

(1) Time-of-flight (TOF) mass analyzer

The TOF mass analyzer uses an electric field to accelerate the ions through the same potential in the flight tube. The lighter ions can travel to the detector faster than heavier ions.

(2) Quadrupole mass analyzer

The quadrupole mass analyzer uses an electrical fields that is created between 4 parallel rods by apply a direct current (DC) and radio frequency (RF) to each rod to selectively stabilize or destabilize the paths of ions. The ions can move along through this electrical field. When, ions are accelerated down to mass analyzer, it was passed to detector by the different of mass/charge in each molecule.

(3) Quadrupole-ion trap mass analyzer

The quadrupole-ion trap mass analyzer uses the same principles as the quadrupole mass analyzer, but it traps ions in a two dimensional quadrupole field. The ions are become unstable and ejected from the trap to the detector by the increasing of mass-to-charge (m/z) ratios.

2.13.5 Detectors

The detector records either the charge when an ion passes and hits on a surface by measuring the value of an indicator quantity as an electron multiplier or a photomultiplier. Thus, the detector provides data for calculating the abundances of each ion present. In a detector, the signal is produced during the scanning as a mass spectrum. The ions are recorded as a function of m/Q by plotting the amount of signal versus m/z ratios.

CHAPTER 3

RESEARCH METHODOLOGY

From the objectives in this study, the experiments were designed to prove the mechanism of apoptosis and paraptosis in HepG2 cells after treated with Hep88 mAb. The mRNA expression level of apoptotic and paraptotic involving genes were quantitated by real-time PCR. The apoptotic mechanism were confirmed again by caspases enzyme activities. Furthermore, the several hallmarks of apoptosis were determined by flow cytometry. The protein profile of Hep88 mAb-treated HepG2 cell was investigated by GeLC-MS/MS method. Overview of the experimental method in this study can be illustrated in the Figure 3.1.

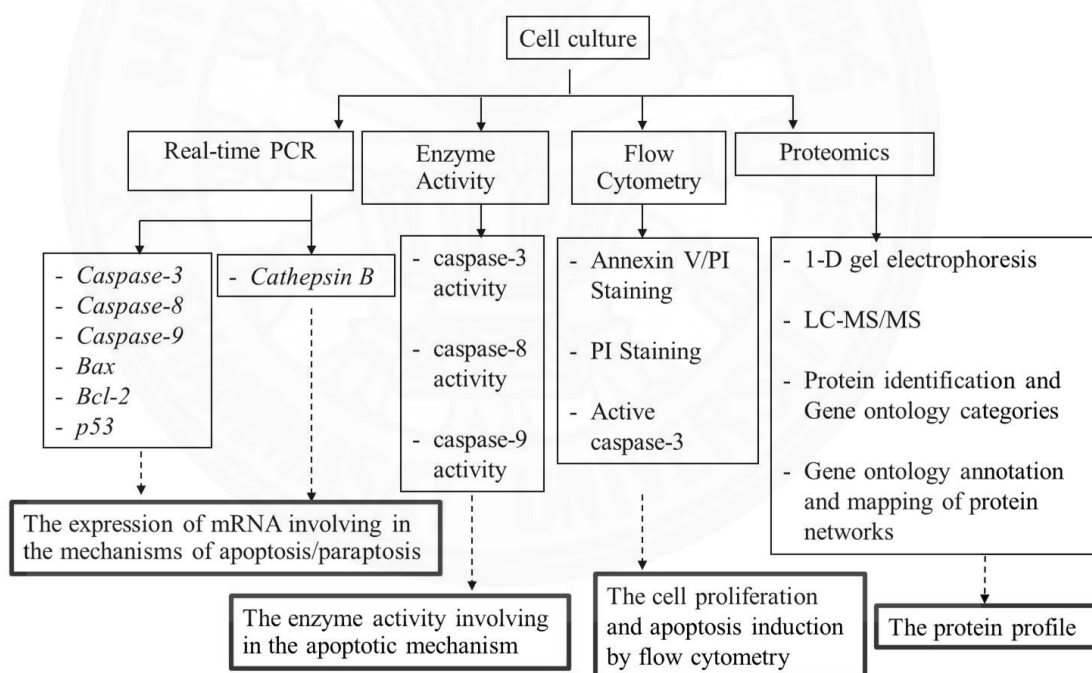


Figure 3.1 A conceptual framework of this study

3.1 Cell culture and cytotoxicity effect of Hep88 mAb

The HepG2 cells were cultured in RPMI 1640 with 10% fetal bovine serum (Biochrom AG, Berlin). It was maintained at 37°C in a CO₂ incubator and subculture every 3-4 days until use. The IC₅₀ concentration of Hep88 mAb against HepG2 cell line was determined by varying dose ranging from 0 to 200 mg/ml for three days incubation via the MTT colorimetric assay as previously described (Manochantr et al., 2011). The 50% growth-inhibitory effect or IC₅₀ concentration had been detected at 12.5 µg/ml for HepG2 cell line.

3.2 Real-time PCR

3.2.1 The apoptotic mechanism of Hep88 mAb treated-HepG2 cell

HepG2 cells (6×10^5 cells) were cultivated in 6-well culture plate with RPMI 1640 medium which is contain 10% fetal bovine serum, and incubated at 37°C in 5% CO₂ for 24 hours prior treatment. HepG2 cells were treated with IC₅₀ concentration of Hep88 mAb for 24, 48 and 72 hours. Whereas, the positive and negative control carried out in this study were a chemotherapeutic drug, IC₅₀ concentration (0.06 µg/ml) of doxorubicin-treated HepG2 cell, and untreated HepG2 cell, respectively.

3.2.2 The early mechanism of PCD in HepG2 cell after treated with Hep88 mAb

HepG2 cells (6×10^5 cells) were cultivated in 6-well culture plate with RPMI 1640 medium which is contain 10% fetal bovine serum, and incubated at 37°C in 5% CO₂ for 24 hours prior treatment. HepG2 cells were treated with IC₅₀ (12.5 µg/ml) and cytotoxic (62.5 µg/ml) concentration of Hep88 mAb for 3, 6, 9, 12, 18 and 24 hours. The untreated HepG2 cells were used as control.

3.2.3 Validating the amplified PCR product

3.2.3.1 Primer design

Primer design was performed by Primer3 program (http://frodo.wi.mit.edu/cgi-bin/primer3/primer3_www.cgi) after identifying the specific sequence from genome databases (GenBank®). The primers were designed in a low Guanine/Cytosine content (20-80 %) region. The amplified size would be in a range between 100 to 200 bp whereas; the melting temperature (T_m) for the primers was limited within 55-65°C.

3.2.3.2 PCR Amplification

Designed primers were used to amplified gene in the sample by 30 cycles of PCR method (denaturation: 95°C 30 seconds, annealing: 55°C, 60°C or 65°C 30 seconds and extension : 72°C 30 seconds). PCR products were run on 2% agarose gel to checking the PCR product size.

3.2.3.3 Gene cloning

PCR products of the expected predicted size were extracted from the gel by Geneaid Gel/PCR DNA Fragments Extraction Kit and ligated into pTZ57R/T vectors and transformed into E.coli DH5α competent cells by TAclone PCR cloning kit.

3.2.3.4 Screening of gene recombinant plasmid

Bacterial clones were placed on LB ampicillin agar plates and grown overnight at 37°C. A maximum of 10 colonies were picked from each plated transformation and were detected by colony PCR technique.

3.2.3.5 Plasmid extraction

The bacterial clone with interesting gene plasmid were cultivated in LB broth containing ampicillin overnight at 37°C, 200 rpm. The cells were pelleted by centrifugation at 8,000 rpm for 3 minutes before following the manufacturing's protocol from QIAprep® Spin Miniprep Kit (QIAGEN).

3.2.3.6 Sequence analysis

The plasmids were diluted as 100 ng/μl and analyzed by Macrogen Inc. (Korea) with the 96-capillary 3730xl DNA Analyzer (Applied Biosystems®). The sequence of gene recombinant plasmid was checked where the gene was by using reverse and forward primer sequence. The location of the primers show location of the gene that means the recombinant plasmid contains the gene. The nucleotide sequences of can be double check again by the nucleotide Basic Local Alignment Search Tool (BLAST) online database program (http://blast.ncbi.nlm.nih.gov/Blast.cgi?PROGRAM=blastn&PAGE_TYPE=BlastSearch&LINK_LOC=blasthome).

3.2.4 Generating standard curve of interesting gene

Copy Number was calculated from plasmid DNA concentration. The plasmid DNA was diluted to (Serial Dilution) 10⁹-10². Diluted plasmid was added into Real-time PCR Master mix. The gene expression was operated and analyzed by using Bio-rad iQ5 and Exicycler™96 Bioneer. The data reported as Ct value of each dilution, we use Ct value compared with copy number to generated standard curve.

3.2.4.1 Copy number calculation

Once the size of the plasmid that contains the gene of interest was estimated, the copy number could be calculated as shown in the equation (Whelan, Russell, & Whelan, 2003):

$$\text{DNA copy} = \frac{6.02 \times 10^{23} \text{ (copy/mol)} \times \text{DNA amount (g)}}{\text{DNA length (bp)} \times 660 \text{ (g/mol/bp)}}$$

3.2.5 Total RNA extraction

Total RNA was extracted from cell culture by using TRI REAGENT[®] Molecular research center, Inc. Cell lysate was transferred into new tube, vortexed thoroughly and incubated at room temperature for a few minutes before centrifuged 10,000 x g for 15 minutes. As a result, the supernatant was separated into 3 phases. The clear phase in the upper part was transferred into new tube and precipitated RNA with absolute isopropanol. The RNA pellet was washed with 70% Ethanol. Finally, the RNA pellet was re-suspended in DEPC water.

3.2.6 Reverse transcription

Total RNA was used as the template for first-strand complementary DNA (cDNA) synthesis. The reaction was started with denatured RNA and oligonucleotide primers (Oligo (dT) primers) at 70°C for 5 minutes, chilled on ice for 1 minute and added 10 µl of Prime RT Premix (2X). The reaction mixture was incubated at 42 °C for 60 minutes, then stopped the reaction by heating at 70°C for 10 minutes and chilled on ice. The cDNA concentration was measured an A260/A280 by NanoDrop 1000.

3.2.7 Quantitative real-time PCR analysis

The 2X Prime Q-Master Mix (with SYBR Green I) was used in the study of apoptosis mechanism after induction with Hep88 mAb for 24, 48 and 72 hours experiment. Real-time PCR was carried out in iCycler iQ[™] Real-Time PCR Detection System (Bio-Rad Laboratories, Inc.). All samples were run in duplicate in final reaction volume of 20 µl. The PCR parameters were 1 cycle of initial denaturation at 94°C for 10 minutes, 40 cycles of at 94°C, 60°C, 72°C for 30 seconds in each temperature. The primers used for PCR amplification of *capase-3,-8,-9* and *EF-2* are listed in the Table 3.1. The *EF-2* gene was used as control to normalize target gene expression.

The 2X KAPA SYBR[®] FAST qPCR Master Mix was used in the study of early mechanism of PCD in IC50 and cytotoxic dose of Hep88 mAb-treated cells experiment. The gene expression was operated and analyzed by using Exicycler[™]96 Bioneer. All samples were run in triplicate in final reaction volume of 10 μ l. The PCR parameters were 1 cycle of initial denaturation at 94°C for 10 minutes, 40 cycles of PCR reaction and hold for 30 seconds in each temperature. The primers used for PCR amplification of *Bax*, *Bcl-2*, *p53*, *cathepsin B*, *caspase-3*, *caspase-9* and *EF-2* are listed in the Table 3.2. The *EF-2* gene was used as control to normalize target gene expression.

The specificity of PCR products was confirmed by the single peak dissociation curves. Threshold cycle (Ct) value was compared with standard curve of each gene to report as copy number. The gene expression was calculated, used the copy number of interesting gene divided with housekeeping gene to normalize, then using the normalize value of treated sample divide with untreated sample. Finally, the results were reported as fold change of gene expression.

Table 3.1

Primer PCR for Real-time PCR

	Primers	sequence of nucleotides (nt)	size (nt)	Product size
<i>Caspase-3</i>	Forward	5'-TGT TTG TGT GCT TCT GAG CC-3'	20	210 bp
	Reverse	5'-CAC GCC ATG TCA TCATCA AC-3'	20	
<i>Caspase-8</i>	Forward	5'-GAT CAA GCC CCA CGA TGA C-3'	19	149 bp
	Reverse	5'-CCT GTC CAT CAG TGC CAT AG-3'	20	
<i>Caspase-9</i>	Forward	5'-CAT TTC ATG GTG GAG GTG AAG-3'	21	149 bp
	Reverse	5'-GGG AAC TGC AGG TGG CTG-3'	18	
<i>EF-2</i>	Forward	5'-CTG AAG CGG CTG GCT AAG TCT GA-3'	23	155 bp
	Reverse	5'-GGG TCA GAT TTC TTG ATG GGG ATG-3'	24	

Table 3.2**Primer PCR for Real-time PCR**

Primers		Sequence of Nucleotides (nt)	Size (nt)	PCR Product length
<i>Bax</i> (55°C)	Forward	5'-ATGTTTTCTGACGGCAACTTC-3'	21	133 bp
	Reverse	5'-AGTCCAATGTCCAGCCCAT-3'	19	
<i>Bcl-2</i> (65°C)	Forward	5'-ATGTGTGTGGAGACCGTCAA-3'	20	141 bp
	Reverse	5'-GCCGTACAGTTCACAAAGG-3'	20	
<i>p53</i> (60°C)	Forward	5'-ATGTTTTGCCAACTGGCCAAG-3'	21	153 bp
	Reverse	5'-TGAGCAGCGCTCATGGTG-3'	18	
<i>Cathepsin B</i> (55°C)	Forward	5'-CAGCGTCTCCAATAGCGA-3'	18	164 bp
	Reverse	5'-AGCCCAGGATGCGGAT-3'	16	
<i>EF-2</i> (60°C)	Forward	5'-CTGAAGCGGCTGGCTAAGTCTGA-3'	23	155 bp
	Reverse	5'-GGGTCAGATTTCTTGATGGGGATG-3'	24	
<i>Caspase-3</i> (60°C)	Forward	5'-TGTTTGTGTGCTTCTGAGCC-3'	20	210 bp
	Reverse	5'-CACGCCATGTCATCATCAAC-3'	20	
<i>Caspase-9</i> (65°C)	Forward	5'-CATTTCATGGTGGAGGTGAAG-3'	21	149 bp
	Reverse	5'-GGGAACTGCAGGTGGCTG-3'	18	

3.3 Enzyme Colorimetric assay

The caspase-3,-8 and -9 activities were assessed by using Caspase-3/ CPP32 Colorimetric assay kit, FLICE/Caspase-8 Colorimetric assay kit and Caspase-9 Colorimetric assay kit (BioVision) according to the manufacturer's instructions, with some modification.

3.3.1 Protein extraction

After treatment with IC50 concentration of Hep88 mAb for 24, 48 and 72 hours, HepG2 cell pellets were protein extracted by 50 μ l of ice cold cell lysis buffer, then incubated for 10 minutes on ice and brought them to sonicate for 10 times. The lysate was centrifuged at 13,800 rpm, 4°C for 20 minutes. The supernatants were cytoplasmic proteins which were transferred into the new tube. The protein concentration in each sample was determined by BCA™ Protein Assay Kit (Pierce, Rockford, IL). The protein concentration was adjusted to 100 μ g/50 μ l with cell lysis buffer.

3.3.2 Caspase-3/ CPP32 Colorimetric assay

Caspase-3 activity was determined by Caspase-3/ CPP32 Colorimetric assay kit. By following the manufacturer's protocols, 50 μ l of 2 μ g/ μ l protein of cell lysate was mixed with 50 μ l of 2X Reaction Buffer (containing 10 mM DTT) and 5 μ l of 4 mM DEVD-pNA substrate (200 μ M final concentration) in 96-well plate. After 37°C, 2 hour incubation, the samples were quantified using a microplate reader PowerWave™ XS Microplate Spectrophotometer (BioTek) at 405nm. The level of fold-increase in CPP32 activity was analyzed and compared with the level of the untreated control.

3.3.3 FLICE/Caspase-8 Colorimetric assay

Caspase-8 activity was determined by FLICE/Caspase-8 Colorimetric assay kit. By following the manufacturer's protocols, 50 μ l of 2 μ g/ μ l protein of cell lysate was mixed with 50 μ l of 2X Reaction Buffer (containing 10 mM DTT) and 5 μ l of 4 mM IETD-pNA substrate (200 μ M final concentration) in 96-well plate. After 37°C, 2 hour incubation, the samples were quantified using a microplate reader PowerWave™ XS Microplate Spectrophotometer (BioTek) at 405nm. The level of fold-increase in FLICE/Caspase-8 activity was analyzed and compared with the level of the untreated control.

3.3.4 Caspase-9 Colorimetric assay

Caspase-9 activity was determined by Caspase-9 Colorimetric assay kit. By following the manufacturer's protocols, 50 μ l of 2 μ g/ μ l protein of cell lysate was mixed with 50 μ l of 2X Reaction Buffer (containing 10 mM DTT) and 5 μ l of 4 mM LEHD -pNA substrate (200 μ M final concentration) in 96-well plate. After 37°C, 2 hour incubation, the samples were quantified using a microplate reader PowerWave™ XS Microplate Spectrophotometer (BioTek) at 405nm. The level of fold-increase in Caspase-9 activity was analyzed and compared with the level of the untreated control.

3.4 Flow cytometry

HepG2 cells were treated with cytotoxic dose of Hep88 mAb for 24, 48 and 72 hours to determine several hallmark of apoptosis such as phosphatidylserine exposure, DNA fragmentation and active caspase-3 formation by the following methods.

3.4.1 Detecting apoptosis

After treatment with Hep88 mAb, 1×10^6 cells/ml of HepG2 cells were washed twice in cold phosphate buffered saline (PBS) and then resuspended in binding buffer (0.02 μ m sterile filtered 0.01M Hepes (pH 7.4), 0.14M NaCl, and 2.5 mM CaCl_2 solution) in the FITC Annexin V Apoptosis Detection Kit I (BD Pharmingen™). Aliquots 100 μ l of this cell suspension were placed in 5 mL tubes with 5 μ l Annexin V/FITC and 10 μ l of 20 μ g/ml propidium iodide. They were mixed thoroughly and incubated at room temperature away from sunlight for 15 minutes. PBS (400 μ l) was then added. The suspension was analyzed with a fluorescence-activated cell sorter (FACS). The cell populations were calculated as the percentage by Cell Quest software (Becton Dickinson). Early apoptotic cells were positive-stained with annexin V and negative-stained with PI; however, Late apoptotic cells were positive-stained both annexin V and PI. The sum of early and late apoptotic cells population are divided with total population to calculate as the percentage of apoptotic cell.

3.4.2 Detecting cell cycle

The cells were washed twice in cold phosphate buffered saline (PBS) and fixed in 90% ethanol by drop the cell suspensions in vertexes ethanol. The fixed cell suspensions were placed at -20°C overnight then, centrifugation to pellet cell. The cell pellets were resuspended with PI/RNase Staining Buffer (BD Pharmingen™). They were mixed thoroughly and incubated at room temperature away from sunlight for 15 minutes. Finally, the suspension was analyzed with a fluorescence-activated cell sorter (FACS).

3.4.3 Active caspase-3

The cells were collected and washed twice in cold phosphate buffered saline (PBS). The cells were fixed with BD Cytotfix/Cytoperm™ solution in Caspase-3, Active Form, Apoptosis Kit (BD Pharmingen™) at a concentration of 1×10^6 cells/0.5 ml for 20 minutes on ice. The cells were pelleted by centrifugation, then washed twice with BD Perm/Wash™ at room temperature. After that, the cells were stained with antibody for 30 minutes at room temperature. The results of active caspase-3 were detected by flow cytometry.

3.5 Proteomics

HepG2 cells were treated with IC50 and cytotoxic dose of Hep88 mAb for 3, 6, 9, 12, 18 and 24 hours. The untreated HepG2 cells were used as control. Three group of treatment were used as the subject for proteomics analysis by a technique which combines SDS-PAGE and LC-MS/MS. This technique is called GeLC-MS/MS.

3.5.1 Total protein extraction

The cell pellets of Hep88 mAb treated HepG2 cells in various concentrations and times were extracted by 0.5% SDS (1:1). The protein concentrations were determined by the Lowry method.

3.5.2 Protein concentration determination by Lowry method

The sample protein concentrations were estimated by using the standard curve of bovine serum albumin (BSA). The cell lysate of sample was mixed with 200 μ l of alkaline copper solution (freshly prepared by mixing solution A and solution B as shown in Appendix A) and then incubated for 30 minutes at room temperature. After incubation, 50 μ l of Folin-Ciocalteu phenol reagent was added and well mixed into the reaction. The reaction mixture was incubated at room temperature for 30 minutes before the absorbance (A_{690}) was measured by using a microplate reader.

3.5.3 Denaturing gel electrophoresis (SDS-PAGE)

SDS-PAGE was performed on 12.5% polyacrylamide gels. The total proteins were mixed with 1/5 volume of sample loading buffer and heated at 95°C for 5 minutes before loading to gel. The reservoir of electrophoresis was filled with electrophoresis buffer (0.025M Tris, 0.192M Glycine, 0.1% SDS). The proteins are separated by applying a current of 20mA/gel for approximately 70 minutes or until tracking dye has reached the bottom of the gel. The proteins bands were visualized by silver staining.

3.5.4 Silver staining

After the electrophoresis, the polyacrylamide gels were fixed in the fixing solution (50% methanol, 10% acetic acid and 50µl/100 ml of 37% formaldehyde) and agitated for 30 minutes. The fixing gel was washed with 35% ethanol 2 times for 5 minutes each and sensitized in 0.02% sodium thiosulfate for 2 minutes. After the sensitizing, the gel was washed with distilled water twice for 5 minutes each. The gel was stained by using 0.2% silver nitrate for 20 minutes, then rinsed with distilled water before being developed by adding developing reagent (6% sodium carbonate, 0.02% sodium thiosulfate and 50 µl/100 ml 37% formaldehyde) to gel and shaking until protein bands were visualized in the gel. When visualized completely development, the reaction was stopped by adding stopping solution (1.46% sodium EDTA) for 20 minutes. The gel was kept in 0.1% acetic acid at room temperature until use.

3.5.5 In-gel digestion

The protein bands were excised into sections. Each band was cut into small pieces approximate 1 mm²/piece. Each band was subjected to in-gel digestion using an in house method developed by Proteomics Research Laboratory, Genome Institute, National Centre for Genetic Engineering and Biotechnology (BIOTEC), National Science and Technology Development Agency (NSTDA), Thailand. The gel pieces were transferred to low binding 96 well plates, washed with distilled water and destained using 5% hydrogen peroxide (H₂O₂) until clear, then washed with distilled water 3 times before dehydration. The gel pieces were dehydrated with 100% acetonitrile (ACN) for 5 minutes and disulfide bond were reduced by adding

10mM dithiothreitol (DTT) in ammonium bicarbonate, and then incubated at 56 °C for an hour. After that 100mM iodoacetamide (IAA) in 10mM ammonium bicarbonate was added and incubated room temperature in the dark for an hour to let protein alkylation. Next, the gel pieces were dehydrated again twice times with 100%acetonitrile (ACN) for 5 minutes each. The gel pieces were available continued with in-gel trypsin digestion step. The in-gel proteins were trypsin digested to short-peptides by stand the reaction at room temperature for 20 minutes, before incubate at 37°C for 3 hours. The peptides were collected from the solutions, then transferred to a new plate. The extraction of remaining peptides in gel pieces were repeated by the addition of 50% ACN in 0.1% formic acid (FA). The peptides solution was then incubated at 40°C until dry. The peptides samples were kept at -80°C until analysis by LC-MS/MS. When analyzing, the peptides were resuspended with 0.1% formic acid. The peptides solutions were transferred into the vial for injection to ESI-QUAD-TOF mass spectrometer.

3.5.6 Nano LC-MS/MS analysis

The proteins that digest from gel electrophoresis were separated in Nanoscale LC-MS for Synapt HDMS system, NanoAcquity system (Waters Corp., Milford, MA) couple to a Symmetry C18 5 µm, 180-µm x Trap column and a BEH130 C18 1.7 µm, 100-µm x 100-mm analytical reverse phase column (Waters Corp., Milford, MA). The samples were transferred with an aqueous 0.1% formic acid solution, loaded by using an autosampler and separated on trap column at a flow rate of 15 µl/min following separation at a flow rate of 1 µl/min. The mobile phase A was 0.1% formic acid in water and mobile phase B was 0.1% formic acid in acetonitrile. The peptides mixture were separated with 15-50% a mobile phase B gradient solution over 15 minutes at flow rate of 600 nl/min followed by a 3-minute rinse with 80% of mobile phase B. The flow-through peptides were sprayed and then detected in ESI-QUAD-TOF mass spectrometer. The [Glu¹]-Fibrinopeptide B was used as the reference sprayer of mass spectrometry, which was adjusted the flow rate to 500 nl/min to maintain a constant concentration at 200 fmol/µl. The tryptic peptides samples were analyzed using a SYNAPT™ HDMS mass spectrometer (Waters Corp., Manchester, UK). The time-of-flight analyzer of the mass spectrometer was also calibrated and corrected using the monoisotopic mass of [Glu¹]-Fibrinopeptide B. The quadrupole mass analyzer was

adjusted that ions for efficiently transmitted on the MS/MS detection. The peptides mixture were completely operated within 40 minutes to detect the peptide.

3.5.7 Protein identification and Gene ontology categories

DeCyder MS Differential Analysis software (GE Healthcare) used to qualify the differentially expressed peptide in all samples. The LC-MS raw data was converted to mzXML file by CompressXport software. All peptides were detected with the software in PepDetect module. The isotropic peaks was determined to assign the charge states of peptide. The MS signal intensities of LC-MS data were used to determine the compatible of consecutive charge states and quantification. The data from PepDetect module was transferred to be a subject in PepMatch module. This module was used to matching peptides across different signal intensity maps. Finally, the PepMatch module reported the quantitative comparison data (MS/MS data). The MS/MS data from DeCyder MS software was submitted to search in human database. While, the Mascot software (Matrix Science) was used to identify the data.

The data was searched with Human database for protein identification. Database inquiry was specified as the following: enzyme - trypsin, fixed modification - carbamidomethyl (C), variable modification - oxidation (M), mass values - Monoisotopic, protein mass - unrestricted, peptide mass tolerance - ± 1.2 Da, fragment mass tolerance - ± 0.6 Da, max missed cleavages - 3, instrument type - ESI-QUAD-TOF and the number of inquiries - 53. Therefore the mascot DAT files were merged and evaluated the peptide level on DeCyder MS software and the data was export to Microsoft Excel.

3.5.8 Gene ontology annotation and mapping of protein networks

The proteins information were obtained from the online database especially, Uniprot Knowledgebase database. It was used to perform gene ontology annotation. All of the gene ontology information contain 3 terms including biological process, cellular component and molecular function. The Search Tool for Retrieval of Interacting Genes (STRING) was using to search interaction of each proteins by Uniprot IDs. The search helps more understanding of cellular functions and annotate all functional interactions among protein in cell.

3.5.9 Quantification of the changes in protein analysis

The MultiExperiment Viewer software (Mev) was used to analyse the changes in the protein between group of treatment and control.

CHAPTER 4

RESULTS AND DISCUSSIONS

From preliminary report, it has been shown that IC₅₀ dose of Hep88 mAb induced HepG2 cell death through paraptosis morphology (Manochantr et al., 2011). In this study, the gene-expression at mRNA level of *caspase-3*, *caspase-8* and *caspase-9* after IC₅₀ dose of Hep88 mAb treatment were considered to compare with anti-cancer drug doxorubicin treatment by real-time PCR. The enzyme activities of caspase-3, caspase-8 and caspase-9 were also determined to compare with anti-cancer drug doxorubicin treatment by enzyme colorimetric assay. Furthermore, the apoptotic PCD morphology of cytotoxic dose of Hep88 mAb-treated HepG2 cells were monitored by flow cytometry. The differences of PCD molecular mechanism between IC₅₀ and cytotoxic dose of Hep88 mAb treated-HepG2 cells were investigated in both mRNA and protein level by real-time PCR and GeLC-MS/MS.

4.1 The expression of mRNA involving the mechanism of apoptosis and paraptosis

Real-time PCR technique was performed to analyze the expression of genes involving paraptosis and apoptosis. Each gene was validated to accurately calculate the expression by the standard curve. Plasmids were constructed as the standard template for copy-number determination. The apoptotic mechanisms and the early mechanisms of PCD in HepG2 cell after Hep88 mAb treatment were performed by this technique.

4.1.1 Plasmids construction and copy-number determination

In this study, the interesting genes were ligated into bacterial plasmid to use as an effective and accurate standard template for real-time PCR. To calculate a molecular weight of plasmid, the length of plasmid (bp) was multiplied by the average weight of a double-stranded base pair (660 g/mol/bp). The copy number was calculated from the concentration of plasmid (g), the Avogadro constant (6.02×10^{23} copy/mol) and the molecular weight (g/mol). The cloned plasmids were

quantified and calculated as the copy number. The standard curve of each gene was generated by serial dilution of plasmid. The standard curve of genes were linear in the range tested for $R^2=0.999$ (*caspase-3*), $R^2=0.997$ (*caspase-8*), $R^2=0.995$ (*caspase-9*) and $R^2=0.994$ (*EF-2*) as shown in Figure 4.1. The standard curves of *Bax*, *Bcl-2*, *p53*, *cathepsin B (CTSB)*, *caspase-3*, *caspase-9* and *EF-2* gene were next set up as shown in Figure 4.2. Linear plot was shown in the range tested for $R^2 = 0.995$ (*Bax*), $R^2 = 0.997$ (*Bcl-2*), $R^2 = 0.991$ (*p53*) $R^2 = 0.999$ (*cathepsin-B*), $R^2 = 0.992$ (*caspase-3*), $R^2 = 0.996$ (*caspase-9*), and $R^2 = 0.997$ (*EF-2*).

These results showed that the regression analysis is extremely closed in linearity (Figure 4.1 and 4.2). These goodness-of-fit statistical results guaranteed that our real-time PCR results were of sufficient reproducibility to quantify those parameters of the genes expression following incubation with Hep88 mAb as formerly discussed by Pfaffl M.W.& Hageleit M. (Pfaffl & Hageleit, 2001).

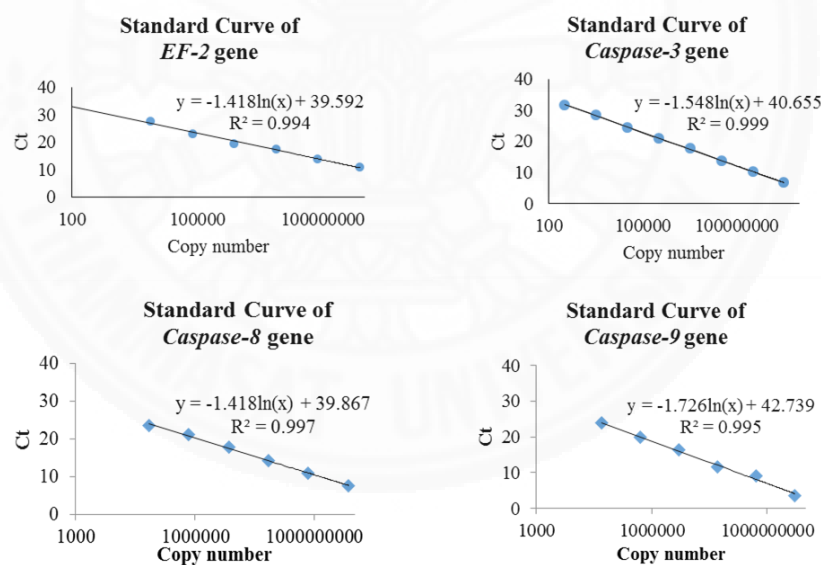


Figure 4.1 Standard curve for *caspase-3*, *-8*, *-9* and *EF-2* gene. The copy number of plasmid DNA template ranges from 10^9 - 10^2 copies. The standard curve of genes were linear in the range tested for $R^2 = 0.999$ (*caspase-3*), $R^2 = 0.997$ (*caspase-8*), $R^2 = 0.995$ (*caspase-9*) and $R^2 = 0.994$ (*EF-2*).

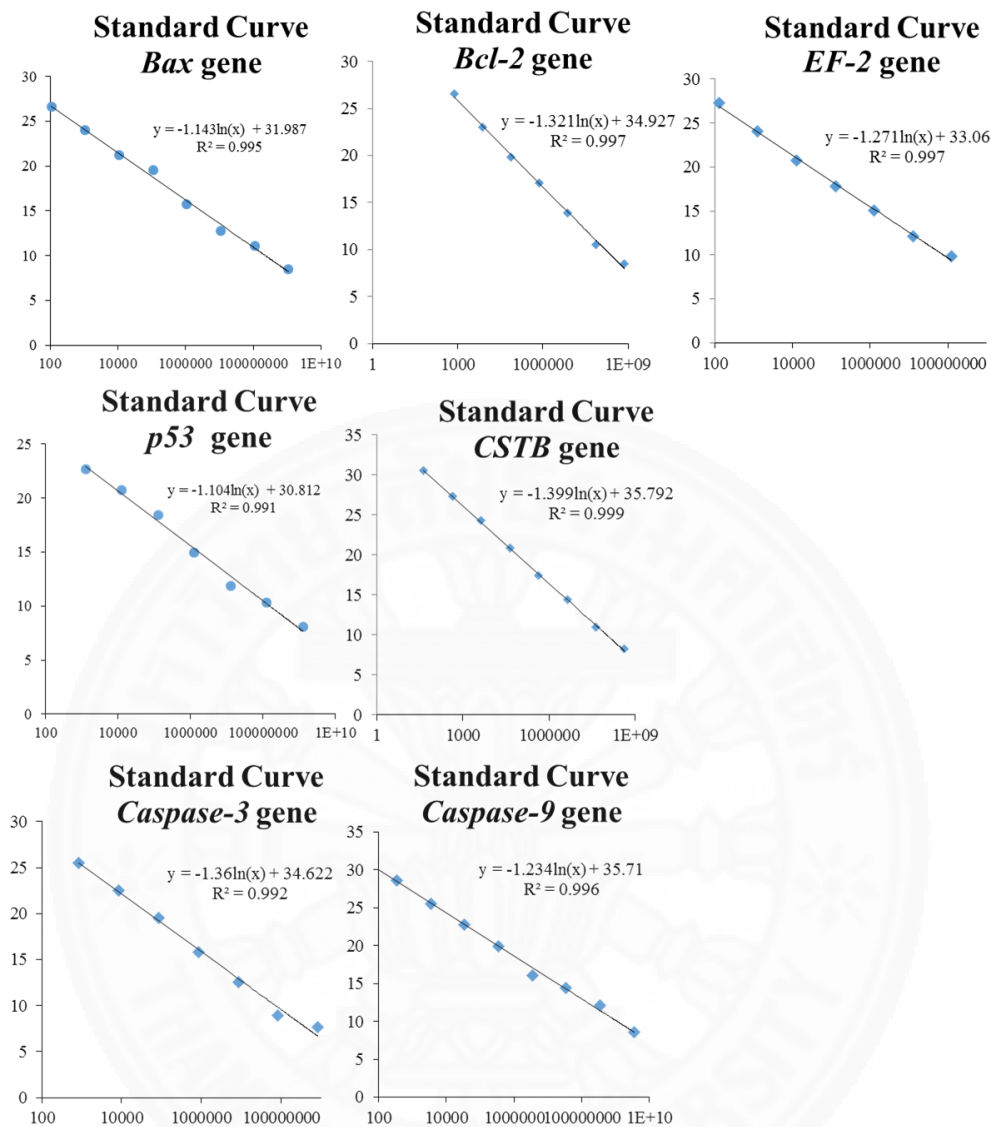


Figure 4.2 Standard curve for *Bax*, *Bcl-2*, *p53*, *cathepsin B (CTSB)*, *caspase-3*, *caspase-9* and *EF-2* gene. The copy number of plasmid DNA template ranges from 10^9 - 10^2 copies. The standard curve of genes were linear in the range tested for for $R^2 = 0.995$ (*Bax*), $R^2 = 0.997$ (*Bcl-2*), $R^2 = 0.991$ (*p53*) $R^2 = 0.999$ (*cathepsin B*), $R^2 = 0.992$ (*caspase-3*), $R^2 = 0.996$ (*caspase-9*), and $R^2 = 0.997$ (*EF-2*).

4.1.2 The mRNA expression of *caspase-3*, *caspase-8* and *caspase-9* at 24, 48 and 72 hours

The expression of the genes in the apoptotic mechanism was quantitated by real-time PCR. Real-time PCR results show statistically significant differences in mRNA expression of *caspase-3*, *caspase-8* and *caspase-9* ($p < 0.05$) in Hep88-treated HepG2 (Figure 4.3). The mRNA expression of *caspase-3*, *caspase-8* and *caspase-9* was higher than in the control group after incubation for 24 hours (*caspase-3*: fold change = 34.08 ± 29.01 ; *caspase-8*: fold change: 43.90 ± 40.48 ; $p < 0.05$, *caspase-9*: fold change = 20.65 ± 1.41 ; $p < 0.001$; Figure 4.3). In addition, after incubation for 48 hours, the *caspase-3* and *caspase-8* expression in Hep88-treated HepG2 was significantly lower than in the control group (*caspase-3*: 0.15 ± 0.14 ; $p < 0.01$, *caspase-8*: 0.32 ± 0.11 ; $p < 0.01$; Figure 4.3). In the HepG2 that had been treated with doxorubicin for 48 and 72 hours, results show statistically significant differences in expression of *caspase-3* and *caspase-9* ($p < 0.05$). By contrast, there were no statistically significant differences in HepG2 treated with doxorubicin for 24 hours in the mRNA expression of *caspase-3*, *caspase-8* and *caspase-9* when compared with control ($p > 0.05$).

The quantitative real-time PCR results confirmed the powerful potency of Hep88 mAb in the induction of HCC cell death by up-regulation of *caspase-3*, -8 and -9 genes expression after 24 hours of incubation when compared with untreated cells. These outcomes were consistent with findings from other researchers (Del Puerto et al., 2010; R. K. Gupta, Banerjee, Pathak, Sharma, & Singh, 2013; Selim & Hendi, 2012), which reported the apoptotic induction pathway significantly increased the presence of *caspase-3*, -8 and -9 mRNA expressions. Interestingly, when compared with the chemotherapeutic drug doxorubicin, an early and remarkably apoptotic induction was outstandingly demonstrated. From these results, it has been confirmed that Hep88 mAb induced the up-regulation of the caspase cascade mechanism after 24 hours of incubation. Meanwhile, doxorubicin induced an up-regulation of those three *caspases* in a time-dependent manner, i.e. from a slightly advanced stage of induction to a completely advanced stage of induction, from 24 hours to 72 hours as shown in Figure 4.3. From a comparison of those up-

regulated fold changes of Hep88 mAb with doxorubicin, it was shown that Hep88 mAb more strongly activated *caspase-3* and *-9* expressions than did doxorubicin ($p < 0.05$). This result demonstrates its effectiveness over the common chemotherapeutic drugs that have been used in cancer therapy up to the present time.

The apoptotic mechanism induced by Hep88 mAb might be started either upon binding with its receptor or just after cellular internalization. Its effect is possible on both an extrinsic and intrinsic pathway. As regards the extrinsically proposed mechanism, it induced the activation of initiator caspase-8, which is the key substance of HCC-inducing apoptosis as reported by Cho *et al.* (Cho *et al.*, 2010). It is subsequently the initiator of the caspase cascade reaction and also activates the effect of the caspase-3. Alternatively, an intrinsic pathway is normally explained scientifically by a mitochondria-mediated mechanism. This process results in the releasing of cytochrome c, which thus stimulates the assembly of procaspase-9 with Apaf-1 and cytochrome c itself to become an apoptosome. It then activates caspase-9, which then ultimately initiates caspase-3 activation (R. K. Gupta *et al.*, 2013; S. Gupta, Kass, Szegezdi, & Joseph, 2009).

4.1.3 The pathway determination through *Bax*, *Bcl-2*, *p53*, *cathepsin B*, *caspase-9* and *caspase-3* mRNA expression at 3, 6, 9, 12, 18 and 24 hours.

4.1.3.1 The mRNA expression of *Bax*, *Bcl-2*, *p53*, *cathepsin B*, *caspase-9* and *caspase-3*

Statistically significant differences in fold change of the early apoptotic genes in the apoptotic mechanism. The mRNA expression levels of *Bax*, *Bcl-2*, *p53*, *cathepsin B*, *caspase-3* and *caspase-9* in Hep88 mAb-treated HepG2 cell comparing with the untreated cells by real-time PCR is shown ($p < 0.05$) (Figure 4.4, 4.5, 4.6, 4.7 and 4.8).

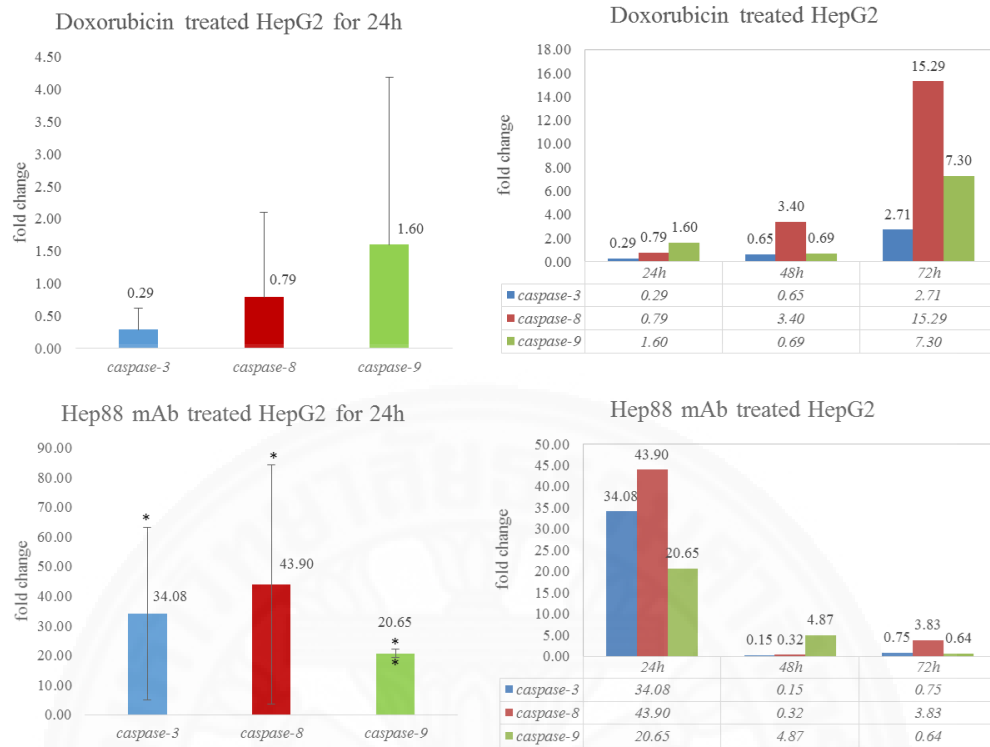


Figure 4.3 Effects on caspase expression of doxorubicin and Hep88 monoclonal antibody-treated HepG2 cells. The charts show fold change of *caspase-3*, *-8*, *-9* gene expression in doxorubicin-treated HepG2 mRNA (upper) and Hep88-treated HepG2 mRNA (lower) after incubation for 24, 48 and 72 hours. The doxorubicin-treated HepG2 of *caspase-3*, *-8* and *-9* mRNA expressions were gradually increased from 24 to 72 hours. Meanwhile, the Hep88 treated HepG2 of *caspase-3*, *-8* and *-9* mRNA expressions were significantly increased during the first 24 hours; after that it was then decreased. Effects on caspases expression of Hep88 monoclonal antibody-treated HepG2 cells were determined using Real-time PCR methods. Data are expressed as fold change, and are means \pm SD ($n \geq 3$). * $p < 0.05$ vs. control, ** $p < 0.001$ vs control.

(1) IC50 dose of Hep88 mAb treatment

Figure 4.4 represented the mRNA expression of *p53*, *Bax*, *caspase-9* gene after 12, 18 and 24 hours of incubation that were regulated in the same direction. While, the *cathepsin B* expression after 12, 18 and 24 hours of incubation was significantly down-regulated. Noticeably, after 18 hours of incubation, the expression of anti-apoptotic *Bcl-2* was started to down-regulate. When considering at the earlier time point (3, 6 and 9 hours) in Figure 4.5, the *cathepsin B* was prominent over-expressed after 3 hours of incubation. Meanwhile, the *caspase-9* and *caspase-3* expression were up-regulated at the same time. When focus at 9 hours of incubation, the expression of *p53*, *Bax* and *caspase-3* was slightly increased. Unfortunately, over-expressed *Bcl-2* had turned over. Therefore, the HepG2 cells were inhibited to undergo to apoptosis cell death, even though the up-regulated apoptotic genes expression were found.

After 12 hours of incubation with IC50 dose of Hep88 mAb, it was demonstrated the significant increase of *Bcl-2* expression and *Bcl-2/Bax* expression ratio (Figure 4.4 and 4.6). The *Bcl-2* expression graph showed highly anti-apoptotic event at 12 hours of treatment before significance decrease (Figure 4.4). A ratio of *Bcl-2/Bax* was used to determine the survival or death of cells following an apoptotic stimulus, which will be indicated apoptosis induction when lower than one (Y. Q. Liu et al., 2014; Pan, Wang, Huang, Luo, & Ling, 2014).

These results imply that IC50 dose of Hep88 mAb can induce apoptosis cell death in HepG2 cell, but at the same time it tries to avoid this process by triggered anti-apoptotic gene expression. On the other way, the overexpression of cathepsins have been demonstrated in many cancers (Gondi & Rao, 2013). The cathepsins are involved either directed or indirect cell death. Cathepsin B involves either in the progression of cancer cells, or cell proliferation and apoptosis induction in HCC (Xu et al., 2014). Previously, Foghsgaard *et al.* reported a role of cathepsins in the execution of caspase-independent cell death, which results in a paraptosis-like morphology (Foghsgaard et al., 2001). This is well correlated with our results that after earliest Hep88 mAb treatment, the rapid up-regulated of *Cathepsin B* (*CTSB*) is strongly expressed at 3 hours incubation.

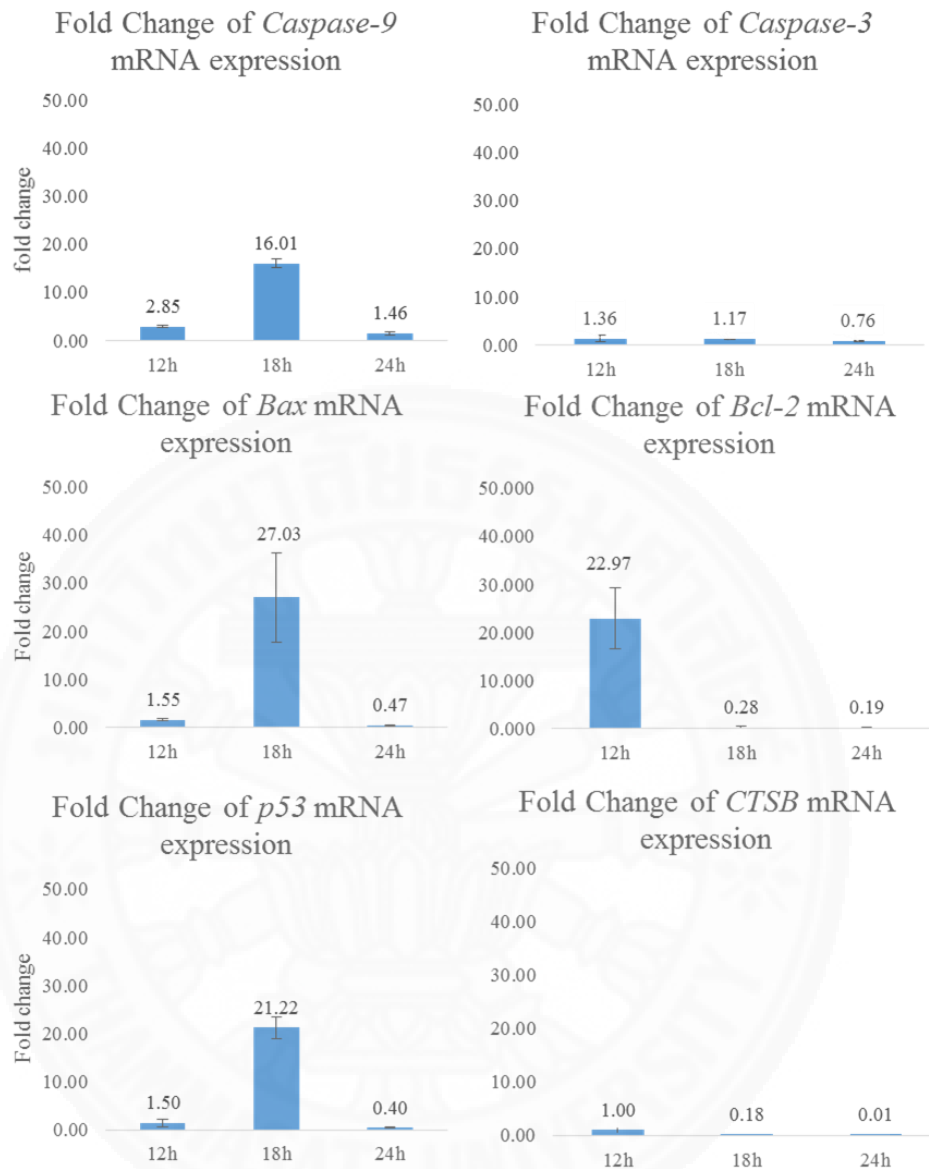


Figure 4.4 Real-time PCR analysis for *Bax*, *Bcl-2*, *p53*, *cathepsin B*, *caspase-3* and *caspase-9* expression in IC₅₀ dose of Hep88 mAb treatment at 12, 18 and 24 hours. The *caspase-9*, *Bax* and *p53* expression at 18 hours after treatment were displayed in the same direction. However, *caspase-3* expression on IC₅₀ dose of Hep88 mAb showed slightly difference in each time point. Overexpressed *Bcl-2* was shown that it was decreased after IC₅₀ dose of treatment for 18 and 24 hours.

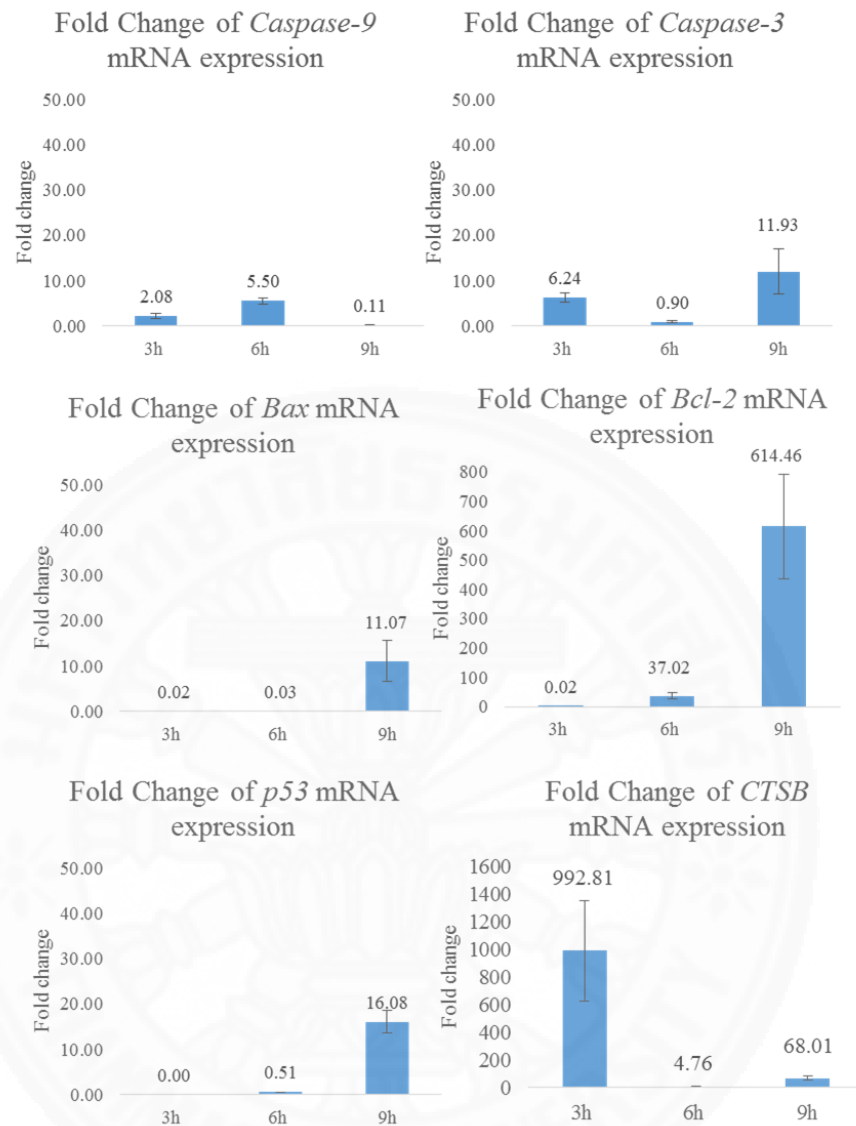


Figure 4.5 Real-time PCR analysis for *Bax*, *Bcl-2*, *p53*, *cathepsin B*, *caspase-3* and *caspase-9* expression in IC50 dose of Hep88 mAb treatment at 3, 6 and 9 hours. *Cathepsin B* was shown highly expression since 3 hours and then significantly decrease when prolong incubation. The up-regulation of *caspase-9* and *caspase-3* expression were represented after 3 hours treatment. At 9 hours of IC50 dose treatment was demonstrated that overexpressed *Bcl-2*. The *p53*, *Bax* and *caspase-3* expression were slightly increased then up-regulated at 9 hours of incubation in the same trend.

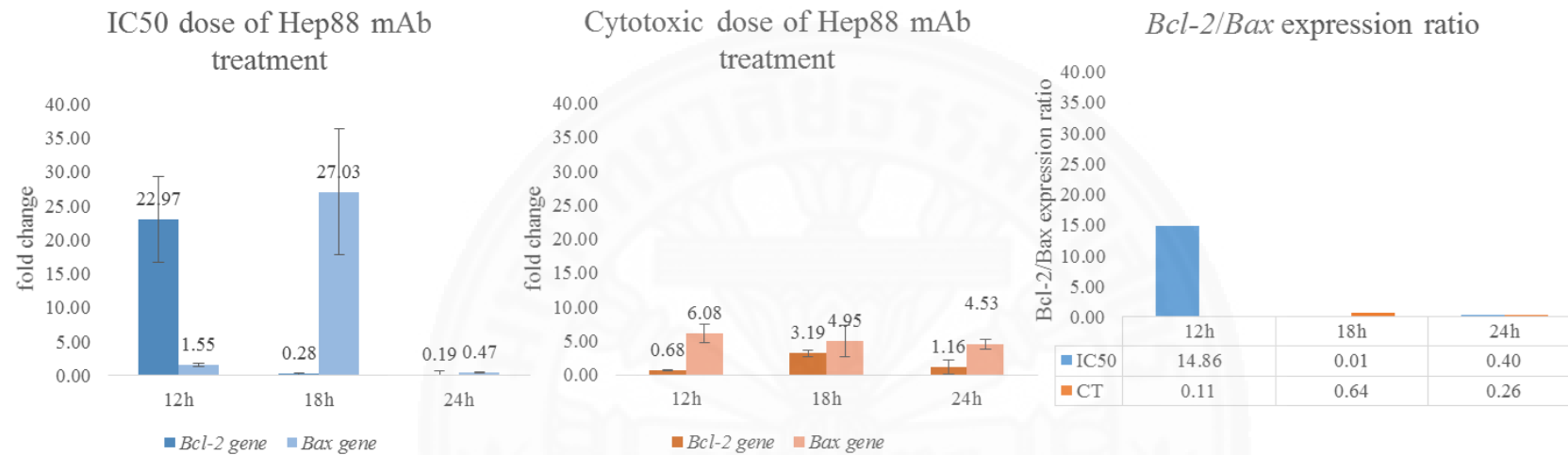


Figure 4.6 Real-time PCR analysis for *Bcl-2* expression, *Bax* expression and the ratio of *Bcl-2/Bax* in IC50 dose and cytotoxic dose of Hep88 mAb treatment at 12, 18 and 24 hours. The graphs show highly anti-apoptotic event in IC50 dose of Hep88 mAb induced-HepG2 cell at 12 hours of treatment. After prolong incubation, the anti-apoptotic *Bcl-2* expression is significantly decreased. The *Bcl-2/Bax* expression ratio shows a value lower than 1. It can be indicated that apoptosis induction is caused through *Bax* activities. In addition, the bar chart of cytotoxic dose treatment represents the expression of *Bax*, which is higher than *Bcl-2*. These results strongly supported the apoptosis induction of Hep88 mAb through an up-regulation of *Bax* together with a down-regulation of *Bcl-2*.

Table 4.1

The fold change of the expression of early apoptotic mechanism involving genes after IC50 dose of Hep88 mAb treatment.

gene	fold change of gene expression					
	3h	6h	9h	12h	18h	24h
<i>CTSB</i>	992.81±365.38	4.76±5.51	68.01±14.74	1.00±0.33	0.18±0.03	0.01±0.00
<i>Bax</i>	0.02±0.00	0.03±0.00	11.07±4.56	1.55±0.24	27.03±9.24	0.47±0.10
<i>p53</i>	0.00±0.00	0.51±0.05	16.08±2.53	1.50±0.79	21.22±2.20	0.40±0.10
<i>Bcl-2</i>	0.02±0.00	37.02±10.96	614.46±178.32	22.97±6.29	0.28±0.16	0.19±0.09
<i>caspase-3</i>	6.24±1.04	0.90±0.30	11.93±5.01	1.36±0.58	1.17±0.08	0.76±0.15
<i>caspase-9</i>	2.08±0.59	5.50±0.65	0.11±0.03	2.85±0.21	16.01±0.85	1.46±0.39

Table 4.2

The fold change of the expression of early apoptotic mechanism involving genes after cytotoxic dose of Hep88 mAb treatment.

gene	fold change of gene expression					
	3h	6h	9h	12h	18h	24h
<i>CTSB</i>	247.92±62.55	2.32±1.35	66.67±11.60	0.70±0.12	196.80±47.15	0.08±0.04
<i>Bax</i>	0.28±0.03	0.04±0.00	22.88±2.67	6.08±1.38	4.95±2.33	4.53±0.70
<i>p53</i>	0.00±0.00	1.92±1.03	25.86±4.04	7.53±3.44	0.07±0.03	39.70±7.90
<i>Bcl-2</i>	0.00±0.00	9.56±5.94	23.78±13.96	0.68±0.11	3.19±0.51	1.16±1.02
<i>caspase-3</i>	6.19±1.58	0.94±0.18	29.85±11.14	1.78±0.99	2.81±0.85	10.68±4.67
<i>caspase-9</i>	5.62±3.74	3.08±1.32	1.06±0.15	5.91±1.00	1.75±0.36	3.67±1.37

(2) Cytotoxic dose of Hep88 mAb treatment

Figure 4.6 represents up-regulation of pro-apoptotic protein, *Bax*, over anti-apoptotic one, *Bcl-2*, in any time of treatment. Interestingly, *Bcl-2/Bax*

expression ratio decreased lower than one. This was strongly supported the apoptotic induction of Hep88 mAb through up-regulation of *Bax* expression while down-regulation of *Bcl-2* expression.

In addition, it has been demonstrated that the *Bax* and *caspase-9* expression were consistent with the *p53* expression along 12, 18 and 24 hours of treatment (Figure 4.7). It shows up- and down- and up- significantly regulation response from the start till the last of treatment (12, 18 and 24 hours of incubation times). On the other hand, the flipped response was found at the *Bcl-2* expression (Table 4.2, Figure 4.7).

To monitor the response of *p53*, *Bax* and *caspase-9* expression at the earlier time of treatment, we also conducted the real-time PCR at 3, 6 and 9 hours of treatment. The results of *p53* expression show gradually increased (Table 4.2, Figure 4.8). It was related to *Bax* expression (Table 4.2, Figure 4.8). While, the *caspase-9* expression at the earlier time of treatment wasn't correlated to *Bax* and *p53* expression. Perhaps Hep88 mAb firstly induced HepG2 cell through the extrinsic pathway. Caspase-8 might be activated by DISC. Active caspase-8 initiated the cascade downstream reaction. Bid was truncated and directly let the releasing of cytochrome c to induce caspase-9 (Chipuk & Green, 2008). Hence, the *caspase-9* expression was up-regulated since 3 hours of treatment.

However, when focused on *caspase-3* expression (Figure 4.7) after 12, 18 and 24 hours of incubation, it is likely to its strongest increase after a prolonged incubation time of treatment, which correspond to flow cytometry results.

Additionally, for the protein involving in paraptosis morphology i.e. *cathepsin B* (*CTSB*), it's strongly expression (Figure 4.7). *Cathepsin B* mRNA expression is up-regulated after 18 hours of treatment but lower to lowest expression is detected either at an early (12 hours) or late treatment (24 hours). This triggered us to reveal what the response would be detected at the earlier point. The data on Figure 4.8 shows the strongest up-regulation of *CTSB* expression at the earliest hours

(3 hours) of treatment. It's possible that, HepG2 cell suddenly up-regulated *cathepsin B* expression from the external induction.

Cathepsin B might be contributed to loss of mitochondria membrane potential and releasing of cytochrome c (Guicciardi et al., 2000). And afterwards, intrinsic apoptotic pathway was initiated by the up-regulation of capase-9 and caspase-3 which is correlated well with the previously reports (Joy et al., 2010; Morchang et al., 2013). Nevertheless, the death induction was further stimulated after Hep88 mAb binding to its specific antigen (Ag) which might be corresponding with death receptor at the cell membrane. The extrinsic apoptotic pathway was subsequently induced (Guicciardi et al., 2000).

However, cathepsin B wasn't completely released because LMP was suppressed by Hsp70 mortalin-Bax and Hsp70 mortalin-p53 binding complexes (Stankiewicz, Lachapelle, Foo, Radicioni, & Mosser, 2005; Taurin et al., 2002; Wadhwa et al., 2006; X.-M. Yuan et al., 2002). Taurin and co-workers found the p53 expression in mortalin-transfected cells was delayed to response death induction (Taurin et al., 2002). Moreover, Stankiewicz et al. also found Hsp70 blocks heat-induced apoptosis by inhibiting Bax activation (Stankiewicz et al., 2005). For this reason, Hep88 mAb-treated HepG2 cells for 3 hours wasn't shown the *p53* and *Bax* up-regulation. Anywise, after prolong the incubation time, Hep88 mAb might be fully internalized into the HepG2 cell as it was widely reported (Jedema et al., 2004; Kovtun & Goldmacher, 2007; Walter, Raden, Kamikura, Cooper, & Bernstein, 2005). It was then binding to Hsp70 mortalin to restore p53-function. Thereby, *p53* was beginning up-regulated. Similarly to Walker and colleagues have been reported, the molecule specific to mortalin was also induced p53 by stealing it from the p53–mortalin complex (Walker, Bottger, & Low, 2006).

Notwithstanding, the cancer cell attempts to combat and escape from the death induction of Hep88 mAb-treatment by up-regulated *Bcl-2* expression. As a results, MOMP and LMP were suppressed to release cytochrome c and cathepsin B. This probably means, cancer cell have adapted to avoid harm. Related to many reports demonstrated that an overexpression of *Bcl-2* has been found associated with apoptotic resistance to anti-cancer treatment (Douarre et al., 2005; Sartorius & Krammer, 2002). The cell after treatment shown the balance between anti-apoptosis and apoptosis which it was occurred like a seesaw board. Whenever this balance is lost, the cell decide to specify their way to living or dead.

Therefore, the excess of death induction in this study lead to HepG2 death via stimulate both cathepsin B and mitochondria mediated-caspase that can lead to paraptosis and apoptosis respectively. It is well correlate with our previous report that the fastest mechanism, the predominant death morphology verification. All of the results from this study confirm the cytotoxic mechanism of Hep88 mAb that it triggered HCC to be death via the paraptosis till apoptosis.

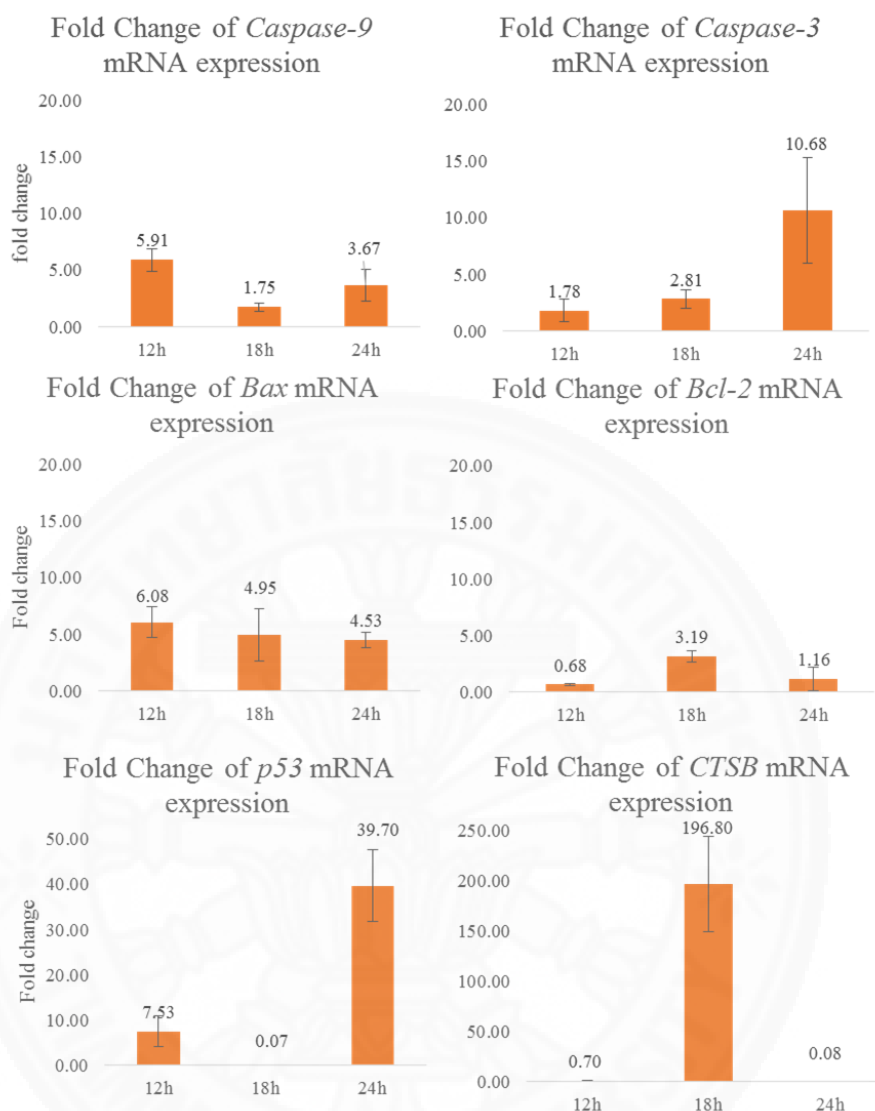


Figure 4.7 Real-time PCR analysis for *Bax*, *Bcl-2*, *p53*, *cathepsin B*, *caspase-3* and *caspase-9* expression in cytotoxic dose of Hep88 mAb treatment at 12, 18 and 24 hours. The *Bax* and *caspase-9* expressions were consistent with the *p53* expression during the period of treatment. *Bcl-2* expression increased at 18 hr of treatment, while it varied in an opposite way with the *p53*, *Bax* and *caspase-9* expression. Similarly, the *cathepsin B* expression revealed the up-regulation after 18 hr of treatment, while the *caspase-3* expression is likely to increase after prolonged incubation time of the treatment.

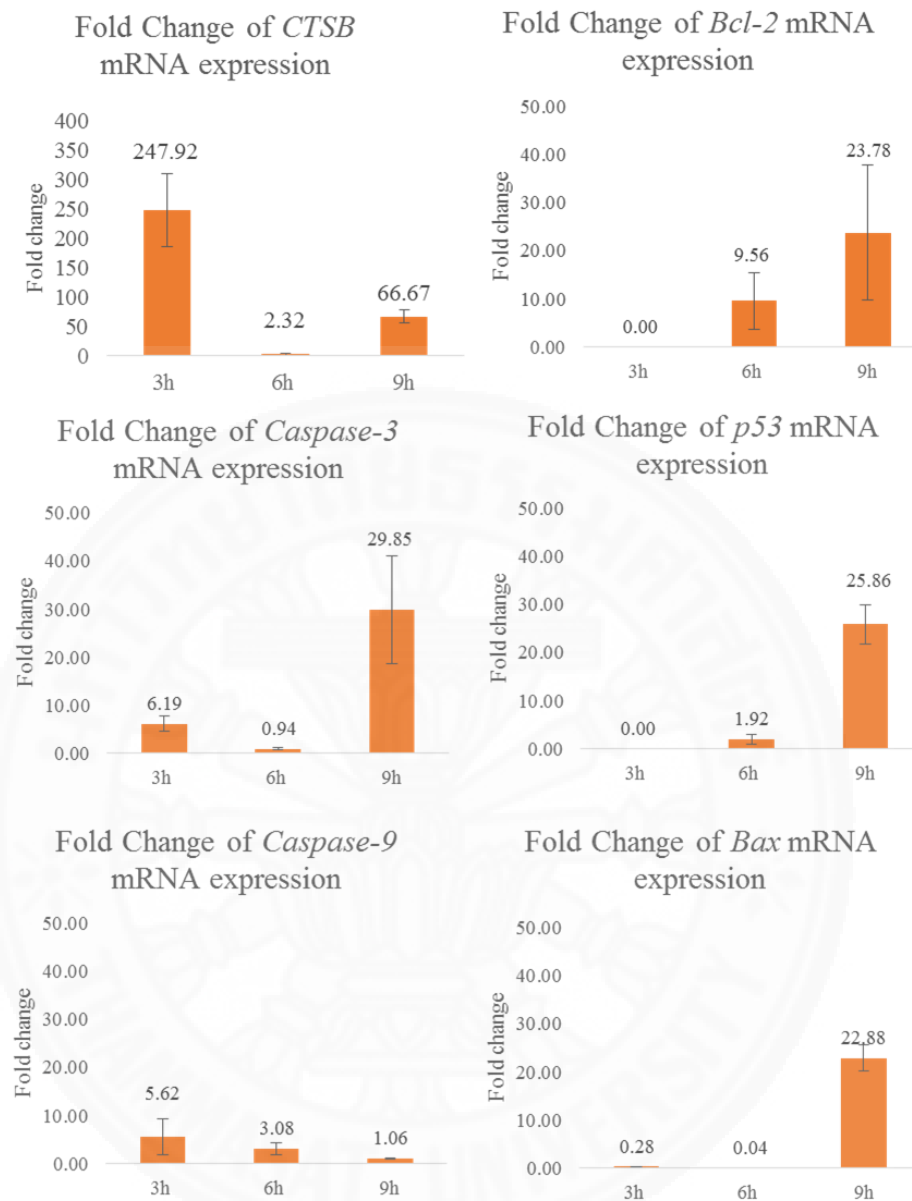


Figure 4.8 Real-time PCR analysis for *Bax*, *Bcl-2*, *p53*, *cathepsin B*, *caspase-3* and *caspase-9* expression in cytotoxic dose of Hep88 mAb treatment at 3, 6 and 9 hours. *Cathepsin B* was shown highly expression at 3 hours, then significantly decreased at 6 hours and up-regulated again at 9 hours of incubation. The graph also represents *caspase-9* and *caspase-3* expression were up-regulated at 3 hours. At 9 hours was demonstrated that overexpressed *Bcl-2*. While, cytotoxic dose treatment was contrary revealed. The *p53*, *Bax* and *caspase-3* expression were slightly increased after 6 hours then up-regulated at 9 hours of incubation in the same trend.

4.2 Enzyme activity involving in the apoptotic mechanism

4.2.1 Caspase-3, -8 and -9 activities

The activation of caspase activity is a unique feature of apoptotic cell death. We determined Hep88-induced activation of the protease activities of caspase-3, caspase-8 and caspase-9. As shown in Figure 4.9, caspase-3, caspase-8 and caspase-9 activities in doxorubicin-treated HepG2 (1.748 ± 0.37 , 3.786 ± 0.21 , 16.889 ± 7.22 ; $p < 0.05$) and Hep88 mAb-treated HepG2 (1.412 ± 0.15 , 5.197 ± 0.90 , 41.228 ± 18.192 ; $p < 0.05$) are significantly different at 24 hours following incubation. By contrast, at 48 and 72 hours, there was no significant effect on caspase-3, caspase-8 and caspase-9 activities in the HepG2 cells (except caspase-8 and caspase-9 in Hep88-treated HepG2 cell for 72h; 1.50 ± 0.27 and 14.334 ± 5.19 ; $p < 0.05$ respectively).

The caspase-3, -8 and -9 activities were induced by Hep88 mAb within 24 hours of incubation, which were correlated well with the mRNA expression results. The apoptotic mechanism induced by Hep88 mAb is involved in the extrinsic and intrinsic pathway. Caspase-8 was activated by the extrinsic induction, then it stimulated the downstream caspases. On the other hand, caspase-9 was activated by the apoptosome formation. It subsequently activated the downstream effector caspases.

The initiator caspase-8 is activated by two subunits of procaspase-8 compact to each other through the death-inducing signaling complex (DISC) that recruited from the ligation of death receptor with cytosolic adapter protein. As a results, activated caspase-8 is the key substance of the extrinsic apoptotic pathway. Even so, an intrinsic pathway can occurred by the caspase-8 through pro-apoptotic Bid cleavage. A truncate form of Bid (tBid) can translocates to the mitochondria and lead to cytochrome c release (Kruidering & Evan, 2000). Procaspase-9 combine with cytochrome c, dATP and Apaf-1 in a multimeric complex, is called apoptosome. As a results, caspase-9, the initiator caspase of the intrinsic apoptosis pathway is activated.

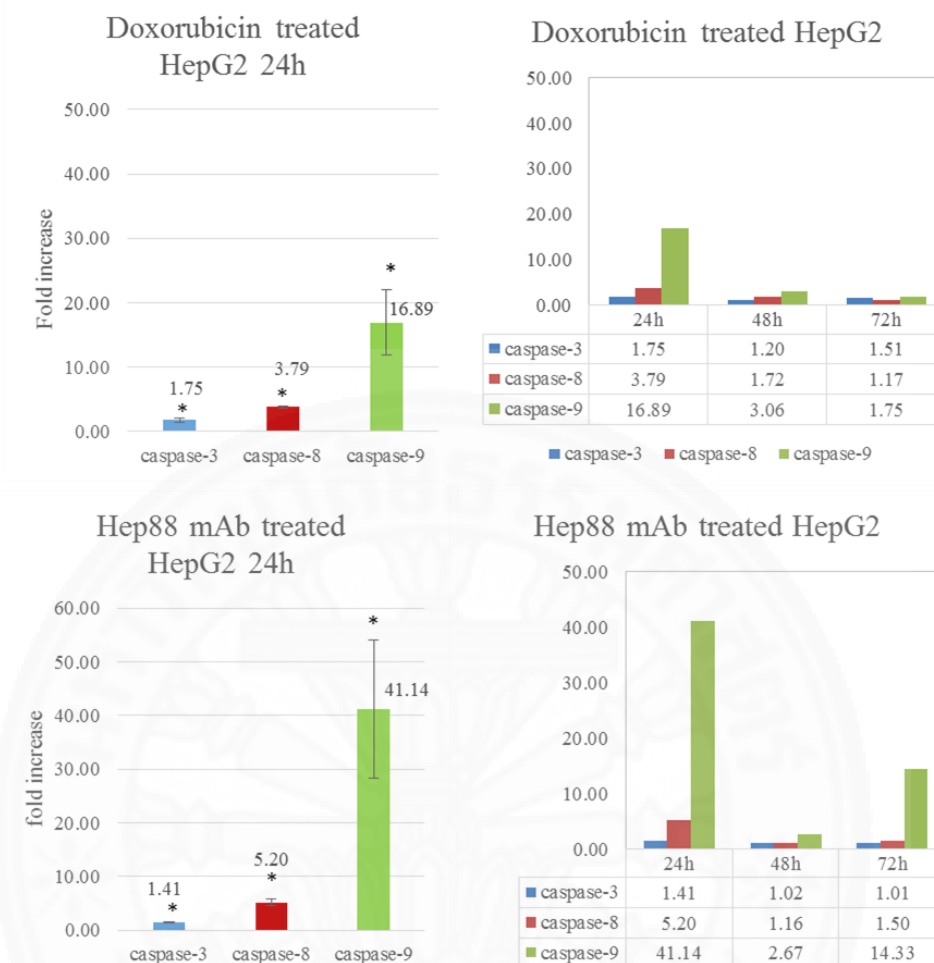


Figure 4.9 Effects on caspase activities of doxorubicin and Hep88 mAb-treated HepG2 cells. The charts show fold increases of caspase-3, -8, -9 enzyme activities in doxorubicin-treated HepG2 (upper) and Hep88-treated HepG2 (lower) after incubation for 24, 48 and 72 hours. The doxorubicin-treated HepG2 of caspase-3,-8 and -9 activities were increased at 24 hours, while the Hep88 mAb-treated HepG2 of caspase-3,-8 and -9 activities also increased highly during the first 24 hours. Effects on caspases activities were determined using HepG2 cells treated as described in the methods. Caspase activities in HepG2 were determined using the caspase-activity detection kits (see Methods). Data are expressed as fold increase, and as means \pm SD ($n \geq 3$). * $p < 0.05$ vs. control.

4.3 Flow cytometry

The principle of apoptotic morphology detection by flow cytometry depends on the hallmarks of apoptosis. Thereby, several flow cytometry techniques can be used to evaluate apoptotic cell population. The phosphatidylserine exposure is observed on the plasma membrane of apoptotic cells by annexin V/FITC staining. The plasma membrane of both healthy cells and early apoptotic cells are integrity, those cells aren't stained with propidium iodide (PI). While, the late apoptotic cells and necrotic cells were loss of plasma membrane integrity, they are stained with PI. In addition, a fluorescent dye PI is used for DNA staining in cell cycle analysis because each phase of cell cycle contains different quantity of the DNA content. The active caspase-3 is a key of apoptosis, it is detected in cells by specific staining with fluorescent tag monoclonal antibody.

4.3.1 Hep88 mAb induced apoptotic cell death in HepG2 cells

The mode of cell death induced by Hep88 mAb in HepG2 cells was confirmed by annexinV/PI double staining. Hep88 mAb-treated cells induced a decrease in the percentage of viable cells (annexinV-/PI-) as compared to control cells with a concurrent increase in the percentage of early apoptotic cells (annexin V+/PI-). The percentage of early apoptotic cells increased in a dose- and time-dependent manner (Figure 4.10 and 4.11). The increase in the apoptotic population is associated with the increase in the sub-G1 population observed in the cell cycle analysis (Figure 4.12). These results suggest that Hep88 mAb induces cell death through an apoptotic mechanism.

As cells are entering the apoptosis state, the earliest feature of this activity is the phosphatidylserine translocation from the inner cytoplasmic membrane to the outer membrane, a movement which can be detected by Annexin V staining. Our Annexin V-PI staining data found a significant increase of an early apoptotic cell population with elevated concentration and prolonged exposure time (Figure 4.10 and 4.11).

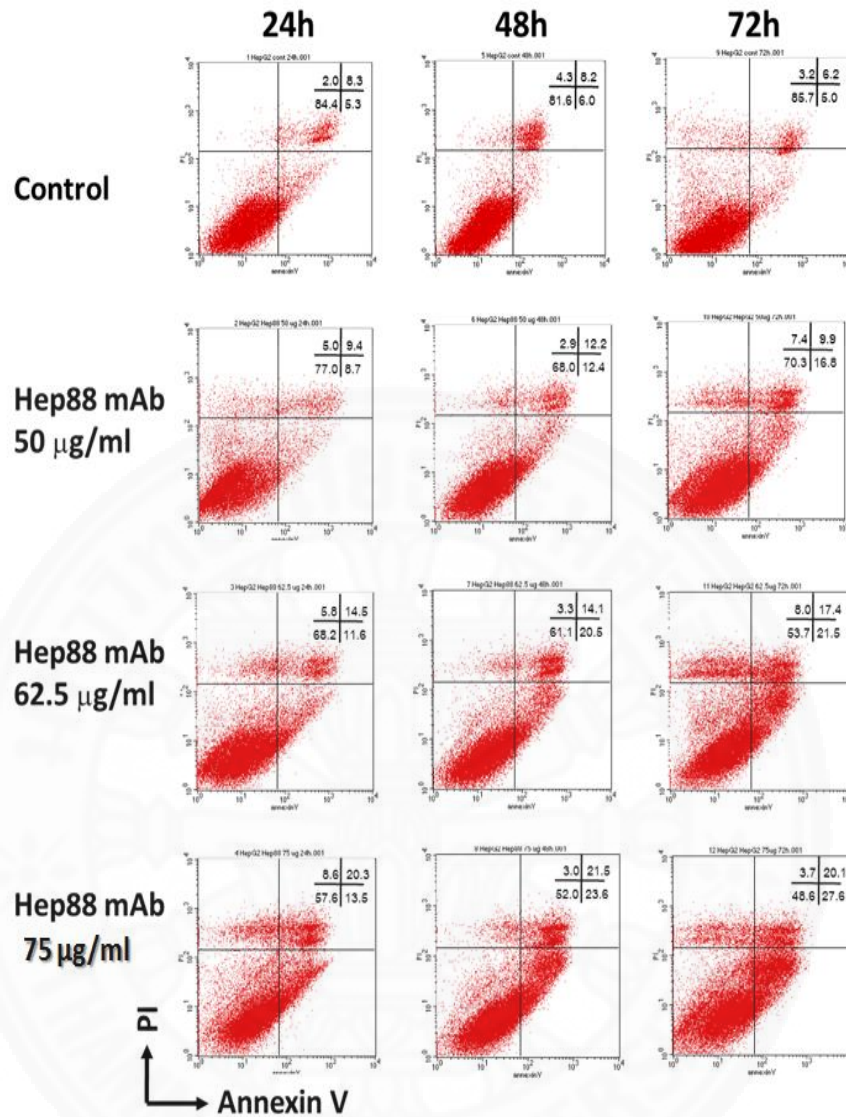


Figure 4.10 Flow cytometry analysis of apoptotic cell death in Hep88 mAb-treated HepG2 cells. HepG2 cells were untreated or treated with Hep88 mAb at 50, 62.5 and 75 µg/ml for 24, 48 and 72 h. Cells were stained with annexin V/PI and subsequently analyzed by flow cytometry. Annexin V⁺/PI⁻ cells were in early stages of apoptosis and double positive cells were in late apoptosis, whereas annexin V⁻/PI⁺ cells were necrosis. The percentage of early apoptotic cells increased in a dose- and time-dependent manner.

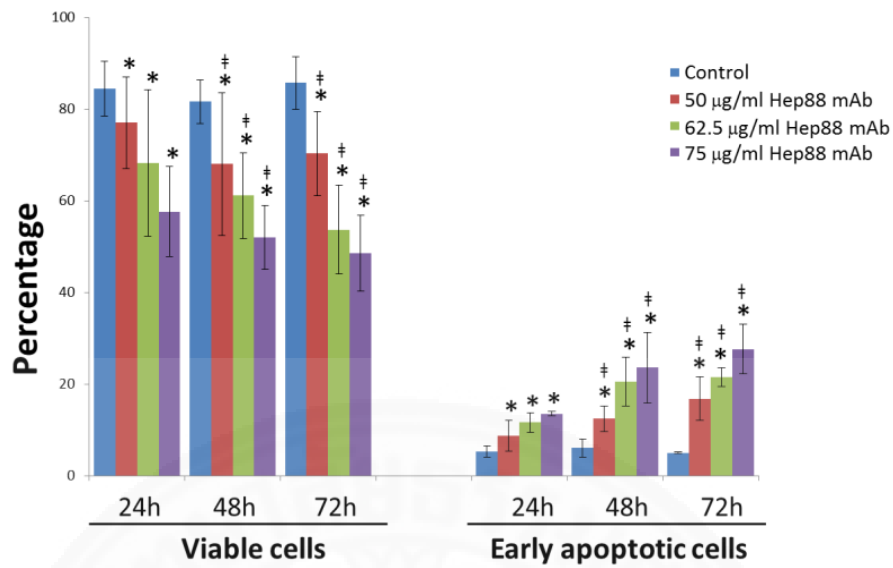


Figure 4.11 Changes in the percentage of early apoptotic and viable HepG2 cells induced by Hep88 mAb. The charts show percentage of early apoptotic and viable cells in Hep88-treated HepG2 after incubation for 24, 48 and 72 hours. The percentage of viable cells in Hep88-treated HepG2 were decreased, while the percentage of early apoptotic cells was increased after elevated dose and prolonged exposure time. Percentage of viable and apoptotic cells of Hep88 mAb-treated cells was analyzed. (mean \pm SD, $n \geq 3$), * $p < 0.05$ vs. control, † $p < 0.05$ 48 and 72-h incubation vs 24-h incubation of their corresponding doses.

4.3.2 Hep88 mAb induced cell cycle progression in HepG2 cells

Apoptotic cells show staining below the G1 population of normal diploid cells. The DNA-specific fluorochrome PI identified a distinct hypo-diploid cell (sub-G1) population as apoptotic cells. Figure 4.12 shows a representative DNA-histogram of HepG2 cells as observed at 24hr, 48hr 72hr after treatment with 50, 62.5 and 75 µg/ml of Hep88 mAb. The percentages of each phase population were measured by Flow cytometry. Populations of apoptotic cells (sub-G1) and G2/M cells were higher in the experimental group than in the control group. Furthermore, at the same concentration of Hep88 mAb, apoptotic cells increased over time. This increase correlates well with many pieces of evidence indicating that apoptosis induction not only involves an extrinsic (caspase-8 activation) apoptosis pathway and a mitochondrial/intrinsic (caspase-9 and caspase-3 activation) apoptosis pathway, but also induces cell cycle arrest as well (Lin, Lu, Wang, Chan, & Chen, 2013; Y. X. Wang, Cai, Jiang, Zhou, & Wu, 2014; B. Yang et al., 2013; Zhu et al., 2013).

From within the scope of these patterns, the cell cycle can be determined by the quantization of DNA content (PI staining) within the cell. The cycle is based on differences in DNA content in each phase by following the cells in pre-replicative phase (G1), replicate DNA- (S phase) and post-replicative plus mitotic (G2/M)- phase cells. Moreover, DNA content can be used to estimate apoptotic cells by sub-G1 (Darzynkiewicz, Halicka, & Zhao, 2010). During the cell cycle, the potential target for cancer therapy is a G2/M checkpoint (Y. Wang et al., 2009), because G2/M is a checkpoint that prevents DNA-damaged cells from entering mitosis and allows for the DNA repair. If cells cannot repair the damage during cell cycle arrest, the cell cycle progression with the DNA damage causes cell death or apoptosis (H. Wang, Zhang, Sit, Lee, & Wan, 2014; Yu & Zhang, 2003). As based on this point, it has been found that many publications on the novel cytotoxic molecule with regard to its role in cancer therapy are concerned with G2/M phase arrest (Lin et al., 2013; Y. X. Wang et al., 2014; B. Yang et al., 2013; Zhu et al., 2013). Remarkably, our results revealed that Hep88 mAb induced HepG2 cells to arrest at the G2/M phase and to increase in the sub-G1 peak (Figure 4.7) in a dose- and-time-dependent manner. This cell cycle data was correlated with significantly increased cell death, as determined by annexin V staining. This correlation might be the result of mortalin depletion after recognition by

Hep88 mAb. It induces the restoration of p53-activating apoptosis induction and finally activates cell cycle arrest (Agarwal, Agarwal, Taylor, & Stark, 1995; Kaul, Aida, Yaguchi, Kaur, & Wadhwa, 2005; Starenki, Hong, Lloyd, & Park, 2014).

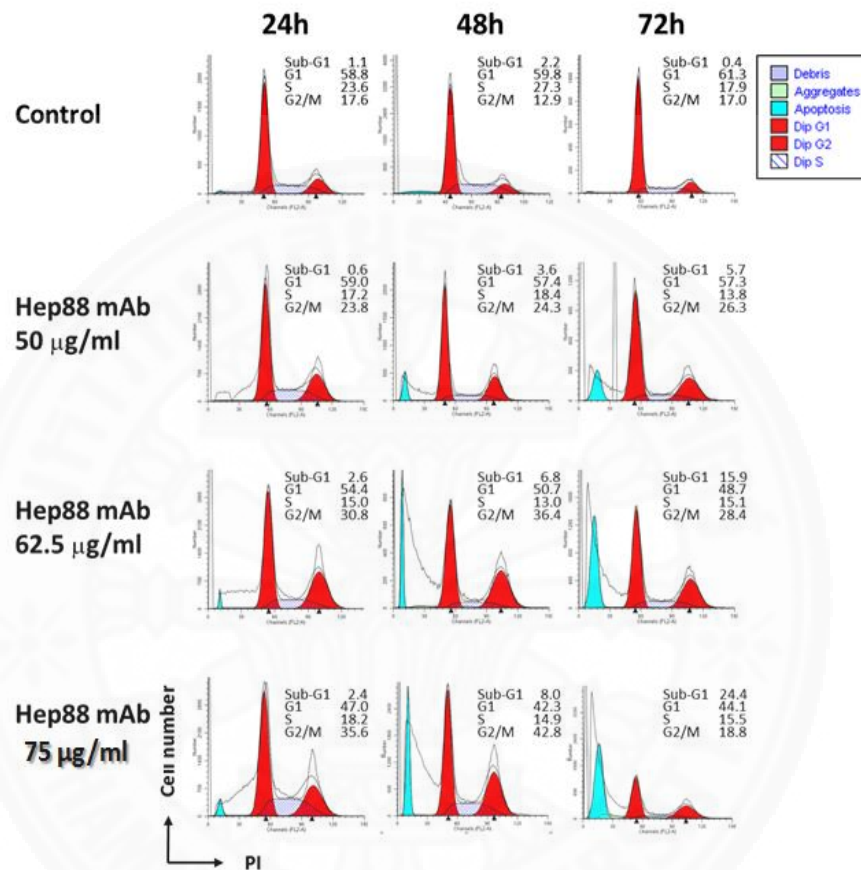


Figure 4.12 Effects on varying doses and times of Hep88 mAb incubation on cell cycle progression in HepG2 cells. HepG2 were seeded into each well of six-well plates and cultured in 10% FBS-RPMI at 37°C. After 24 h, the cells were treated with Hep88 mAb for 24 h, 48 h and 72 h in varying doses. The cells were then collected for PI staining assay. The DNA-histogram showed that Hep88 mAb promoted altered HepG2 cell cycle progression. The G2/M cell cycle arrest and apoptosis (sub-G1) were found with increases in doses and incubation times of Hep88 mAb.

4.3.3 Effect of Hep88 mAb on an active caspase-3 expression

The caspase-3 has also been confirmed as active following incubation with Hep88 mAb by using an antibody that specifically recognizes the active form of caspase-3 for staining. After treatment with various concentrations of Hep88 mAb, the mean intensity of the content in the samples increased, indicating increased active caspase-3. According to the concentration of Hep88 mAb at 72 h, active caspase-3 staining was 125.46%, 145.34% and 167.31% higher than in the control group, which was statistically significant as shown in Table 4.3 and Figure 4.13. The results also correlated well with another analytical apoptosis study in a time- and dose-dependent manner.

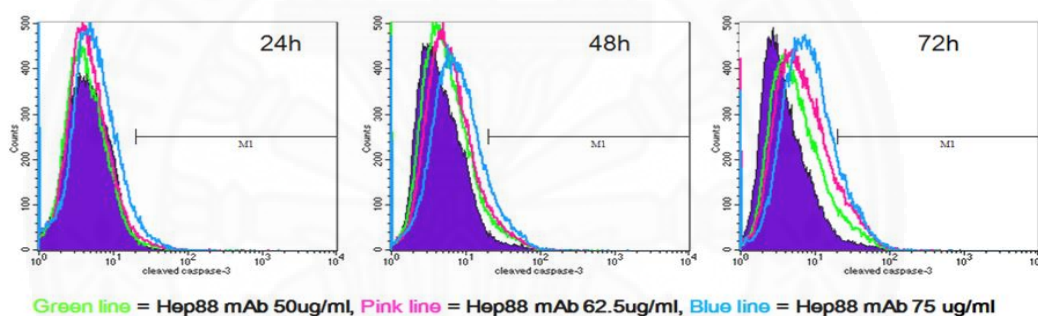


Figure 4.13 Effect of Hep88 monoclonal antibody on active caspase-3 in HepG2. The overlay untreated control HepG2 cell is shown with various Hep88 mAb concentrations during treatment at 24, 48 and 72 hours. The mean intensity of active caspase-3 showed a greater increase than in the control group in a dose- and time-dependent manner.

Table 4.3

Effect of Hep88 monoclonal antibody on active caspase-3 expression in HepG2.

Time	Mean intensity			
	Control	50 µg/ml Hep88 mAb	62.5 µg/ml Hep88 mAb	75 µg/ml Hep88 mAb
24h	8.04 ± 2.88	7.67 ± 2.51	8.28 ± 3.06	9.12 ± 3.20
48h	7.99 ± 2.16	8.96 ± 2.49	9.28 ± 2.70	11.06 ± 3.39
72h	8.30 ± 2.80	10.41 ± 3.33	12.06 ± 3.80*	13.89 ± 4.46*

(mean ± SD, n = 3)* $p < 0.05$ vs. control group

4.4 GeLC-MS/MS

4.4.1 The differentially expressed proteins in the Hep88 mAb-treated HepG2 cells from GeLC-MS/MS analysis

GeLC-MS/MS analysis revealed a total of 323 differentially expressed proteins (Figure 4.14). We found that 29 differentially expressed proteins were appeared after treated HepG2 cell line with Hep88 mAb (as shown in Figure 4.14, Table 4.5). Two of that 29 differentially expressed proteins only found in IC50 concentration treatment (ankyrin repeat domain 32 and spindlin-1) after 3 hours of incubation (Figure 4.18). In addition, there were 2 interesting proteins that did not found in cytotoxic concentration treatment but found in untreated control and IC50 concentration treatment. In turn, there were 4 interesting proteins that did not found in IC50 concentration treatment but found in untreated control and cytotoxic concentration treatment.

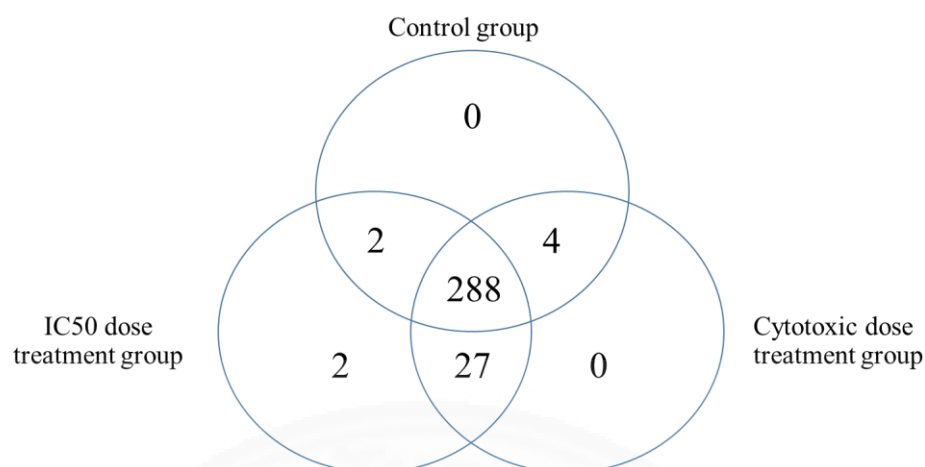


Figure 4.14 The Venn diagram comparison of the differentially expressed proteins from the Hep88 mAb-treated HepG2 cells.

Ankyrin repeat domain 32 is a member in the ankyrin repeat family protein that mainly mediated protein-protein interaction. It is involved in DNA repair and/or DNA damage signaling pathways. The ankyrin repeat domain 32 has been shown to interact with an E3 ligase. The binding of ankyrin repeat domain 32 to E3 ligase is required for E3 ligase function in the promoting ubiquitination (T. Liu et al., 2012). E3 ligase is functioned as a mediator for DNA damage response signals to activate the G2/M checkpoint for maintain the genome integrity and cell survival after induced-damage exposure (Sasatani et al., 2015). Interestingly, after treated HepG2 cell with IC50 dose of Hep88 mAb also found the ankyrin repeat domain 32 protein. This indicated that HepG2 cell try to survive by produced this protein after treatment, and rapidly repairs the damage. In the same time, this protein wasn't found in the cytotoxic dose of treatment. The results correlated well with the cell cycle data in this studies which shown the G2/M arrest after increasing dose of Hep88 mAb treatment.

In addition, the G2/M phase cell cycle arrest is involved the nuclear protein spindlin-1. It increased the G2/M phase cells and made cell growth faster in mouse embryonic fibroblast cells (Gao et al., 2005). Spindlin-1 contains three tandem tudor-like domains which play an important role in epigenetic control of gene

expression and DNA damage response. Spindlin-1 can binding with histone peptide by the interaction between aspartic acid residue and N-terminal group of histone protein to stimulate rRNA transcription (W. Wang et al., 2011; N. Yang et al., 2012). These data suggest that spindlin-1 is also involved in regulation of transcription. It's possible that HepG2 cell try to increase the G2/M phase cell to repair the damage from the Hep88 mAb induction by spindlin-1 activity. However, when the intracellular damage had been accumulated in a large number, cell turn from arrest to apoptotic cell death pathway.

When the cells were treated with cytotoxic dose of Hep88 mAb, it was contributed to absent two proteins (Figure 4.14). Two absented proteins were plectin and pterin-4-alpha carbinolamine dehydratase. Plectin is an essential protein that involve in the cell structure maintaining. The deficiency of plectin mediates the collapse of cytoskeleton (Cheng et al., 2015; Y. H. Liu et al., 2008) which may turn the cancer cell to apoptosis. While another one protein was an enzyme in tetrahydrobiopterin synthesis, named pterin-4-alpha-carbinolamine dehydratase. This enzyme is also a cofactor for hepatocyte nuclear factor 1 alpha (HNF1A) transcription (Thony, Neuheiser, Blau, & Heizmann, 1995). If this enzyme is depleted, it might be contributed to reach the defect on the transcription in liver cell. From such data (Figure 4.17) probably means the cytotoxic dose of Hep88 mAb causes the cytoskeleton damage and the malfunction of transcription.

While, the cells were treated with IC50 dose of Hep88 mAb, led to lack in four proteins including X-prolyl aminopeptidase (aminopeptidase P) 1, potassium channel regulatory protein, keratin type II cytoskeletal 6B and HFSE-1.

X-prolyl aminopeptidase 1 is a catalytic exopeptidase enzyme that cleavage on the N-terminal of peptide, which may play a role in degradation and maturation of many peptides (Iyer et al., 2015). The potassium channel regulatory protein can upregulate the potassium channel to increase the potassium efflux at early apoptosis (Wible et al., 2002). This two proteins were also up-regulated after treated with cytotoxic dose of Hep88 mAb when compare with the expression of protein in untreated control cell.

4.4.2 Mapping proteins network from the GeLC-MS/MS data

The identified proteins in this studies were grouped according to their biological functions, derived from the annotated in the UniprotKB database (Figure 4.15 and 4.16). There were 29 apoptotic proteins that involved in apoptotic signaling pathway (7 proteins), apoptotic process (21 proteins) and an apoptotic cell clearance (as shown in Table 4.4). All of apoptotic proteins in Hep88 mAb-treated HepG2 cell were used as the subject to network interaction analysis by STRING database, which integrates protein-protein interaction data from various sources (Figure 4.19 and 4.20).

Interestingly, its functional partners of 60 kDa heat shock protein (HSPD1) is 10 kDa heat shock protein (HSPE1), a major heat shock protein which functions as a chaperonin that helps to correct the folding of other proteins. Besides that HSPD1 can link to the negative regulation of apoptosis proteins, heat shock protein 75 (TRAP1) and heat shock protein 70 (HSPA5) as shown in Figure 4.20.

The HSPD1 also links with a regulator protein of oxidative stress-induced intrinsic apoptotic signaling pathway named protein disulfide-isomerase precursor (P4HB), and protein disulfide-isomerase A6 (PDIA6), protein in the group of apoptotic cell clearance protein. Both of them are the protein in ER stress response, which is involved in the intrinsic apoptotic pathway. P4HB acts as a molecular chaperon that improve the misfolded proteins in ER stress response (Sun et al., 2013). While, PDIA6 is the protein that control the ER response. The hyperresponse of ER stress was found in PDIA6-deficient cells, it resulting in overstated upregulated the unfolded protein response (UPR) target genes and increased apoptosis via activation of apoptotic mediators (Eletto, Eletto, Dersh, Gidalevitz, & Argon, 2014). These proteins were inhibited when the intrinsic apoptotic PCD is happened. However, the up-regulated of these chaperon proteins has wildly reported that correlated with the therapeutic resistance.

Three apoptotic process proteins; the voltage-dependent anion-selective channel protein 1 (VDAC1), glyceraldehyde-3-phosphate dehydrogenase (GAPDH) and albumin (ALB) were the differentially expressed proteins, which found in this study. GAPDH can be interacted with VDAC1 in mitochondria which it lead to mitochondria permeabilization and release of cytochrome c (Tarze et al., 2007). While, excessive albumin uptake is initiated the increase of calcium concentration in mitochondria that let cytochrome c release (Erkan, Devarajan, & Schwartz, 2007). The relation of these proteins indicated that Hep88 mAb caused apoptosis by the intracellular damage that induced intrinsic apoptotic PCD.

Furthermore, the apoptotic signaling pathway was stimulated through the Fas (TNFRSF6)-associated via death domain (FASLG) and tumor necrosis factor ligand super family 8 (TNFSF8), which were linked to many functional partner proteins in the extrinsic apoptosis induction such as FADD, FAS, and CASP8. This might be interpreted that the apoptosis cell death induction by Hep88 mAb through Fas ligand and tumor necrosis factor ligand triggered extrinsic apoptotic induction process.

In addition, the expression of many proteins after cytotoxic dose of Hep88 mAb treatment were increased when compared with IC50 dose of Hep88 mAb treatment and untreated control by using MultiExperiment Viewer software (Mev) (Figure 4.18). The proteins are involved in transcription, metabolic process, transport and proteolysis (Table 4.5). These data can be used to predict the effect of Hep88 mAb on HepG2 cells in the near future.

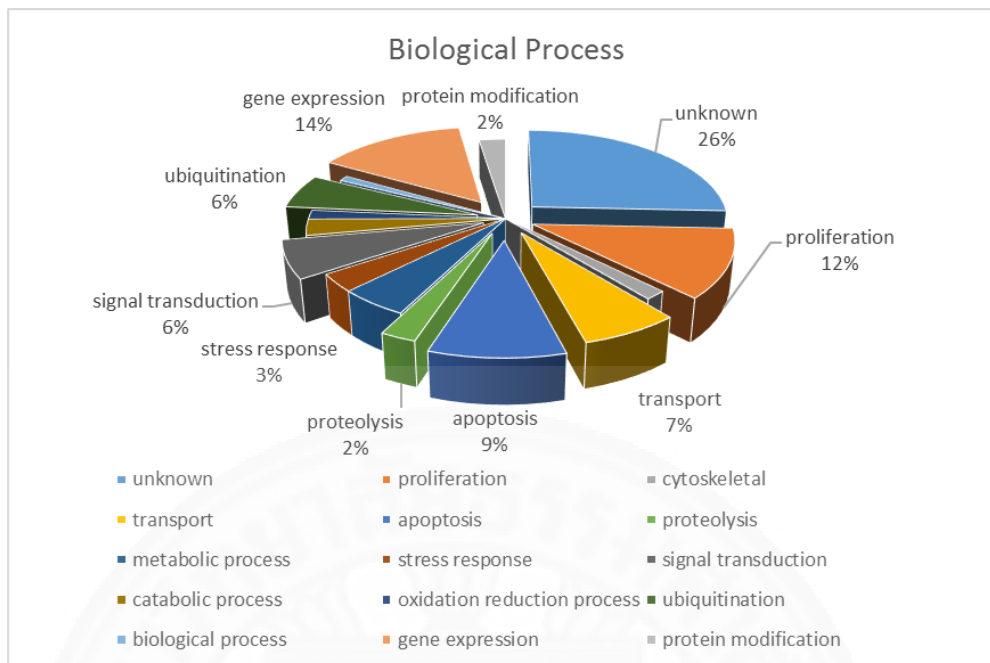


Figure 4.15 The functional distribution of proteins significantly differentially expressed in Hep88 mAb-treated HepG2 cells.

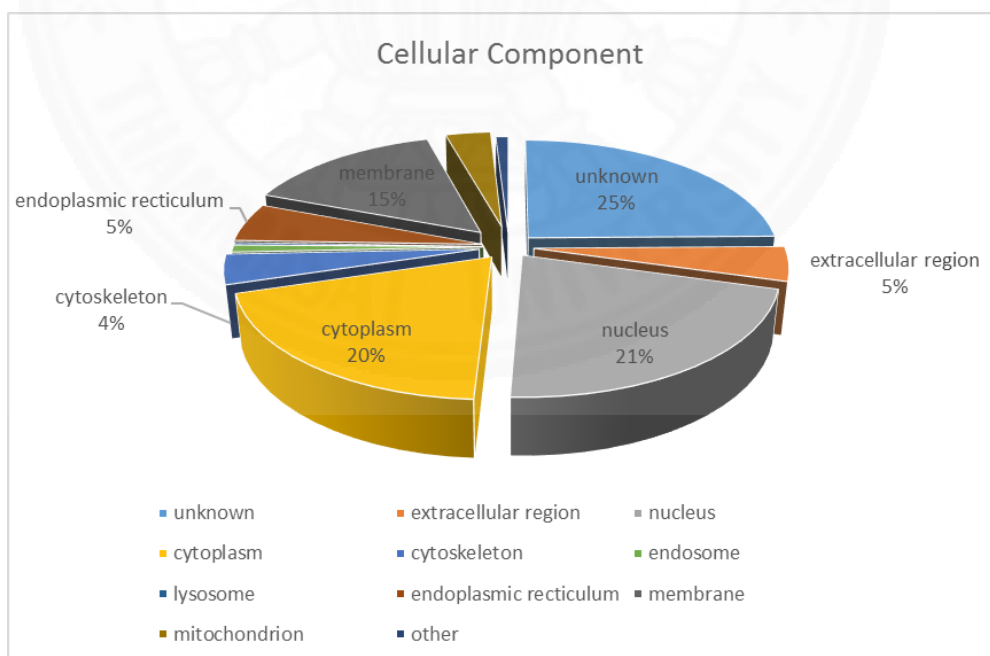


Figure 4.16 The cellular component distribution of proteins significantly differentially expressed in Hep88 mAb-treated HepG2 cells.

Table 4.4**Apoptotic proteins altered after Hep88 monoclonal antibody treatment.**

Accession number	Gene name	Protein name	Biological process	Localization
Apoptotic process				
gi 578816051	PLEC	plectin	apoptotic process	Cytoplasm
gi 578817995	TNFSF8	tumor necrosis factor ligand superfamily member 8	apoptotic process	Membrane
gi 578825607	ACIN1	apoptotic chromatin condensation inducer in the nucleus	apoptotic process	Nucleus
gi 62089230	SLC25A6	ADP,ATP carrier protein, liver isoform T2 variant	apoptotic process	Mitochondria
gi 530380137	VDAC1	voltage-dependent anion-selective channel protein 1	apoptotic process	Mitochondria
gi 9956035	GAPDH	Homo sapiens glyceraldehyde-3-phosphate dehydrogenase (GAPDH)	apoptotic process	Cytoplasm
gi 55743092	ALX4	homeobox protein aristaless-like 4	regulation of apoptotic process	Nucleus
gi 530413039	BECN1	beclin-1	negative regulation of apoptotic process	Cytoplasm
gi 530389399	MTDH	protein LYRIC	negative regulation of apoptotic process	Endoplasmic reticulum
gi 32189392	PRDX2	peroxiredoxin-2	negative regulation of apoptotic process	Cytoplasm

Table 4.4 (Continue)

Accession number	Gene name	Protein name	Biological process	Localization
gi 530370277	HSPD1	60 kDa heat shock protein, mitochondrial	negative regulation of apoptotic process	Mitochondria
gi 578814707	KRIT1	krev interaction trapped protein 1	negative regulation of endothelial cell apoptotic process	Cytoplasm
gi 332356380	ALB	albumin	negative regulation of apoptotic process	Extracellular region
gi 71043932	ZSWIM2	E3 ubiquitin-protein ligase	apoptotic process	Nucleus
gi 530366444	TP53BP2	apoptosis-stimulating of p53 protein 2	apoptotic process	Cytoplasm
gi 578831071	SEPT4	septin-4	apoptotic process	Mitochondria
gi 78101187	EIF2AK2	Chain B, Pkr Kinase Domain-Eif2alpha Complex	negative regulation of apoptotic process	Cytoplasm
gi 372466577	KRT8	keratin, type II cytoskeletal 8	hepatocyte apoptotic process	Cytoplasm
gi 40354195	KRT18	keratin, type I cytoskeletal 18	hepatocyte apoptotic process	Cytoplasm
gi 16507237	HSPA5	78 kDa glucose-regulated protein	negative regulation of apoptotic process	Endoplasmic reticulum

Table 4.4 (Continue)

Accession number	Gene name	Protein name	Biological process	Localization
gi 530389873	ACER2	alkaline ceramidase 2	activation of cysteine-type endopeptidase activity involved in apoptotic process	Golgi membrane
Apoptotic signaling pathway				
gi 20070125	P4HB	protein disulfide-isomerase precursor	regulation of oxidative stress-induced intrinsic apoptotic signaling pathway	Endoplasmic reticulum
gi 578833135	ARHGEF18	rho guanine nucleotide exchange factor 18	apoptotic signaling pathway	Cytoplasm
gi 530361574	VAV3	guanine nucleotide exchange factor VAV3	apoptotic signaling pathway	Cytoplasm
gi 119595168	FASLG	Fas (TNFRSF6)-associated via death domain	apoptotic signaling pathway	Extracellular region
gi 545719855	BCAP31	Chain B, Crystal Structure Of Bap31 Vded At Acidic Ph	positive regulation of intrinsic apoptotic signaling pathway	Endoplasmic reticulum
gi 148887400	MCF2L	Guanine nucleotide exchange factor DBS	apoptotic signaling pathway	Cytoplasm

Table 4.4 (Continue)

Accession number	Gene name	Protein name	Biological process	Localization
gi 440309857	TRAP1	heat shock protein 75 kDa, mitochondrial	negative regulation of oxidative stress-induced intrinsic apoptotic signaling pathway	Mitochondria
Apoptotic cell clearance				
gi 578802476	PDIA6	protein disulfide-isomerase A6	apoptotic cell clearance	Endoplasmic reticulum

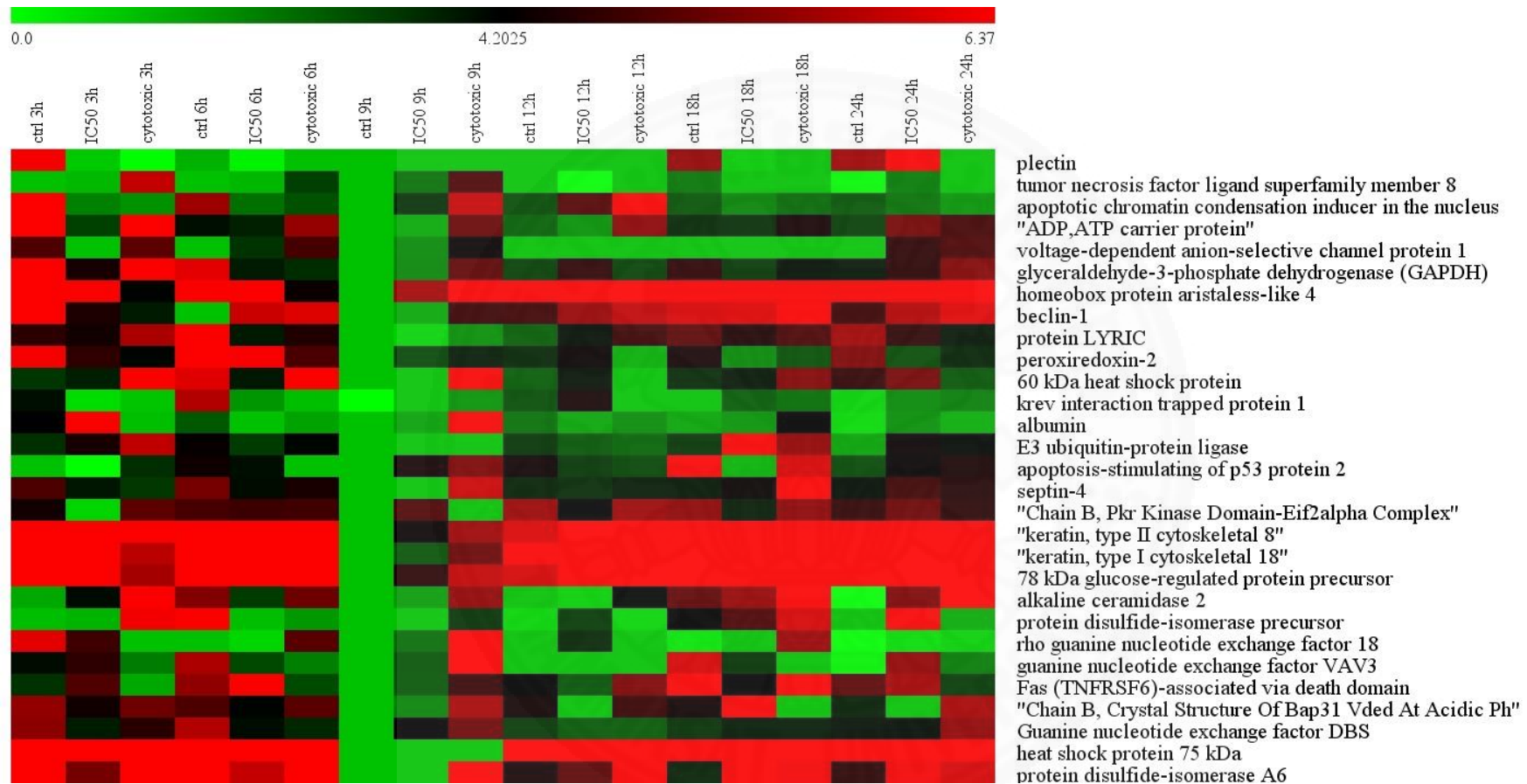


Figure 4.17 The quantification of the change of 29 apoptotic proteins differentially expressed proteins in HepG2 cell after treated with Hep88 mAb.

Table 4.5

The differentially expressed proteins altered after Hep88 monoclonal antibody treatment.

Accession number	Protein name	Gene Name	Biological processes	Localization	Hep88 mAb treatment effect	
					IC ₅₀ conc.	Cytotoxic conc.
Gene expression						
gi 578830602	nucleosome-remodeling factor	BPTF	transcription	Nucleus	1.09	0.09
gi 238908505	DNA-directed RNA polymerase III	POLR3B	transcription	Nucleus	3.05	7.19
gi 187608750	cellular nucleic acid-binding protein	CNBP	transcription	Nucleus	3.93	5.89
gi 4884564	vitamin D3 receptor interacting protein	MED24	transcription	Nucleus	5.53	5.05
gi 145275210	ribosome production factor 1	RPF1	rRNA processing	Nucleus	2.01	6.53
gi 83700235	eukaryotic initiation factor 4A-II	EIF4A2	gene expression	Cytoplasm	5.34	6.03
gi 157384182	ubiquitously transcribed tetratricopeptide repeat protein Y-linked transcript variant 241	UTY	regulation of gene expression	Unknown	6.04	8.96
Metabolic process						
gi 514830150	Chain B, The Crystal Structure Of Apo Human Hdh4 From Se-mad	NANP	metabolic process	Cytoplasm	3.03	5.95
gi 3005599	katanin p80 subunit	KATNB1	metabolic process	Cytoplasm	3.41	4.11
gi 530367796	NADH dehydrogenase [ubiquinone] complex I, assembly factor 7	NDUFAF7	mitochondrial respiratory chain complex I assembly	Mitochondria	4.11	3.79

Table 4.5 (continue)

Accession number	Protein name	Gene Name	Biological processes	Localization	Hep88 mAb treatment effect	
					IC ₅₀ conc.	Cytotoxic conc.
Transport						
gi 21729876	ATP-binding cassette sub-family C member 11	ABCC11	transport	Membrane	5.46	7.50
gi 154759255	collagen alpha-1(XXVIII) chain	COL28A1	negative regulation of endopeptidase activity	Endoplasmic reticulum	4.08	3.87
gi 13194195	chloride channel CLIC-like protein 1	CLCC1	transport	Endoplasmic reticulum	2.89	7.30
Cell cycle						
gi 112293285	spindlin-1	SPIN1	cell cycle	Nucleus	7.45	0
gi 194385806	unnamed protein product	TJP3	regulation of G1/S transition of mitotic cell cycle	Tight junction	5.53	5.84
gi 530413971	Polycomb group protein	ASXL3	regulation of cell growth	Nucleus	3.28	5.95
gi 578803172	structural maintenance of chromosomes protein 6	SMC6	DNA repair	Nucleus	4.87	0.62
gi 578807117	disks large homolog 1	DLG1	mitotic cell cycle checkpoint	Membrane	4.35	7.23

Table 4.5 (continue)

Accession number	Protein name	Gene Name	Biological processes	Localization	Hep88 mAb treatment effect	
					IC ₅₀ conc.	Cytotoxic conc.
gi 119609684	CASK interacting protein 2	CASKIN2	biological process	Cytoplasm	4.36	6.13
gi 530394858	probable G-protein coupled receptor 123	GPR123	signal transduction	Membrane	5.28	6.24
gi 578807017	adenylate cyclase type 5	ADCY5	signal transduction	Membrane	6.21	5.45
gi 2565061	CAGH32, partial	EP400	chromatin modification	Nucleus	4.66	4.67
Proteolysis gi 2065171	CAPN5 protein	CAPN5	proteolysis	Cytoplasm	4.67	6.36
Unknown gi 578831523	glutamine-rich protein 2	QRICH2	unknown	Unknown	3.87	7.49
gi 109698611	mast cell-expressed membrane protein 1	MCEMP1	unknown	Membrane	4.52	5.71
gi 119574967	hCG1781322	unknown	unknown	Unknown	3.92	5.61
gi 119568809	hCG1793313	unknown	unknown	Unknown	4.22	5.12
gi 119616435	ankyrin repeat domain 32	ANKRD32	unknown	Nucleus	6.55	0
gi 119603197	hCG1639851 [Homo sapiens]	unknown	unknown	Unknown	8.06	7.80

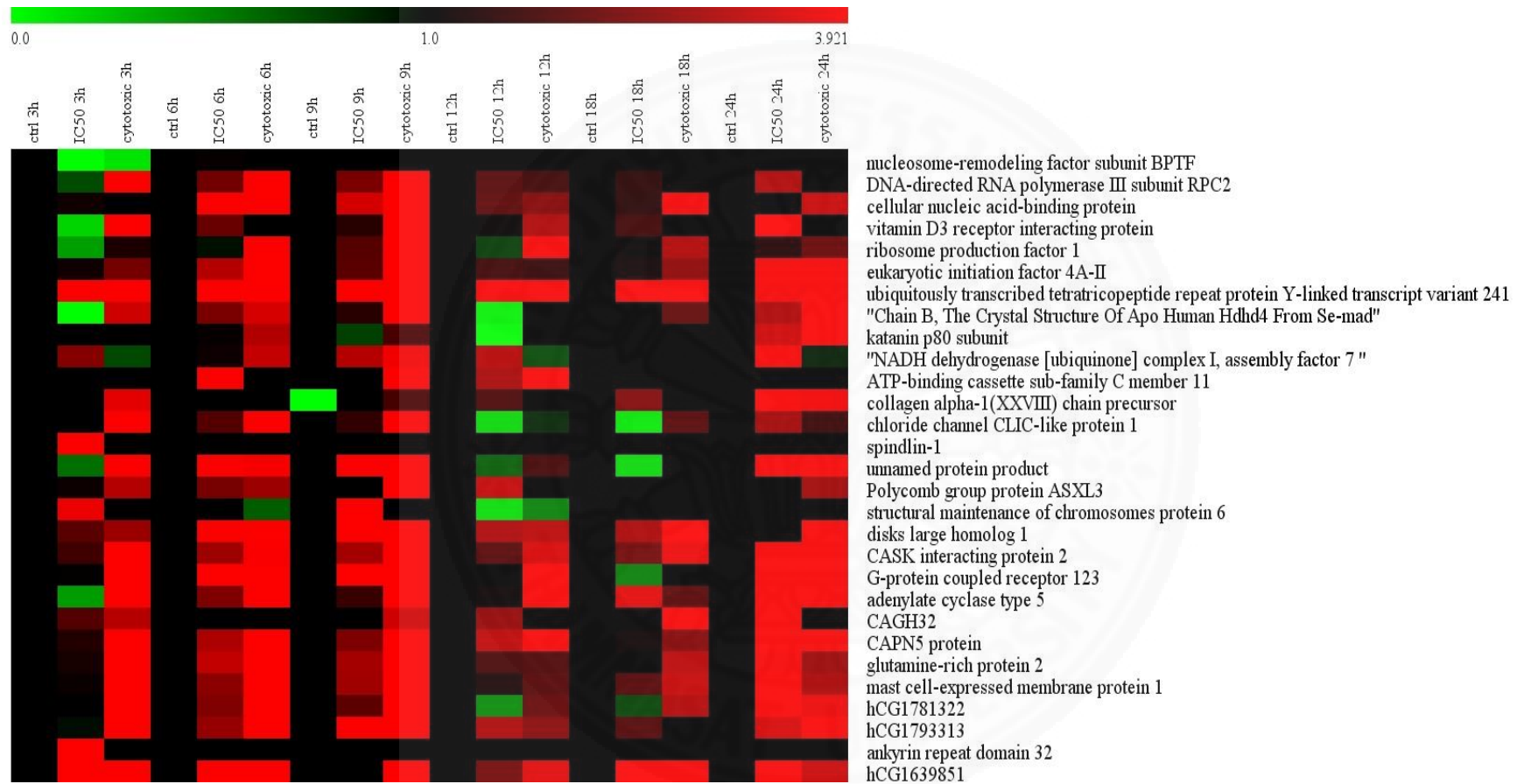


Figure 4.18 The quantification of the change of 29 proteins differentially expressed proteins in HepG2 cell after treated with Hep88 mAb.

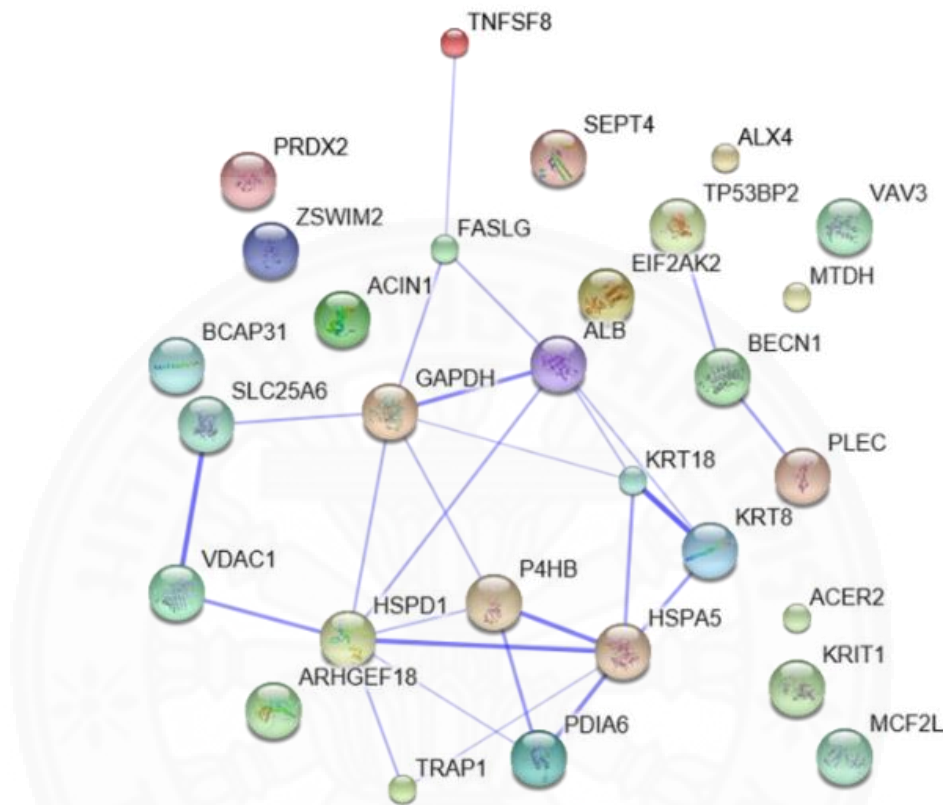


Figure 4.19 The 29 apoptotic proteins of 323 differentially expressed proteins in **Hep88 mAb-treated HepG2 cells**. The network of apoptotic proteins in this study were mostly involved in apoptotic process and apoptotic signaling pathway.

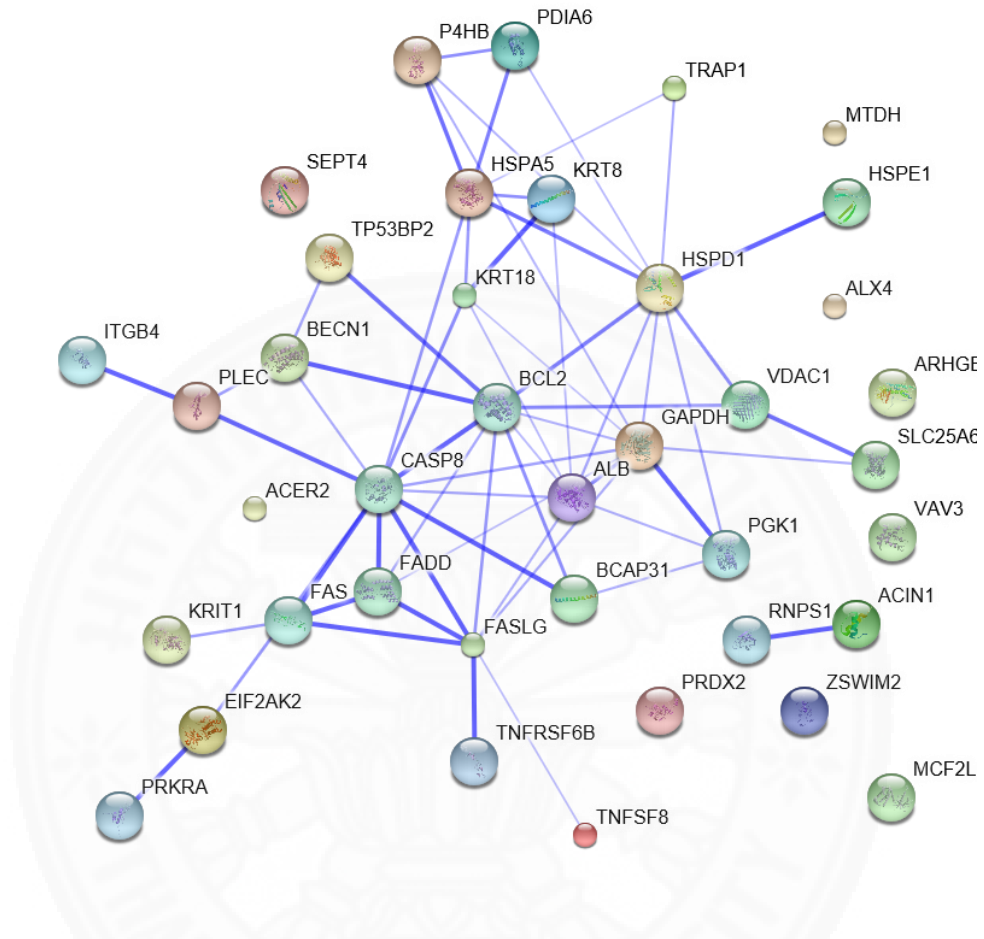


Figure 4.20 The 29 apoptotic proteins of 323 differentially expressed proteins in Hep88 mAb-treated HepG2 cells with its functional partners' proteins. The network of these differentially expressed proteins and their linked proteins can be used to predict the apoptotic effects after Hep88 mAb treatment. The linked proteins are a group of negative regulation of apoptotic proteins, a group of intrinsic apoptotic proteins and a group of extrinsic apoptotic proteins.

CHAPTER 5

CONCLUSIONS AND RECOMMENDATIONS

Although many therapeutic strategies have shown remarkable anticancer effect, but toxicity to normal cells are unavoidable. The novel anticancer that effective but less toxic has great interesting. Especially, the anticancer effect to HCC, because it is a cancer with a complex disease and multiple signaling pathways involved. Its pathogenesis of HCC contributes to difficult treatment. For this reason, targeted therapy like monoclonal antibody appear to be a promising tool for HCC treatment. The recently report of Hep88 mAb had an anticancer activity effect in HCC cell lines, but its mechanism is still unclear. Therefore, in this present study informed about the death induction mechanisms in hepatocellular carcinoma (HepG2) treated with Hep88 mAb. Firstly, the expression at mRNA level of *caspase-3*, *caspase-8*, *caspase-9* (apoptotic genes involving in the apoptotic mechanism after 24, 48, 72 hours of incubation) including their enzymes activities were evaluated compare with chemotherapeutic drug. Afterwards, the Hep88 mAb-treated HepG2 cells were detected to confirm the active caspase-3 induction, cell cycle proliferation and apoptosis induction by using flow cytometry. Early apoptotic mechanism during 3-24 hours of treatment were determined by the expression at mRNA level of *Bax*, *Bcl-2*, *p53*, *caspase-9*, *caspase-3* and *cathepsin B*. Finally, the protein profiles were determined by 1-D gel electrophoresis and LC-MS/MS.

The expression of caspases and their enzyme activities after treated with IC50 dose of Hep88 mAb were demonstrated. It can induced apoptosis in HepG2 cells after 24 hours of incubation through the up-regulation of *caspase-3*, *caspase-8* and *caspase-9* mRNA expression. While, doxorubicin induced the up-regulation of those three caspases in the time dependent manner. However, the caspases induction of IC50 dose of doxorubicin treated HepG2 cells were less than Hep88 mAb. This result demonstrates its effectiveness over the common chemotherapeutic drug normally use in the cancer therapy up to date.

When Hep88 mAb concentration was varied to cytotoxic dose, Hep88 mAb caused the increasing of apoptotic cells and increasing of active caspase-3 in time- and

dose-dependent manner. In addition, G2/M phase cell cycle arrest was increased after increasing the concentration of Hep88 mAb to cytotoxic dose.

The mechanism involved cell death induction in cytotoxic dose of Hep88 mAb-treated HepG2 cells were demonstrated. It was found that the up-regulation of tumor suppressor *p53*, pro-apoptotic *Bax*, *cathepsin B*, *caspase-3*, *caspase-9* while decreasing of anti-apoptotic *Bcl-2*. This was suggested that the cancer cell undergoing paraptosis and apoptosis via cascade reaction as the proposed mechanism as shown in Figure 5.1-5.6.

IC50 dose of Hep88 mAb can induce apoptosis cell death in HepG2 cell, but at the same time the cells tried to escape death phenomenon. It was noticeable from an upregulation of anti-apoptotic gene, *Bcl-2* expression as shown in Figure 5.7-5.12. On the other way, the overexpression of *cathepsin B* in an early treatment (3, 6 and 9 hours of treatment) are involved either directed or indirect cell death by a role in the execution of caspase-independent cell death. It results in a paraptosis-like morphology.

The protein profile in Hep88 mAb-treated HepG2 cells were explored, it revealed 323 differentially expressed peptides. Interestingly, the protein profile of IC50 dose of Hep88 mAb treatment had shown ankyrin repeat domain 32 and spindlin-1. These two proteins were involved G2/M phase cell. From the data, we suggest that HepG2 cell try to survive by these proteins. The G2/M phase cells were increased to rapidly repair the damage from the Hep88 mAb induction. Moreover, it was related with the cell cycle analysis by flow cytometry, IC50 dose of Hep88 mAb-treated HepG2 cells were not mediated G2/M phase cell cycle arrest.

Furthermore, the protein profile of cytotoxic dose of Hep88 mAb-treated HepG2 cell was contributed to the absent of plectin and pterin-4-alpha carbinolamine dehydratase. Plectin is an essential protein that involve in the cell structure maintaining and pterin-4-alpha carbinolamine dehydratase is a cofactor for hepatocyte nuclear factor 1 alpha (HNF1A) transcription. It probably means the cytoskeleton damage and the malfunction of transcription was caused by the cytotoxic dose of Hep88 mAb.

When mapping proteins in Hep88 mAb-treated HepG2 cell were found 29 apoptotic proteins. The apoptotic signaling pathway was stimulated through Fas ligand and tumor necrosis factor ligand to trigger extrinsic apoptotic induction process. While, the proteins involved in the intracellular damage that induced intrinsic apoptotic PCD

was also found. Besides this, the molecular chaperon proteins in ER stress response were involved in the intrinsic apoptotic pathway. These proteins were inhibited when the intrinsic apoptotic PCD is happened. However, the up-regulated of these chaperon proteins has widely reported that correlated with the therapeutic resistance.

The interesting outcomes of our study shown the possibility of the Hep88 mAb mechanism on the induction program cell death of HCC in both cytotoxic and IC50 dose. However, further study on the electron microscope will be certificated in order to confirm the apoptosis cellular alteration morphology of cytotoxic dose of Hep88 mAb treatment. The step of post-transcriptional and post-translational mechanisms are also needed to be clear understood in the relationship between mRNA and protein expression. These activities should be further investigated. The interesting outcomes of Hep88 mAb study might be a promising tool to develop new drugs for the effective treatment of HCC in the near future.

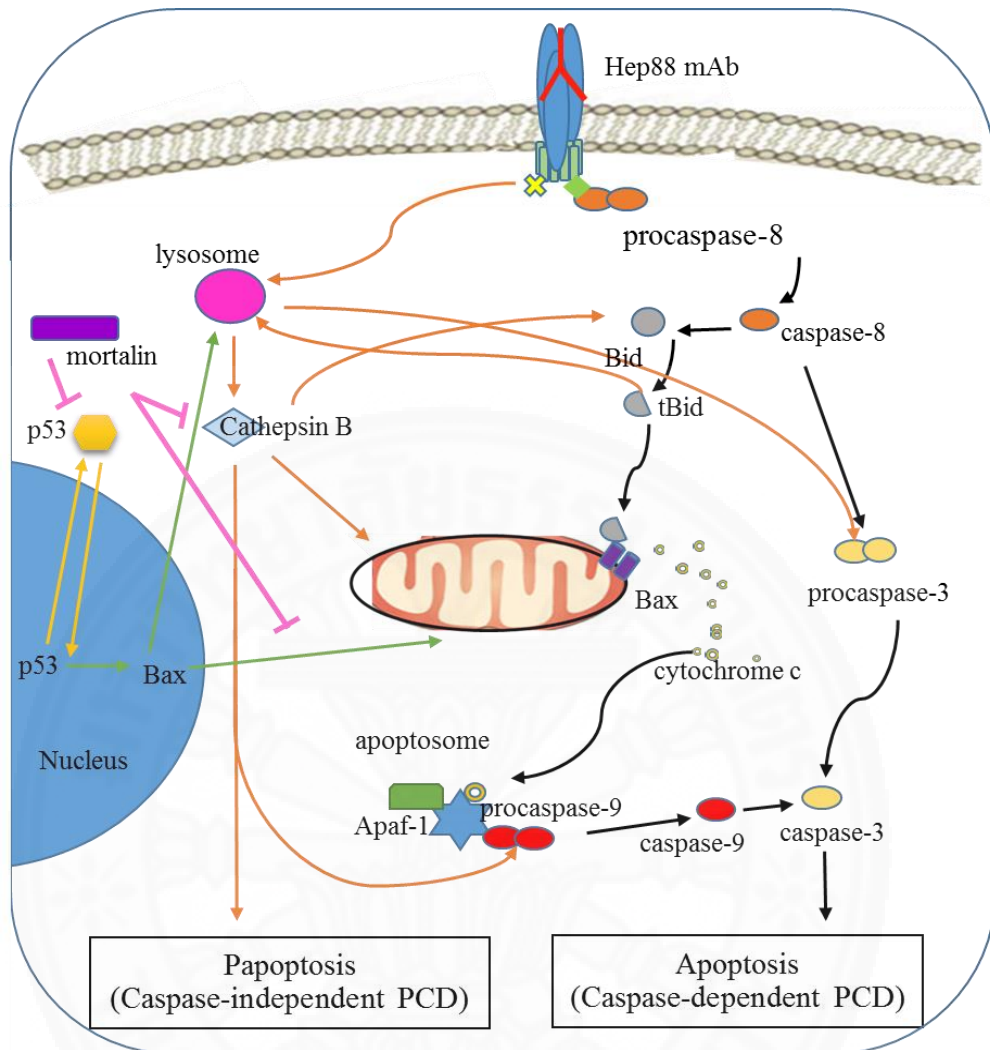


Figure 5.1 The proposed mechanism of cytotoxic dose of Hep88 mAb-treated HepG2 cell at 3 hours. *Cathepsin B* was up-regulated, the loss of mitochondria membrane potential was developed resulting in the releasing of cytochrome c and then initiating the up-regulation of *capase-9* and *caspase-3*. The death induction was further stimulated after Hep88 mAb binding to its specific antigen (Ag) which might be corresponding with death receptor at the cell membrane. The extrinsic apoptotic pathway was subsequently induced.

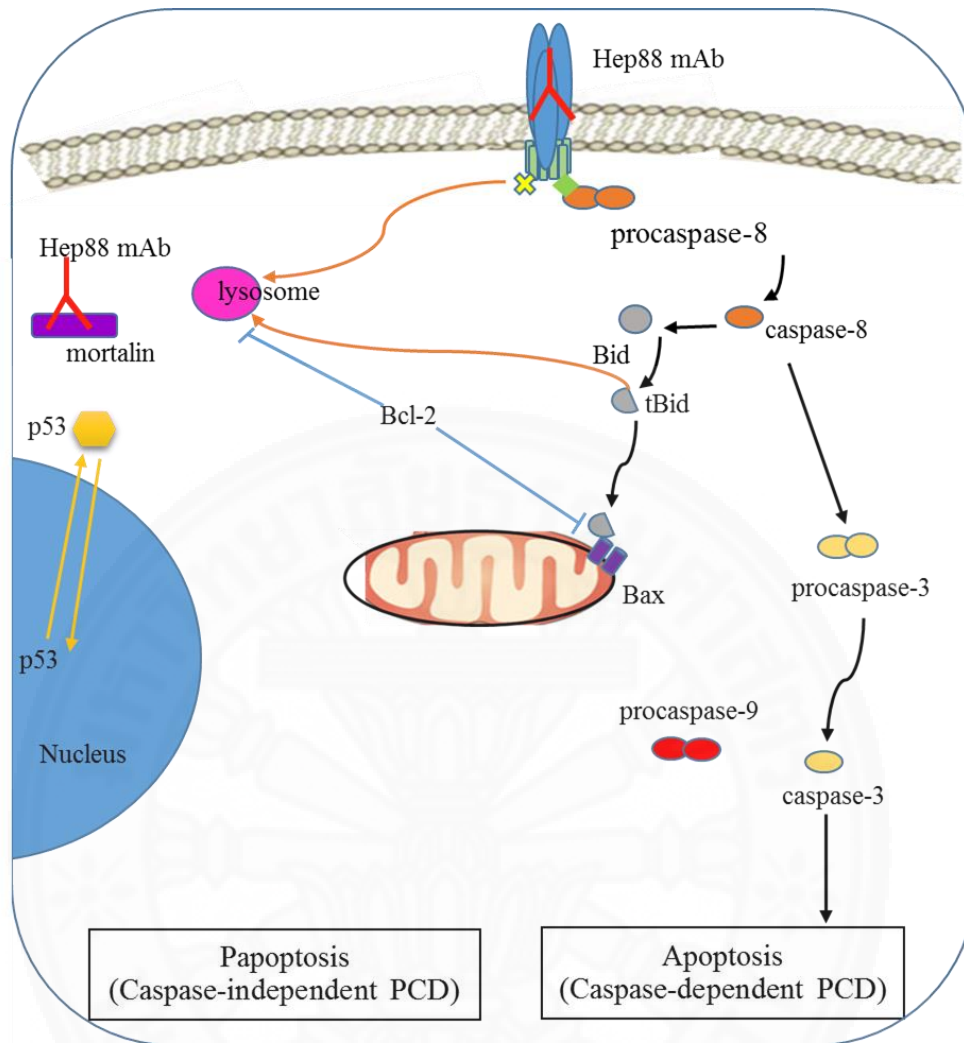


Figure 5.2 The proposed mechanism of cytotoxic dose of Hep88 mAb-treated HepG2 cell at 6 hours. The up-regulated *Bcl-2* caused the remarkable reduction of regulation of *cathepsin B*, *caspase-9* and *caspase-3* in Hep88 mAb-treated HepG2 cell at 6 hours. During these escape phenomenon was risen, Hep88 mAb is still ongoing induction the cell to apoptosis from the extrinsic apoptotic pathway. This initial induced tumor suppressor *p53* gene to be up-regulated.

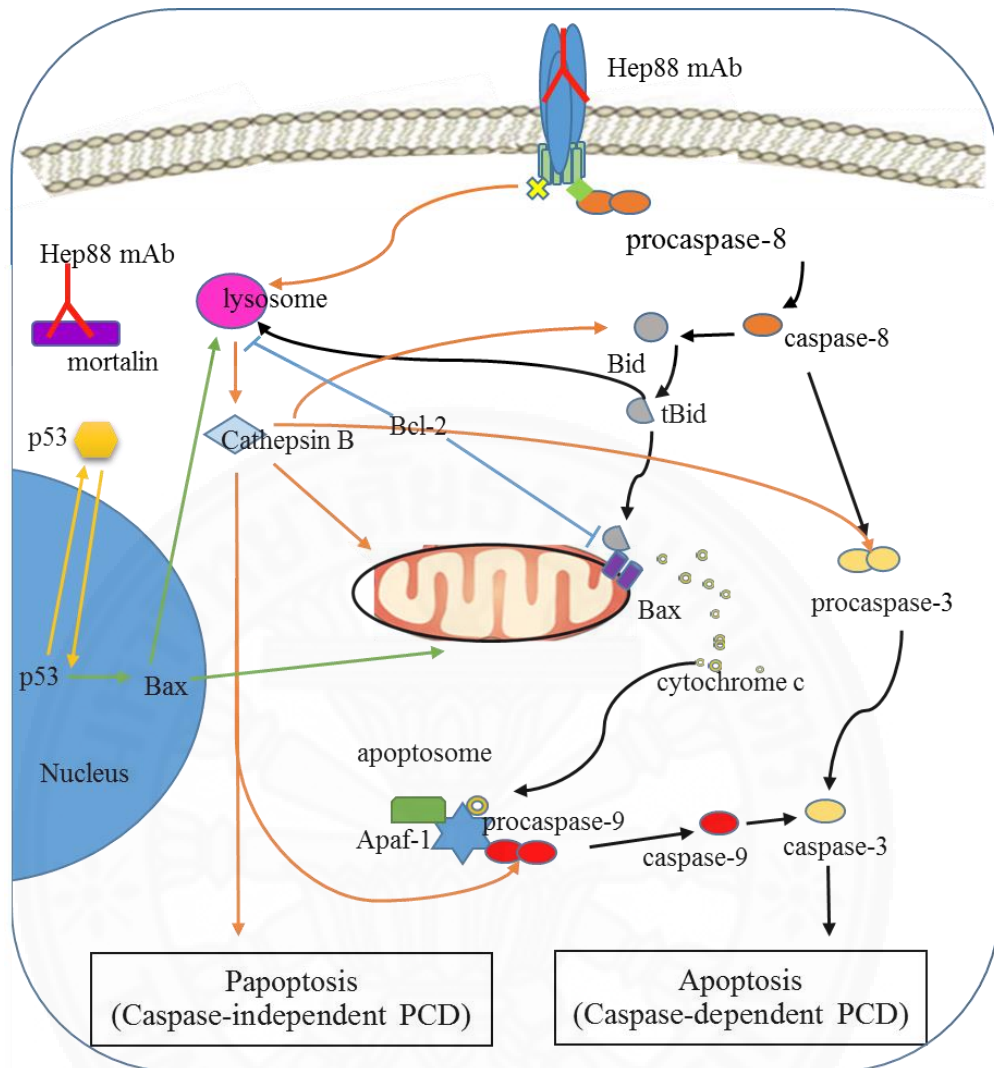


Figure 5.3 The proposed mechanism of cytotoxic dose of Hep88 mAb-treated HepG2 cell at 9 hours. *Cathepsin B*, *caspase-3*, *p53* and *Bax* expression were drastically increased. For gradually increased and released from lysosome of *Cathepsin B*, dead-escape phenomenon was no longer withstand while the strongest and fastest characteristic of cell death was dramatically induced. At this time, however, an overt up-regulation of *Bcl-2* was come into sight. This initiated the signaling pathway of gradual inhibition of LMP and MOMP.

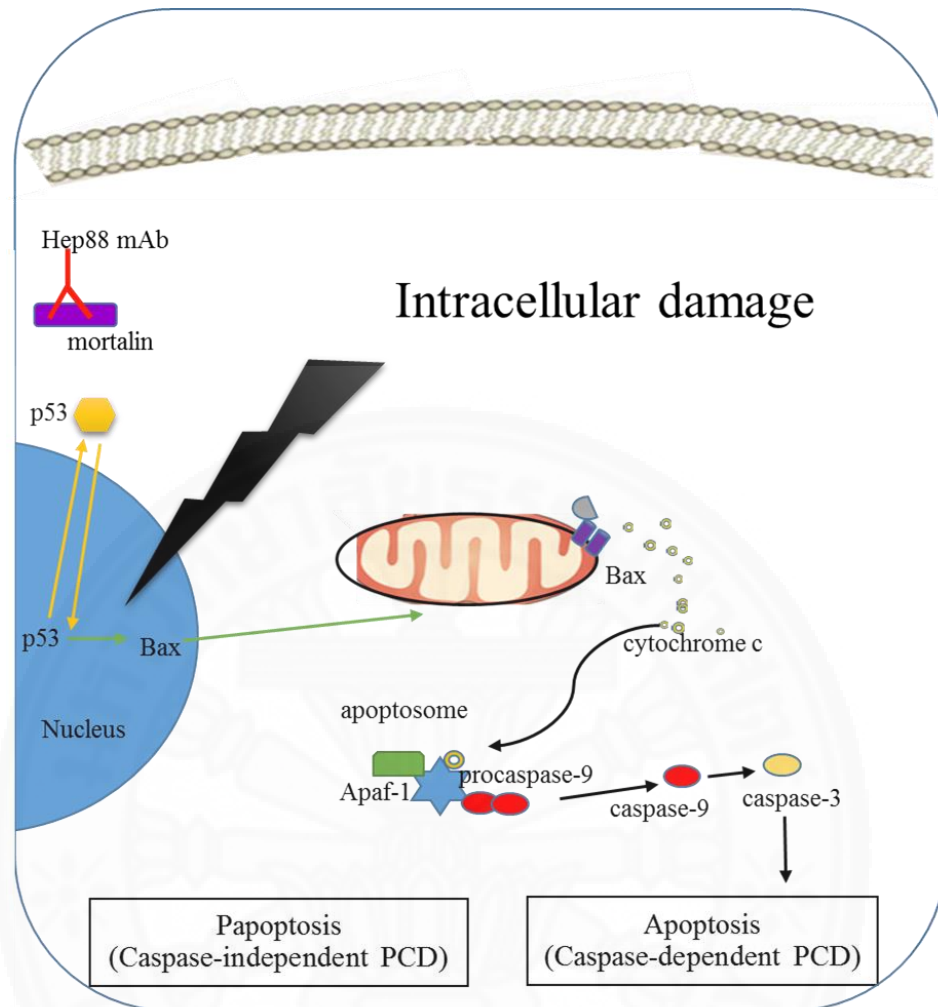


Figure 5.4 The proposed mechanism of cytotoxic dose of Hep88 mAb-treated HepG2 cell at 12 hours. Many damages were accumulated in cell. It still induced *p53*, *Bax*, *caspase-9* and *caspase-3* to up-regulated. While, *cathepsin B* and the anti-apoptotic *Bcl-2* was down-regulated. In the DNA damage response, *p53* was accumulated in the nucleus which was transactivated pro-apoptotic gene *Bax* to stimulate the intrinsic apoptotic pathway entering. When *Bax* protein level increases, it plays a dominant role to generate MOMP at the mitochondria. Eventually, cytochrome *c* is released to activate cascade caspases.

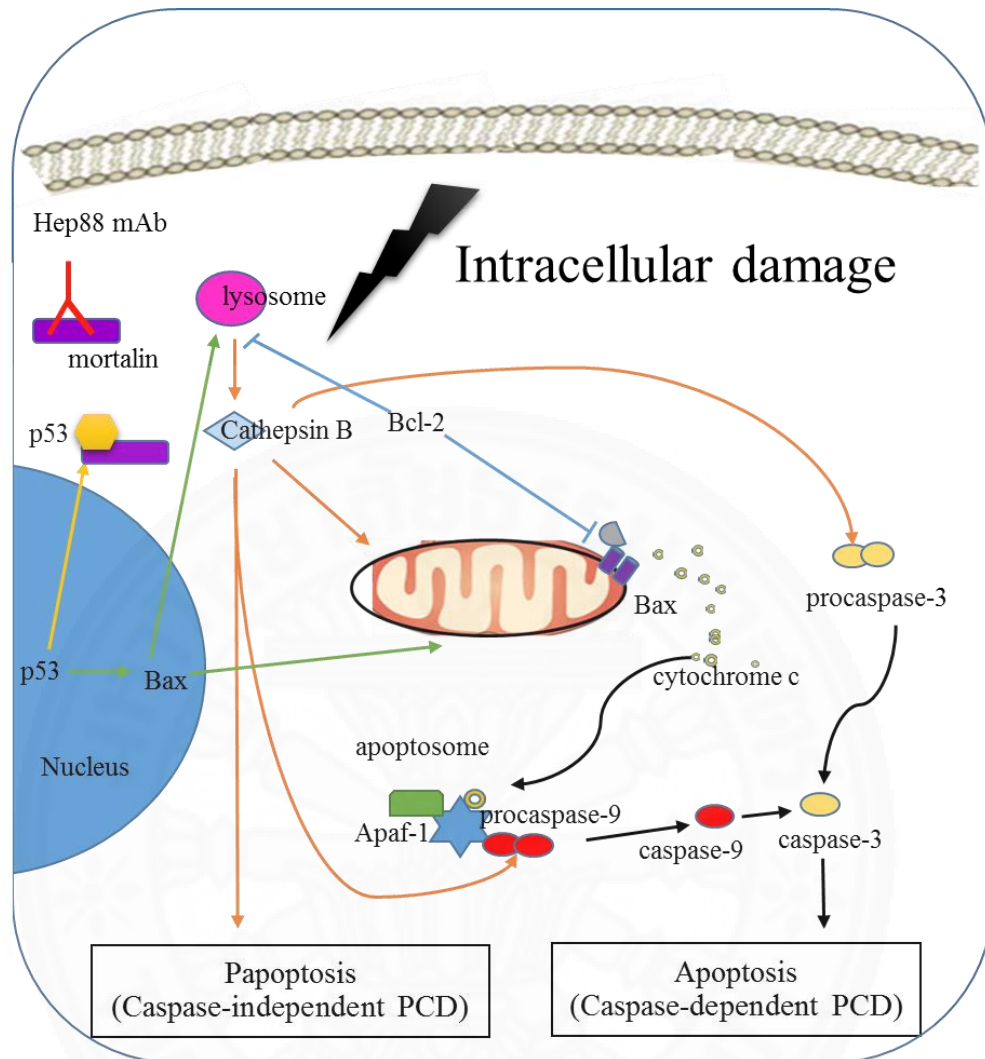


Figure 5.5 The proposed mechanism of cytotoxic dose of Hep88 mAb-treated HepG2 cell at 18 hours. *Cathepsin B* and *Bcl-2* expression was outstanding up-regulated again, *Cathepsin B* was translated, accumulated in lysosome and finally released into cytosol to cleave another intracellular proteins. Besides that, it can induce Bax translocate to mitochondria to release cytochrome c, then activate caspase-9 and caspase-3. As a result, the apoptosis cell death induction was still significant increased, although, anti-apoptotic *Bcl-2* was up-regulated and *p53* was down-regulated

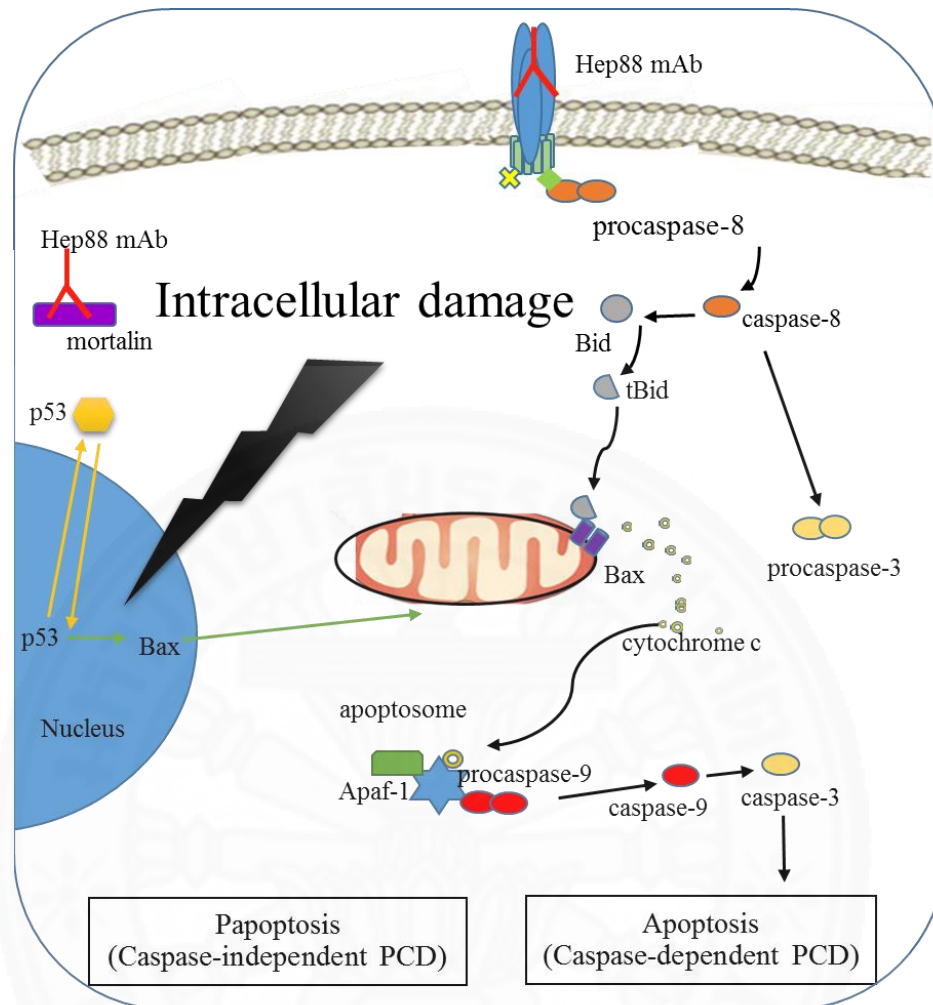


Figure 5.6 The proposed mechanism of cytotoxic dose of Hep88 mAb-treated HepG2 cell at 24 hours. At 24 hours, up-regulation of pro-apoptotic protein i.e. *p53*, *Bax*, *caspase-9* and *caspase -3* were strikingly detected. On the other hand, down-regulation of anti-apoptosis *Bcl-2* and paraptosis engagement protein, *cathepsin B* was conversely remarked. This is well correlate with our previous report that the fastest mechanism, the predominant death morphology verification. All of the results from this study confirm the cytotoxic mechanism of Hep88 mAb that it triggered HCC to be death via the paraptosis till apoptosis.

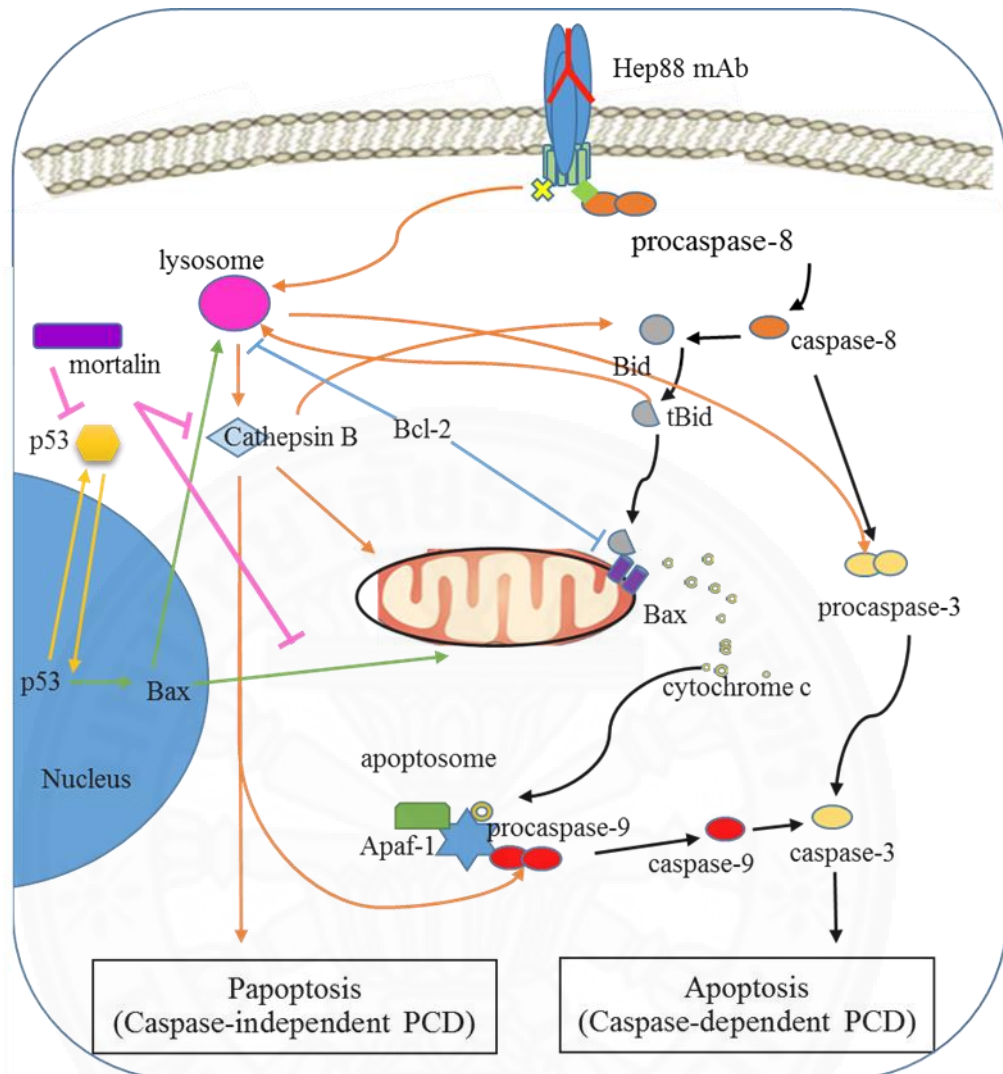


Figure 5.8 The proposed mechanism of IC50 dose of Hep88 mAb-treated HepG2 cell at 6 hours. HepG2 was treated with Hep88 mAb for 6 hours. The cancer cell try to escape the death induction of Hep88 mAb-treated HepG2 cell by up-regulated *Bcl-2* expression. MOMP and LMP were suppressed to release cytochrome c and cathepsin B by *Bcl-2* activity. However, the death induction was still induced through extrinsic apoptotic PCD.

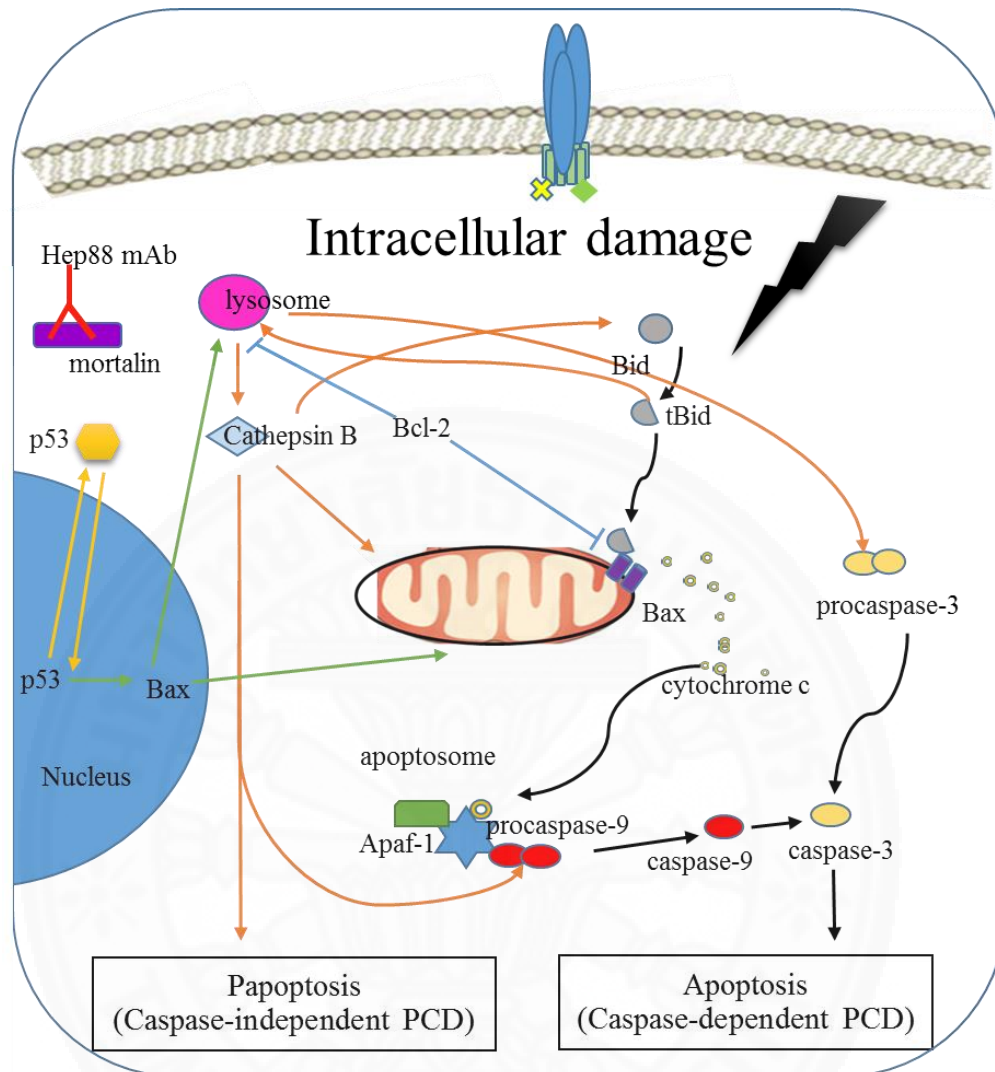


Figure 5.10 The proposed mechanism of IC50 dose of Hep88 mAb-treated HepG2 cell at 12 hours. HepG2 was treated with Hep88 mAb for 12 hours. The expression of *p53* was still up-regulated in small amount than previously time point to induces transcription-dependent apoptosis through transcriptional activation of pro-apoptotic gene *Bax*. The expression of *Bax* and *caspase-9* gene was correlated well with *p53* up-regulation. However, *Bcl-2* expression was still overexpressed. On the other hand, *caspase-9* expression was up-regulated. It possible that *Bax* was oligomerized to generate MOMP and release cytochrome c to cytosol. The death induction was induced through mitochondria mediated caspase that lead to apoptosis.

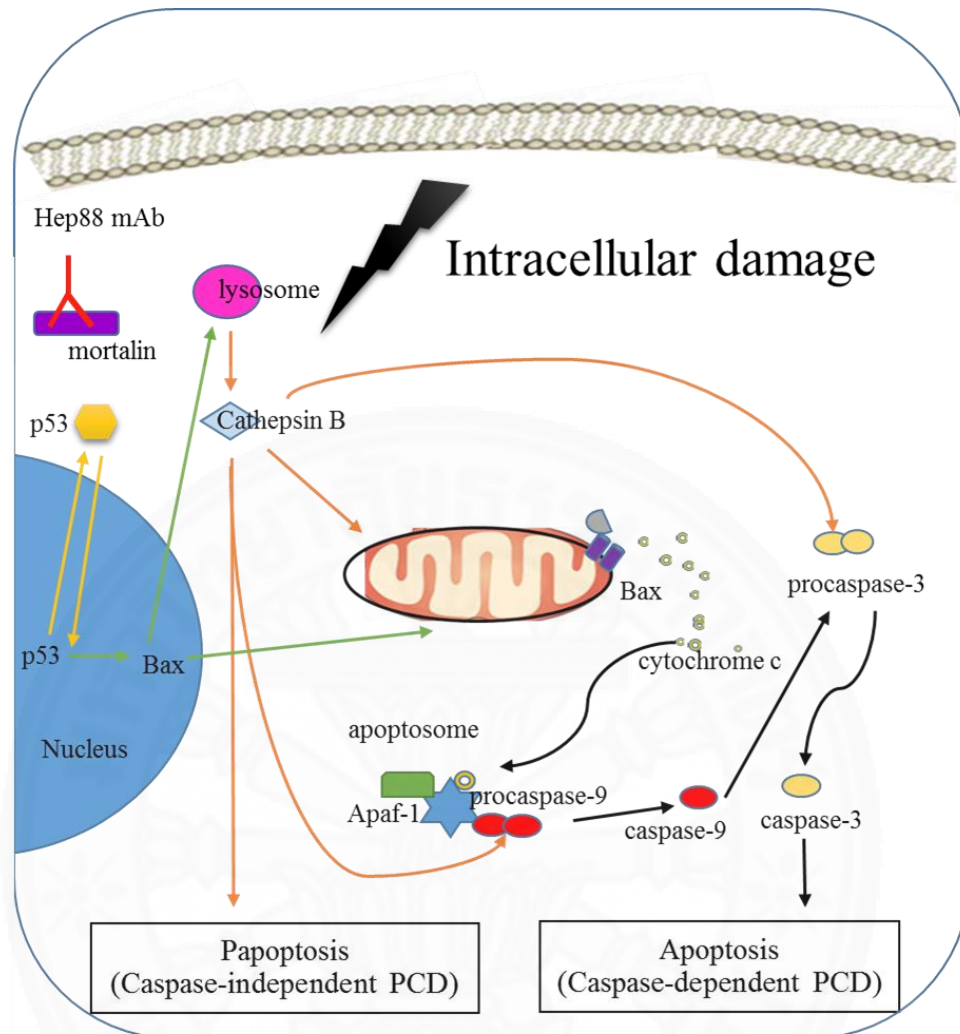


Figure 5.11 The proposed mechanism of IC₅₀ dose of Hep88 mAb-treated HepG2 cell at 18 hours. HepG2 was treated with Hep88 mAb for 18 hours. The expression of *p53* was up-regulated again and lead to up-regulated *Bax* and *caspase-9* gene. The death induction in HepG2 cell was induced through mitochondria mediated-caspase that can lead to apoptosis by Hep88 mAb. However, the induction wasn't strong enough to activate *caspase-3* transcription and activation to apoptosis.

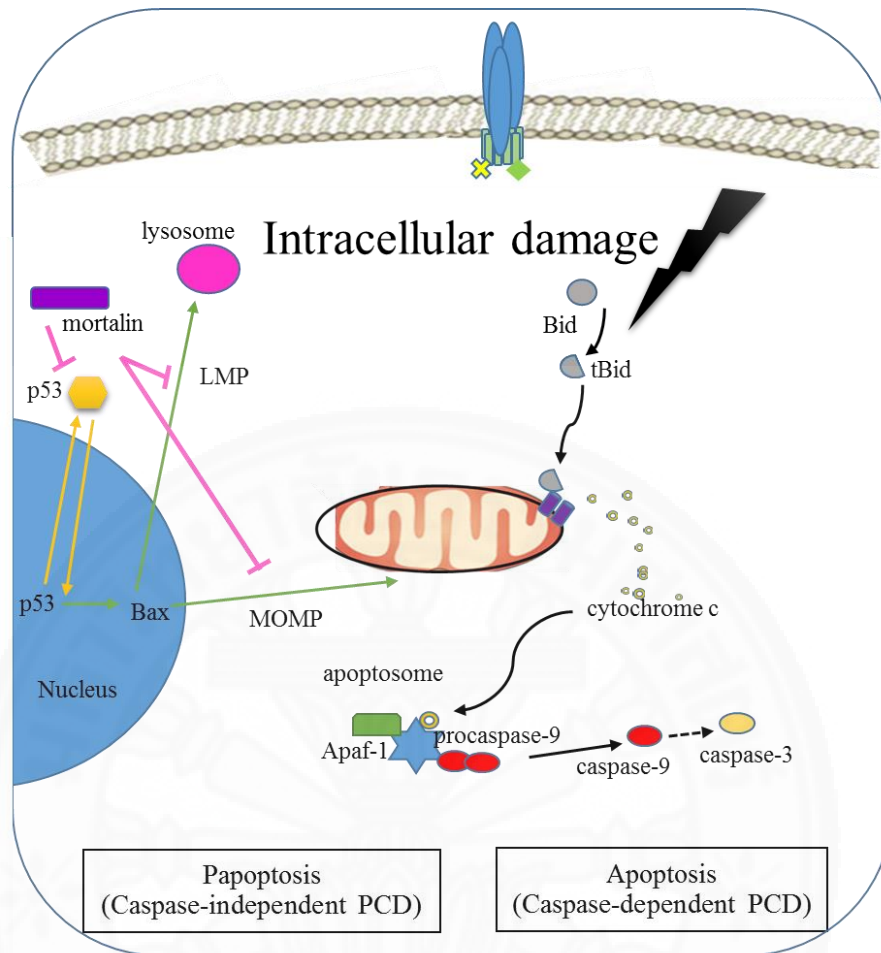


Figure 5.12 The proposed mechanism of IC₅₀ dose of Hep88 mAb-treated HepG2 cell at 24 hours. HepG2 was treated with Hep88 mAb for 24 hours. At this moment, *cathepsin B* and *Bcl-2* expression were down-regulated. This might be possible that mortalin is increased by intracellular stress and sequestered to cytoplasmic p53. p53 can't translocate into nucleus. So, p53 was down-regulated. Moreover, *Bax*, and *caspase-3* expression was also down-regulated. The *caspase-9* expression was shown decrease than the earlier time point, but it still up-regulated.

REFERENCES

- Agarwal, M. L., Agarwal, A., Taylor, W. R., & Stark, G. R. (1995). p53 controls both the G2/M and the G1 cell cycle checkpoints and mediates reversible growth arrest in human fibroblasts. *Proc Natl Acad Sci U S A*, *92*(18), 8493-8497.
- Altekruse, S. F., McGlynn, K. A., & Reichman, M. E. (2009). Hepatocellular carcinoma incidence, mortality, and survival trends in the United States from 1975 to 2005. *J Clin Oncol*, *27*(9), 1485-1491. doi: 10.1200/JCO.2008.20.7753
- Bhoopathi, P., Chetty, C., Gujrati, M., Dinh, D. H., Rao, J. S., & Lakka, S. (2010). Cathepsin B facilitates autophagy-mediated apoptosis in SPARC overexpressed primitive neuroectodermal tumor cells. *Cell Death Differ*, *17*(10), 1529-1539. doi: 10.1038/cdd.2010.28
- Boya, P., & Kroemer, G. (2008). Lysosomal membrane permeabilization in cell death. *Oncogene*, *27*(50), 6434-6451. doi: 10.1038/onc.2008.310
- Broker, L. E., Kruyt, F. A., & Giaccone, G. (2005). Cell death independent of caspases: a review. *Clin Cancer Res*, *11*(9), 3155-3162. doi: 10.1158/1078-0432.CCR-04-2223
- Bruix, J., & Sherman, M. (2005). Management of hepatocellular carcinoma. *Hepatology*, *42*(5), 1208-1236. doi: Doi 10.1002/Hep20933
- Buron, N., Porceddu, M., Brabant, M., Desgue, D., Racœur, C., Lassalle, M., . . . Borgne-Sanchez, A. (2010). Use of human cancer cell lines mitochondria to explore the mechanisms of BH3 peptides and ABT-737-induced mitochondrial membrane permeabilization. *PLoS One*, *5*(3), e9924. doi: 10.1371/journal.pone.0009924
- Byam, J., Renz, J., & Millis, J. M. (2013). Liver transplantation for hepatocellular carcinoma. *Hepatobiliary Surg Nutr*, *2*(1), 22-30. doi: 10.3978/j.issn.2304-3881.2012.11.03
- Cheng, C. C., Lai, Y. C., Lai, Y. S., Hsu, Y. H., Chao, W. T., Sia, K. C., . . . Liu, Y. H. (2015). Transient knockdown-mediated deficiency in plectin alters hepatocellular motility in association with activated FAK and Rac1-GTPase. *Cancer Cell International*, *15*, 29. doi: 10.1186/s12935-015-0177-1

- Chevaliez, S., & Pawlotsky, J. M. (2006). HCV Genome and Life Cycle. In S. L. Tan (Ed.), *Hepatitis C Viruses: Genomes and Molecular Biology*. Norfolk (UK).
- Chipuk, J. E., & Green, D. R. (2005). Do inducers of apoptosis trigger caspase-independent cell death? *Nat Rev Mol Cell Biol*, 6(3), 268-275. doi: 10.1038/nrm1573
- Chipuk, J. E., & Green, D. R. (2008). How do BCL-2 proteins induce mitochondrial outer membrane permeabilization? *Trends Cell Biol*, 18(4), 157-164. doi: 10.1016/j.tcb.2008.01.007
- Cho, S., Lee, J. H., Cho, S. B., Yoon, K. W., Park, S. Y., Lee, W. S., . . . Rew, J. S. (2010). Epigenetic methylation and expression of caspase 8 and survivin in hepatocellular carcinoma. *Pathol Int*, 60(3), 203-211. doi: 10.1111/j.1440-1827.2009.02507.x
- Crescence, L., Beraud, E., Sbarra, V., Bernard, J. P., Lombardo, D., & Mas, E. (2012). Targeting a novel onco-glycoprotein antigen at tumoral pancreatic cell surface by mAb16D10 induces cell death. *J Immunol*, 189(7), 3386-3396. doi: 10.4049/jimmunol.1102647
- Danaila, L., Popescu, I., Pais, V., Riga, D., Riga, S., & Pais, E. (2013). Apoptosis, paraptosis, necrosis, and cell regeneration in posttraumatic cerebral arteries. *Chirurgia (Bucur)*, 108(3), 319-324.
- Darzynkiewicz, Z., Halicka, H. D., & Zhao, H. (2010). Analysis of cellular DNA content by flow and laser scanning cytometry. *Adv Exp Med Biol*, 676, 137-147.
- de Weers, M., Tai, Y. T., van der Veer, M. S., Bakker, J. M., Vink, T., Jacobs, D. C., . . . Parren, P. W. (2011). Daratumumab, a novel therapeutic human CD38 monoclonal antibody, induces killing of multiple myeloma and other hematological tumors. *J Immunol*, 186(3), 1840-1848. doi: 10.4049/jimmunol.1003032
- Del Puerto, H. L., Martins, A. S., Moro, L., Milsted, A., Alves, F., Braz, G. F., & Vasconcelos, A. C. (2010). Caspase-3/-8/-9, Bax and Bcl-2 expression in the cerebellum, lymph nodes and leukocytes of dogs naturally infected with canine distemper virus. *Genet Mol Res*, 9(1), 151-161. doi: 10.4238/vol9-1gmr717
- Douarre, C., Gomez, D., Morjani, H., Zahm, J. M., O'Donohue M, F., Eddabra, L., . . . Trentesaux, C. (2005). Overexpression of Bcl-2 is associated with apoptotic

- resistance to the G-quadruplex ligand 12459 but is not sufficient to confer resistance to long-term senescence. *Nucleic Acids Res*, 33(7), 2192-2203. doi: 10.1093/nar/gki514
- Du, C., Fang, M., Li, Y., Li, L., & Wang, X. (2000). Smac, a mitochondrial protein that promotes cytochrome c-dependent caspase activation by eliminating IAP inhibition. *Cell*, 102(1), 33-42.
- El-Serag, H. B. (2012). Epidemiology of viral hepatitis and hepatocellular carcinoma. *Gastroenterology*, 142(6), 1264-1273 e1261. doi: 10.1053/j.gastro.2011.12.061
- Eletto, D., Eletto, D., Dersh, D., Gidalevitz, T., & Argon, Y. (2014). Protein disulfide isomerase A6 controls the decay of IRE1alpha signaling via disulfide-dependent association. *Mol Cell*, 53(4), 562-576. doi: 10.1016/j.molcel.2014.01.004
- Elmore, S. (2007). Apoptosis: a review of programmed cell death. *Toxicol Pathol*, 35(4), 495-516. doi: 10.1080/01926230701320337
- Erkan, E., Devarajan, P., & Schwartz, G. J. (2007). Mitochondria are the major targets in albumin-induced apoptosis in proximal tubule cells. *J Am Soc Nephrol*, 18(4), 1199-1208. doi: 10.1681/ASN.2006040407
- Estaquier, J., Vallette, F., Vayssiere, J.-L., & Mignotte, B. (2012). The Mitochondrial Pathways of Apoptosis. In R. Scatena, P. Bottoni & B. Giardina (Eds.), *Advances in Mitochondrial Medicine* (Vol. 942, pp. 157-183): Springer Netherlands.
- Ferlay, J., Shin, H. R., Bray, F., Forman, D., Mathers, C., & Parkin, D. M. (2010). Estimates of worldwide burden of cancer in 2008: GLOBOCAN 2008. *Int J Cancer*, 127(12), 2893-2917. doi: 10.1002/ijc.25516
- Foghsgaard, L., Wissing, D., Mauch, D., Lademann, U., Bastholm, L., Boes, M., . . . Jaattela, M. (2001). Cathepsin B acts as a dominant execution protease in tumor cell apoptosis induced by tumor necrosis factor. *J Cell Biol*, 153(5), 999-1010.
- Gao, Y., Yue, W., Zhang, P., Li, L., Xie, X., Yuan, H., . . . Pei, X. (2005). Spindlin1, a novel nuclear protein with a role in the transformation of NIH3T3 cells. *Biochem Biophys Res Commun*, 335(2), 343-350. doi: 10.1016/j.bbrc.2005.07.087

- Gondi, C. S., & Rao, J. S. (2013). Cathepsin B as a cancer target. *Expert Opin Ther Targets*, *17*(3), 281-291. doi: 10.1517/14728222.2013.740461
- Guicciardi, M. E., Deussing, J., Miyoshi, H., Bronk, S. F., Svingen, P. A., Peters, C., . . . Gores, G. J. (2000). Cathepsin B contributes to TNF-alpha-mediated hepatocyte apoptosis by promoting mitochondrial release of cytochrome c. *J Clin Invest*, *106*(9), 1127-1137. doi: 10.1172/JCI9914
- Guo, W. J., Chen, T. S., Wang, X. P., & Chen, R. (2010). Taxol induces concentration-dependent apoptotic and paraptosis-like cell death in human lung adenocarcinoma (ASTC-a-1) cells. *J Xray Sci Technol*, *18*(3), 293-308. doi: 10.3233/XST-2010-0261
- Gupta, R. K., Banerjee, A., Pathak, S., Sharma, C., & Singh, N. (2013). Induction of mitochondrial-mediated apoptosis by *Morinda citrifolia* (Noni) in human cervical cancer cells. *Asian Pac J Cancer Prev*, *14*(1), 237-242.
- Gupta, S., Kass, G. E., Szegezdi, E., & Joseph, B. (2009). The mitochondrial death pathway: a promising therapeutic target in diseases. *J Cell Mol Med*, *13*(6), 1004-1033. doi: 10.1111/j.1582-4934.2009.00697.x
- Handayani, T., Sakinah, S., Nallappan, M., & Pihie, A. H. (2007). Regulation of p53-, Bcl-2- and caspase-dependent signaling pathway in xanthorrhizol-induced apoptosis of HepG2 hepatoma cells. *Anticancer Res*, *27*(2), 965-971.
- Iyer, S., La-Borde, P. J., Payne, K. A., Parsons, M. R., Turner, A. J., Isaac, R. E., & Acharya, K. R. (2015). Crystal structure of X-prolyl aminopeptidase from *Caenorhabditis elegans*: A cytosolic enzyme with a di-nuclear active site. *FEBS Open Bio*, *5*, 292-302. doi: 10.1016/j.fob.2015.03.013
- Jedema, I., Barge, R. M., van der Velden, V. H., Nijmeijer, B. A., van Dongen, J. J., Willemze, R., & Falkenburg, J. H. (2004). Internalization and cell cycle-dependent killing of leukemic cells by Gemtuzumab Ozogamicin: rationale for efficacy in CD33-negative malignancies with endocytic capacity. *Leukemia*, *18*(2), 316-325. doi: 10.1038/sj.leu.2403205
- Jemal, A., Siegel, R., Ward, E., Hao, Y., Xu, J., Murray, T., & Thun, M. J. (2008). Cancer statistics, 2008. *CA Cancer J Clin*, *58*(2), 71-96. doi: 10.3322/CA.2007.0010

- Johansson, A. C., Appelqvist, H., Nilsson, C., Ka°gedal, K., Roberg, K., & O' llinger, K. (2010). Regulation of apoptosis-associated lysosomal membrane permeabilization. *Apoptosis*, 5(15), 527–540. doi: 10.1007/s10495-009-0452-5
- Joy, B., Sivadasan, R., Abraham, T. E., John, M., Sobhan, P. K., Seervi, M., & T, R. S. (2010). Lysosomal destabilization and cathepsin B contributes for cytochrome c release and caspase activation in embelin-induced apoptosis. *Mol Carcinog*, 49(4), 324-336. doi: 10.1002/mc.20599
- Kaul, S. C., Aida, S., Yaguchi, T., Kaur, K., & Wadhwa, R. (2005). Activation of wild type p53 function by its mortalin-binding, cytoplasmically localizing carboxyl terminus peptides. *Journal of Biological Chemistry*, 280(47), 39373-39379. doi: DOI 10.1074/jbc.M500022200
- Keinan, N., Tyomkin, D., & Shoshan-Barmatz, V. (2010). Oligomerization of the mitochondrial protein voltage-dependent anion channel is coupled to the induction of apoptosis. *Mol Cell Biol*, 30(24), 5698-5709. doi: 10.1128/MCB.00165-10
- Kelekar, A., & Thompson, C. B. (1998). Bcl-2-family proteins: the role of the BH3 domain in apoptosis. *Trends Cell Biol*, 8(8), 324-330.
- Kew, M. C. (2013). Aflatoxins as a cause of hepatocellular carcinoma. *J Gastrointestin Liver Dis*, 22(3), 305-310.
- Kischkel, F. C., Hellbardt, S., Behrmann, I., Germer, M., Pawlita, M., Krammer, P. H., & Peter, M. E. (1995). Cytotoxicity-dependent APO-1 (Fas/CD95)-associated proteins form a death-inducing signaling complex (DISC) with the receptor. *EMBO J*, 14(22), 5579-5588.
- Kohler, G., & Milstein, C. (1975). Continuous cultures of fused cells secreting antibody of predefined specificity. *Nature*, 256(5517), 495-497.
- Kook, S. H., Son, Y. O., Chung, S. W., Lee, S. A., Kim, J. G., Jeon, Y. M., & Lee, J. C. (2007). Caspase-independent death of human osteosarcoma cells by flavonoids is driven by p53-mediated mitochondrial stress and nuclear translocation of AIF and endonuclease G. *Apoptosis*, 12(7), 1289-1298. doi: 10.1007/s10495-007-0056-x

- Kordestani, R., Mirshafiee, H., Hosseini, S. M., & Sharifi, Z. (2014). Effect of Hepatitis B Virus X Gene on the Expression Level of p53 Gene using Hep G2 Cell Line. *Avicenna J Med Biotechnol*, 6(1), 3-9.
- Kovtun, Y. V., & Goldmacher, V. S. (2007). Cell killing by antibody-drug conjugates. *Cancer Lett*, 255(2), 232-240. doi: 10.1016/j.canlet.2007.04.010
- Kruidering, M., & Evan, G. I. (2000). Caspase-8 in apoptosis: the beginning of "the end"? *IUBMB Life*, 50(2), 85-90. doi: 10.1080/713803693
- Laohathai, K., & Bhamarapravati, N. (1985). Culturing of human hepatocellular carcinoma. A simple and reproducible method. *Am J Pathol*, 118(2), 203-208.
- Lauring, A. S., & Andino, R. (2010). Quasispecies theory and the behavior of RNA viruses. *PLoS Pathog*, 6(7), e1001005. doi: 10.1371/journal.ppat.1001005
- Li, B., Zhao, J., Wang, C. Z., Searle, J., He, T. C., Yuan, C. S., & Du, W. (2011). Ginsenoside Rh2 induces apoptosis and paraptosis-like cell death in colorectal cancer cells through activation of p53. *Cancer Lett*, 301(2), 185-192. doi: 10.1016/j.canlet.2010.11.015
- Li, W., Wang, Y., Song, Y., Xu, L., Zhao, J., & Fang, B. (2015). A preliminary study of the effect of curcumin on the expression of p53 protein in a human multiple myeloma cell line. *Oncol Lett*, 9(4), 1719-1724. doi: 10.3892/ol.2015.2946
- Liang, T. J. (2009). Hepatitis B: the virus and disease. *Hepatology*, 49(5 Suppl), S13-21. doi: 10.1002/hep.22881
- Lin, C. H., Lu, W. C., Wang, C. W., Chan, Y. C., & Chen, M. K. (2013). Capsaicin induces cell cycle arrest and apoptosis in human KB cancer cells. *BMC Complement Altern Med*, 13, 46. doi: 10.1186/1472-6882-13-46
- Liu, T., Chen, H., Kim, H., Huen, M. S., Chen, J., & Huang, J. (2012). RAD18-BRCTx interaction is required for efficient repair of UV-induced DNA damage. *DNA Repair (Amst)*, 11(2), 131-138. doi: 10.1016/j.dnarep.2011.10.012
- Liu, Y. H., Cheng, C. C., Ho, C. C., Chao, W. T., Pei, R. J., Hsu, Y. H., . . . Lai, Y. S. (2008). Degradation of plectin with modulation of cytokeratin 18 in human liver cells during staurosporine-induced apoptosis. *In Vivo*, 22(5), 543-548.
- Liu, Y. Q., Li, Y., Qin, J., Wang, Q., She, Y. L., Luo, Y. L., . . . Xie, X. D. (2014). Matrine reduces proliferation of human lung cancer cells by inducing apoptosis

- and changing miRNA expression profiles. *Asian Pac J Cancer Prev*, 15(5), 2169-2177.
- Llovet, J. M., Schwartz, M., & Mazzaferro, V. (2005). Resection and liver transplantation for hepatocellular carcinoma. *Semin Liver Dis*, 25(2), 181-200. doi: 10.1055/s-2005-871198
- Lv, J., Yu, Y. Q., Li, S. Q., Luo, L., & Wang, Q. (2014). Aflatoxin B1 promotes cell growth and invasion in hepatocellular carcinoma HepG2 cells through H19 and E2F1. *Asian Pac J Cancer Prev*, 15(6), 2565-2570.
- Malhi, H., Guicciardi, M. E., & Gores, G. J. (2010). Hepatocyte death: a clear and present danger. *Physiol Rev*, 90(3), 1165-1194. doi: 10.1152/physrev.00061.2009
- Manochantr, S., Puthong, S., Gamnarai, P., Roittrakul, S., Kittisenachai, S., Kangsadalampai, S., & Rojpibulstit, P. (2011). Hep 88 mAB induced ultrastructural alteration through apoptosis like program cell death in hepatocellular carcinoma. *J Med Assoc Thai*, 94 Suppl 7, S109-116.
- Martinelli, E., De Palma, R., Orbitura, M., De Vita, F., & Ciardiello, F. (2009). Anti-epidermal growth factor receptor monoclonal antibodies in cancer therapy. *Clin Exp Immunol*, 158(1), 1-9. doi: 10.1111/j.1365-2249.2009.03992.x
- Minguez, B., Tovar, V., Chiang, D., Villanueva, A., & Llovet, J. M. (2009). Pathogenesis of hepatocellular carcinoma and molecular therapies. *Curr Opin Gastroenterol*, 25(3), 186-194. doi: 10.1097/MOG.0b013e32832962a1
- Morchang, A., Panaampon, J., Suttitheptumrong, A., Yasamut, U., Noisakran, S., Yenchitsomanus, P. T., & Limjindaporn, T. (2013). Role of cathepsin B in dengue virus-mediated apoptosis. *Biochem Biophys Res Commun*, 438(1), 20-25. doi: 10.1016/j.bbrc.2013.07.009
- Munagala, R., Kausar, H., Munjal, C., & Gupta, R. C. (2011). Withaferin A induces p53-dependent apoptosis by repression of HPV oncogenes and upregulation of tumor suppressor proteins in human cervical cancer cells. *Carcinogenesis*, 32(11), 1697-1705. doi: 10.1093/carcin/bgr192
- Muntener, K., Zwicky, R., Csucs, G., Rohrer, J., & Baici, A. (2004). Exon skipping of cathepsin B: mitochondrial targeting of a lysosomal peptidase provokes cell death. *J Biol Chem*, 279(39), 41012-41017. doi: 10.1074/jbc.M405333200

- Murakami, Y., Saigo, K., Takashima, H., Minami, M., Okanou, T., Brechot, C., & Paterlini-Brechot, P. (2005). Large scaled analysis of hepatitis B virus (HBV) DNA integration in HBV related hepatocellular carcinomas. *Gut*, *54*(8), 1162-1168. doi: 10.1136/gut.2004.054452
- Oberle, C., Huai, J., Reinheckel, T., Tacke, M., Rassner, M., Ekert, P. G., . . . Borner, C. (2010). Lysosomal membrane permeabilization and cathepsin release is a Bax/Bak-dependent, amplifying event of apoptosis in fibroblasts and monocytes. *Cell Death Differ*, *17*(7), 1167-1178. doi: 10.1038/cdd.2009.214
- Osaki, Y., & Nishikawa, H. (2014). Treatment for hepatocellular carcinoma in Japan over the last three decades: Our experience and published work review. *Hepatol Res*. doi: 10.1111/hepr.12378
- Pan, L. L., Wang, A. Y., Huang, Y. Q., Luo, Y., & Ling, M. (2014). Mangiferin induces apoptosis by regulating Bcl-2 and Bax expression in the CNE2 nasopharyngeal carcinoma cell line. *Asian Pac J Cancer Prev*, *15*(17), 7065-7068.
- Pang, T. C., & Lam, V. W. (2015). Surgical management of hepatocellular carcinoma. *World J Hepatol*, *7*(2), 245-252. doi: 10.4254/wjh.v7.i2.245
- Park, H. H. (2012). Structural features of caspase-activating complexes. *Int J Mol Sci*, *13*(4), 4807-4818. doi: 10.3390/ijms13044807
- Pavlidis, E. T., & Pavlidis, T. E. (2013). Role of bevacizumab in colorectal cancer growth and its adverse effects: a review. *World J Gastroenterol*, *19*(31), 5051-5060. doi: 10.3748/wjg.v19.i31.5051
- Pfaffl, M. W., & Hageleit, M. (2001). Validities of mRNA quantification using recombinant RNA and recombinant DNA external calibration curves in real-time RT-PCR. *Biotechnology Letters*, *23*(4), 275-282. doi: 10.1023/A:1005658330108
- Puthong, S., Rojpibulstit, P., & Buakeaw, A. (2009). Cytotoxic effect of Hep88 mAb: a novel monoclonal antibody against hepatocellular carcinoma. *Thammasat Int. J. Sc. Tech*, *14*(1), 95-104.
- Riccio, M., Di Giaimo, R., Pianetti, S., Palmieri, P. P., Melli, M., & Santi, S. (2001). Nuclear localization of cystatin B, the cathepsin inhibitor implicated in myoclonus epilepsy (EPM1). *Exp Cell Res*, *262*(2), 84-94. doi: 10.1006/excr.2000.5085

- Rojpibulstit, P., Kittisenachai, S., Puthong, S., Manochantr, S., Gamnarai, P., Jitrapakdee, S., & Roytrakul, S. (2014). Hep88 mAb-initiated paraptosis-like PCD pathway in hepatocellular carcinoma cell line through the binding of mortalin (HSPA9) and alpha-enolase. *Cancer Cell International*, *14*. doi: Artn 69 Doi 10.1186/S12935-014-0069-9
- Ruchalski, K., Mao, H., Li, Z., Wang, Z., Gillers, S., Wang, Y., . . . Borkan, S. C. (2006). Distinct hsp70 domains mediate apoptosis-inducing factor release and nuclear accumulation. *J Biol Chem*, *281*(12), 7873-7880. doi: 10.1074/jbc.M513728200
- Salvesen, G. S., & Riedl, S. J. (2008). Caspase mechanisms. *Adv Exp Med Biol*, *615*, 13-23. doi: 10.1007/978-1-4020-6554-5_2
- Sartorius, U. A., & Krammer, P. H. (2002). Upregulation of Bcl-2 is involved in the mediation of chemotherapy resistance in human small cell lung cancer cell lines. *Int J Cancer*, *97*(5), 584-592.
- Sasatani, M., Xu, Y., Kawai, H., Cao, L., Tateishi, S., Shimura, T., . . . Kamiya, K. (2015). RAD18 activates the G2/M checkpoint through DNA damage signaling to maintain genome integrity after ionizing radiation exposure. *PLoS One*, *10*(2), e0117845. doi: 10.1371/journal.pone.0117845
- Selim, M. E., & Hendi, A. A. (2012). Gold nanoparticles induce apoptosis in MCF-7 human breast cancer cells. *Asian Pac J Cancer Prev*, *13*(4), 1617-1620.
- Sergio, A., Cristofori, C., Cardin, R., Pivetta, G., Ragazzi, R., Baldan, A., . . . Farinati, F. (2008). Transcatheter arterial chemoembolization (TACE) in hepatocellular carcinoma (HCC): the role of angiogenesis and invasiveness. *Am J Gastroenterol*, *103*(4), 914-921. doi: 10.1111/j.1572-0241.2007.01712.x
- Smela, M. E., Currier, S. S., Bailey, E. A., & Essigmann, J. M. (2001). The chemistry and biology of aflatoxin B(1): from mutational spectrometry to carcinogenesis. *Carcinogenesis*, *22*(4), 535-545.
- Solozobova, V., Rolletschek, A., & Blattner, C. (2009). Nuclear accumulation and activation of p53 in embryonic stem cells after DNA damage. *BMC Cell Biol*, *10*, 46. doi: 10.1186/1471-2121-10-46

- Somboon, K., Siramolpiwat, S., & Vilaichone, R. K. (2014). Epidemiology and survival of hepatocellular carcinoma in the central region of Thailand. *Asian Pac J Cancer Prev*, *15*(8), 3567-3570.
- Sperandio, S., Poksay, K., de Belle, I., Lafuente, M. J., Liu, B., Nasir, J., & Bredesen, D. E. (2004). Paraptosis: mediation by MAP kinases and inhibition by AIP-1/Alix. *Cell Death Differ*, *11*(10), 1066-1075. doi: 10.1038/sj.cdd.4401465
- Srivatanakul, P., Sriplung, H., & Deerasmee, S. (2004). Epidemiology of liver cancer: An Overview. *Asian Pac J Cancer Prev*(5), 118-125.
- Stankiewicz, A. R., Lachapelle, G., Foo, C. P., Radicioni, S. M., & Mosser, D. D. (2005). Hsp70 inhibits heat-induced apoptosis upstream of mitochondria by preventing Bax translocation. *J Biol Chem*, *280*(46), 38729-38739. doi: 10.1074/jbc.M509497200
- Starenki, D., Hong, S. K., Lloyd, R. V., & Park, J. I. (2014). Mortalin (GRP75/HSPA9) upregulation promotes survival and proliferation of medullary thyroid carcinoma cells. *Oncogene*. doi: 10.1038/onc.2014.392
- Stoka, V., Turk, B., & Turk, V. (2005). Lysosomal cysteine proteases: structural features and their role in apoptosis. *IUBMB Life*, *57*(4-5), 347-353. doi: 10.1080/15216540500154920
- Sun, S., Lee, D., Ho, A. S., Pu, J. K., Zhang, X. Q., Lee, N. P., . . . Leung, G. K. (2013). Inhibition of prolyl 4-hydroxylase, beta polypeptide (P4HB) attenuates temozolomide resistance in malignant glioma via the endoplasmic reticulum stress response (ERSR) pathways. *Neuro Oncol*, *15*(5), 562-577. doi: 10.1093/neuonc/not005
- Szegezdi, E., Macdonald, D. C., Ni Chonghaile, T., Gupta, S., & Samali, A. (2009). Bcl-2 family on guard at the ER. *Am J Physiol Cell Physiol*, *296*(5), C941-953. doi: 10.1152/ajpcell.00612.2008
- Tan, G. J., Peng, Z. K., Lu, J. P., & Tang, F. Q. (2013). Cathepsins mediate tumor metastasis. *World J Biol Chem*, *4*(4), 91-101. doi: 10.4331/wjbc.v4.i4.91
- Tardy, C., Codogno, P., Autefage, H., Levade, T., & Andrieu-Abadie, N. (2006). Lysosomes and lysosomal proteins in cancer cell death (new players of an old struggle). *Biochim Biophys Acta*, *1765*(2), 101-125. doi: 10.1016/j.bbcan.2005.11.003

- Tarze, A., Deniaud, A., Le Bras, M., Maillier, E., Molle, D., Larochette, N., . . . Brenner, C. (2007). GAPDH, a novel regulator of the pro-apoptotic mitochondrial membrane permeabilization. *Oncogene*, *26*(18), 2606-2620. doi: 10.1038/sj.onc.1210074
- Taurin, S., Seyrantepe, V., Orlov, S. N., Tremblay, T. L., Thibault, P., Bennett, M. R., . . . Pshezhetsky, A. V. (2002). Proteome analysis and functional expression identify mortalin as an antiapoptotic gene induced by elevation of $[Na^+]_i/[K^+]_i$ ratio in cultured vascular smooth muscle cells. *Circ Res*, *91*(10), 915-922.
- Tawa, P., Hell, K., Giroux, A., Grimm, E., Han, Y., Nicholson, D. W., & Xanthoudakis, S. (2004). Catalytic activity of caspase-3 is required for its degradation: stabilization of the active complex by synthetic inhibitors. *Cell Death Differ*, *11*(4), 439-447. doi: 10.1038/sj.cdd.4401360
- Thony, B., Neuheiser, F., Blau, N., & Heizmann, C. W. (1995). Characterization of the human PCBD gene encoding the bifunctional protein pterin-4 alpha-carbinolamine dehydratase/dimerization cofactor for the transcription factor HNF-1 alpha. *Biochem Biophys Res Commun*, *210*(3), 966-973. doi: 10.1006/bbrc.1995.1751
- Topalian, S. L., Weiner, G. J., & Pardoll, D. M. (2011). Cancer immunotherapy comes of age. *J Clin Oncol*, *29*(36), 4828-4836. doi: 10.1200/JCO.2011.38.0899
- Tseng, T. C., Liu, C. J., Yang, H. C., Su, T. H., Wang, C. C., Chen, C. L., . . . Kao, J. H. (2012). High levels of hepatitis B surface antigen increase risk of hepatocellular carcinoma in patients with low HBV load. *Gastroenterology*, *142*(5), 1140-1149 e1143; quiz e1113-1144. doi: 10.1053/j.gastro.2012.02.007
- Turk, V., Stoka, V., Vasiljeva, O., Renko, M., Sun, T., Turk, B., & Turk, D. (2012). Cysteine cathepsins: from structure, function and regulation to new frontiers. *Biochim Biophys Acta*, *1824*(1), 68-88. doi: 10.1016/j.bbapap.2011.10.002
- Turk, V., Turk, B., & Turk, D. (2001). Lysosomal cysteine proteases: facts and opportunities. *EMBO J*, *20*(17), 4629-4633. doi: 10.1093/emboj/20.17.4629
- Vatanasapt, V., Sriamporn, S., & Vatanasapt, P. (2002). Cancer control in Thailand. *Jpn J Clin Oncol*, *32 Suppl*, S82-91.
- Vousden, K. H., & Lu, X. (2002). Live or let die: the cell's response to p53. *Nat Rev Cancer*, *2*(8), 594-604. doi: 10.1038/nrc864

- Wadhwa, R., Takano, S., Kaur, K., Deocaris, C. C., Pereira-Smith, O. M., Reddel, R. R., & Kaul, S. C. (2006). Upregulation of mortalin/mthsp70/Grp75 contributes to human carcinogenesis. *Int J Cancer*, *118*(12), 2973-2980. doi: 10.1002/ijc.21773
- Walker, C., Bottger, S., & Low, B. (2006). Mortalin-based cytoplasmic sequestration of p53 in a nonmammalian cancer model. *Am J Pathol*, *168*(5), 1526-1530. doi: 10.2353/ajpath.2006.050603
- Walter, R. B., Raden, B. W., Kamikura, D. M., Cooper, J. A., & Bernstein, I. D. (2005). Influence of CD33 expression levels and ITIM-dependent internalization on gemtuzumab ozogamicin-induced cytotoxicity. *Blood*, *105*(3), 1295-1302. doi: 10.1182/blood-2004-07-2784
- Wang, H., Zhang, J., Sit, W. H., Lee, C. Y., & Wan, J. M. (2014). Cordyceps cicadae induces G2/M cell cycle arrest in MHCC97H human hepatocellular carcinoma cells: a proteomic study. *Chin Med*, *9*, 15. doi: 10.1186/1749-8546-9-15
- Wang, W., Chen, Z., Mao, Z., Zhang, H., Ding, X., Chen, S., . . . Zhu, B. (2011). Nucleolar protein Spindlin1 recognizes H3K4 methylation and stimulates the expression of rRNA genes. *EMBO Rep*, *12*(11), 1160-1166. doi: 10.1038/embor.2011.184
- Wang, Y., Ji, P., Liu, J., Broaddus, R. R., Xue, F., & Zhang, W. (2009). Centrosome-associated regulators of the G(2)/M checkpoint as targets for cancer therapy. *Mol Cancer*, *8*, 8. doi: 10.1186/1476-4598-8-8
- Wang, Y. X., Cai, H., Jiang, G., Zhou, T. B., & Wu, H. (2014). Silibinin inhibits proliferation, induces apoptosis and causes cell cycle arrest in human gastric cancer MGC803 cells via STAT3 pathway inhibition. *Asian Pac J Cancer Prev*, *15*(16), 6791-6798.
- Wei, M. C., Lindsten, T., Mootha, V. K., Weiler, S., Gross, A., Ashiya, M., . . . Korsmeyer, S. J. (2000). tBID, a membrane-targeted death ligand, oligomerizes BAK to release cytochrome c. *Genes Dev*, *14*(16), 2060-2071.
- Wible, B. A., Wang, L., Kuryshv, Y. A., Basu, A., Haldar, S., & Brown, A. M. (2002). Increased K⁺ efflux and apoptosis induced by the potassium channel modulatory protein KChAP/PIAS3beta in prostate cancer cells. *J Biol Chem*, *277*(20), 17852-17862. doi: 10.1074/jbc.M201689200

- Wolf, B. B., Schuler, M., Echeverri, F., & Green, D. R. (1999). Caspase-3 is the primary activator of apoptotic DNA fragmentation via DNA fragmentation factor-45/inhibitor of caspase-activated DNase inactivation. *J Biol Chem*, *274*(43), 30651-30656.
- Yamaguchi, H., Bhalla, K., & Wang, H. G. (2003). Bax plays a pivotal role in thapsigargin-induced apoptosis of human colon cancer HCT116 cells by controlling Smac/Diablo and Omi/HtrA2 release from mitochondria. *Cancer Res*, *63*(7), 1483-1489.
- Yamamoto, J., Okada, S., Shimada, K., Okusaka, T., Yamasaki, S., Ueno, H., & Kosuge, T. (2001). Treatment strategy for small hepatocellular carcinoma: comparison of long-term results after percutaneous ethanol injection therapy and surgical resection. *Hepatology*, *34*(4 Pt 1), 707-713. doi: 10.1053/jhep.2001.27950
- Yang, B., Wang, Y. Q., Cheng, R. B., Chen, J. L., Chen, J., Jia, L. T., & Zhang, R. S. (2013). Induction of cytotoxicity and apoptosis in human gastric cancer cell SGC-7901 by isovaltrate acetoxymethine isolated from *Patrinia heterophylla* bunge involves a mitochondrial pathway and G2/M phase cell cycle arrest. *Asian Pac J Cancer Prev*, *14*(11), 6481-6486.
- Yang, J. D., & Roberts, L. R. (2010). Epidemiology and management of hepatocellular carcinoma. *Infect Dis Clin North Am*, *24*(4), 899-919, viii. doi: 10.1016/j.idc.2010.07.004
- Yang, N., Wang, W., Wang, Y., Wang, M., Zhao, Q., Rao, Z., . . . Xu, R. M. (2012). Distinct mode of methylated lysine-4 of histone H3 recognition by tandem tudor-like domains of Spindlin1. *Proc Natl Acad Sci U S A*, *109*(44), 17954-17959. doi: 10.1073/pnas.1208517109
- Yu, J., & Zhang, L. (2003). No PUMA, no death: implications for p53-dependent apoptosis. *Cancer Cell*, *4*(4), 248-249.
- Yuan, S., Yu, X., Topf, M., Ludtke, S. J., Wang, X., & Akey, C. W. (2010). Structure of an apoptosome-procaspase-9 CARD complex. *Structure*, *18*(5), 571-583. doi: 10.1016/j.str.2010.04.001

- Yuan, X.-M., Li, W., Dalen, H., Lotem, J., Kama, R., Sachs, L., & Brunk, U. T. (2002). Lysosomal destabilization in p53-induced apoptosis. *Proceedings of the National Academy of Sciences*, 99(9), 6286-6291.
- Zhou, H., Xu, M., Gao, Y., Deng, Z., Cao, H., Zhang, W., . . . Hu, T. (2014). Matrine induces caspase-independent program cell death in hepatocellular carcinoma through bid-mediated nuclear translocation of apoptosis inducing factor. *Mol Cancer*, 13, 59. doi: 10.1186/1476-4598-13-59
- Zhu, Y., Mao, Y., Chen, H., Lin, Y., Hu, Z., Wu, J., . . . Xie, L. (2013). Apigenin promotes apoptosis, inhibits invasion and induces cell cycle arrest of T24 human bladder cancer cells. *Cancer Cell International*, 13(1), 54. doi: 10.1186/1475-2867-13-54

The image features a large, faint watermark of the Thammasat University seal in the background. The seal is circular and contains a central emblem with a crown and a lotus flower, surrounded by Thai script and the English text "THAMMASAT UNIVERSITY".

APPENDICES

APPENDIX A

CHEMICAL REAGENTS PREPARATION

1. Protein extraction reagents

1.1 0.5% SDS

Sodium dodecylsulphate (SDS)	0.5	g
Deionized water	100.0	ml

2. Protein determination reagents

2.1 Lowry method

2.1.1 Alkaline copper solution

2.1.1.1 Solution A

$\text{CuSO}_4 \cdot 7\text{H}_2\text{O}$	40	mg
Sodium citrate dehydrate	100	mg
Deionized water	10.0	ml

2.1.1.2 Solution B

Sodium carbonate	2.0	g
Sodium hydroxide	0.4	g
Deionized water	100.0	ml

2.1.2 20% Folin-Ciocalteu phenol reagent

Folin-Ciocalteu phenol	10	ml
Deionized water	10	ml

3. SDS-PAGE preparation reagents

3.1 (5X) SDS-loading buffer

SDS	5.0	g
DTT	3.850	g
Bromophenol blue	0.012	g
1M Tris-HCl, pH 6.8	6.5	ml
87% Glycerol	25.0	ml
Deionized water	17.5	ml

3.2 (10X) Electrophoresis running buffer

Tris-base	3.0	g
Glycine	14.0	g
10% SDS	10.0	ml
Deionized water	add to 100.0	ml

3.3 5% Stacking gel

40% Acrylamide	0.200	ml
Deionized water	0.908	ml
10% SDS	0.015	ml
10% Ammonium persulphate	12.5	μ l
TEMED	0.85	μ l

3.4 12.5% Separating gel

40% Acrylamide	3.130	ml
Deionized water	4.230	ml
10% SDS	0.125	ml
10% Ammonium persulphate (APS)	50	μ l
TEMED	10	μ l

4. Silver staining reagents

4.1 Fixing solution

99.8% Methanol	100	ml
100% Acetic acid	24	ml
37% Formaldehyde	100	µl
Deionized water	add to 200	ml

4.2 Washing solution (35% ethanol)

95% ethanol	73	ml
Deionized water	add to 200	ml

4.3 Sensitizing solution (0.02% sodium thiosulfate)

Sodium thiosulfate	40	mg
Deionized water	add to 200	ml

4.4 Staining solution (0.2% silver nitrate)

Silver nitrate	0.4	g
Deionized water	add to 200	ml

4.5 Developing solution (6% Sodium carbonate)

Sodium carbonate	12	g
37% Formaldehyde	100	µl
0.02% Sodium thiosulfate	4	ml
Deionized water	add to 200	ml

4.6 Stopping solution (1.46% Sodium EDTA)

Sodium EDTA	2.92	g
Deionized water	add to 200	ml

5. In-gel digestion reagents**5.1 10mM Ammonium bicarbonate**

Ammonium bicarbonate	39.5 g
Deionized water	add to 50 ml

5.2 Reducing solution

DTT	15.42 mg
10mM Ammonium bicarbonate	10 ml

5.3 Alkylating solution

Iodoacetamide	185 mg
10mM Ammonium bicarbonate	10 ml

5.4 50% acetonitrile in 10 mM ammonium bicarbonate

100% Acetonitrile	5 ml
10mM Ammonium bicarbonate	5 ml

5.5 10 ng/ μ l Trypsin solution

Trypsin	10 mg
50% acetonitrile in 10 mM ammonium bicarbonate	1 ml

5.6 30% Acetonitrile

100% Acetonitrile	3 ml
Deionized water	7 ml

5.7 50% Acetonitrile

100% Acetonitrile	5 ml
Deionized water	5 ml

5.8 0.1% Formic acid

Formic acid	5 ml
Deionized water	5 ml

5.9 Peptide extraction solution

0.1% Formic acid	5 ml
100% Acetonitrile	5 ml

6. Chemicals lists

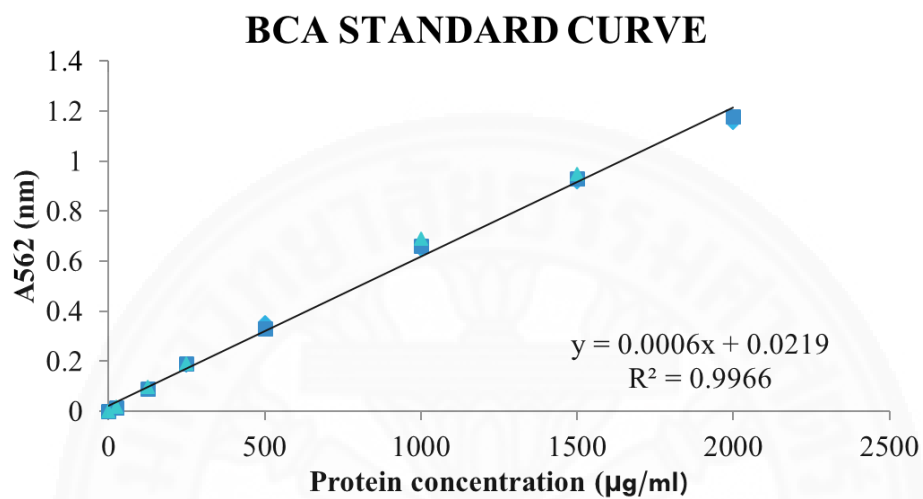
Water (LC grade)	(Labscan, Thailand)
Absolute Ethanol (AR grade)	(Labscan, Thailand)
Acetone	(Labscan, Thailand)
40% Acrylamide	(BIO-RAD, China)
Agarose	(BIO-active)
Ammonium persulfate (APS)	(USB corporation, USA)
Ammonium sulfate	(Sigma Aldrich, France)
Ammonium bicarbonate	(Sigma, USA)
Acetonitrile (AR grade)	(Labscan, Thailand)
β -mercaptoethanol	(GE Healthcare, Sweden)
Bovine serum albumin (BSA)	(Damsldt, Germany)
Bromophenol blue	(Sigma, USA)
Calcium chloride ($\text{CaCl}_2 \cdot 2\text{H}_2\text{O}$)	(BIO BASIC INC., Thailand)
Copper sulfate ($\text{CuSO}_4 \cdot 7\text{H}_2\text{O}$)	(Fisher scientific, UK)
Chloroform	(Labscan, Thailand)
DEPC treat-water	(USB corporation, USA)
Dithiothreitol (DTT)	(GE Healthcare, Sweden)
Folin-Ciocalteu phenol	(Merck, Germany)
37% Formaldehyde	(Sigma, USA)
Formic acid	(Scharlau, Spain)
Glycerol (87% w/w)	(GE Healthcare, UK)

Glacial acetic acid	(Labsan, Thailand)
Hydrochloric acid	(Labsan, Thailand)
Iodoacetamide (IAA)	(GE Healthcare, UK)
Isopropanol	(VWR International 201)
Mercaptoethanol	(GE Healthcare, Sweden)
Methanol (AR grade)	(Labsan, Thailand)
Phenol	(Amresco, Thailand)
Protein standard marker	(Bio-Sciences AB, Sweden)
Silver nitrate	(AppliChem, UK)
Sodium EDTA	(USB Corporation, USA)
Sodium citrate	(Merck, Germany)
Sodium chloride	(Labsan, Thailand)
Sodium carbonate	(Sigma, Germany)
Sodium hydroxide	(Saharlau, Spain)
Sodium dodecyl sulfate (SDS)	(Uppsala, Sweden)
Sodium thiosulfate	(Sigma, USA)
TEMED	(USB corporation, USA)
Tris-base	(USB corporation, USA)
Trypsin	(PROMEGA, USA)

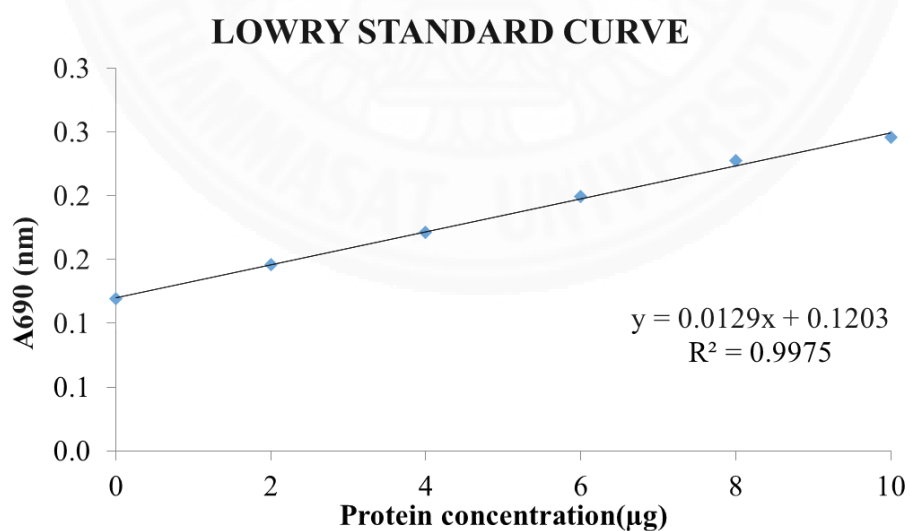
APPENDIX B

PROTEIN STANDARD CURVE

1. Protein standard curve of BCA method



2. Protein standard curve of Lowry method



APPENDIX C

PLASMID DNA PREPARATION

1. Competent cell preparation by Calcium chloride (CaCl₂) method

- 1.1. A colony of DH5 α from LB plate was inoculated in 3 ml of LB medium, then incubated overnight at 37°C shaking 200 rpm.
- 1.2. 1 ml of overnight grown culture of *E.coli* DH5 α was inoculated to 100 ml of LB medium and shaken at 37°C, 200 rpm until the OD₆₀₀ reaches between 0.4-0.6 (typically 4-6 hr).
- 1.3. All bacterial cells were collected by centrifugation at 5,000 rpm, 4°C for 3 min.
- 1.4. The bacterial pellet was gently resuspended in 5 ml of ice-cold CaCl₂ (about 1/20 of original volume), then incubated on ice 5-10 min and collected by centrifugation at 5,000 rpm, 4°C for 3 min.
- 1.5. The bacterial pellet was gently resuspended again in 5 ml of ice-cold 14% glycerol in 0.1 M CaCl₂ (about 1/20 of original volume), then incubated on ice 10-15 min and aliquot (50 μ l) in new tube.
- 1.6. Flash freeze in liquid nitrogen, then store at -80°C.

2. Ligation

- 2.1 The interesting genes were amplified with PCR technique.
- 2.2 PCR products of the expected predicted size were ligated into pTZ57R/T vectors by 4°C incubation for 1 hour (TAcloning kit).
- 2.3 The ligated vector was transformed into *E.coli* DH5 α competent cells by heat shock method.

<i>Components</i>	<i>Condition Volume 1 (μl)</i>	<i>Condition Volume 2 (μl)</i>
Vector pTZ57R/T	1	1
PCR product	1	3
5X ligation buffer	2	2
Water	5.7	3.7
T4 DNA ligase, 5u	0.3	0.3

3. Heat shock method

- 3.1. The competent cells in -80°C were thaw on ice for 20-30 min.
- 3.2. 4 μl of the ligated DNA was mixed into 50 μl of competent cells by gently flinking tube with finger a few times. Control for ligation we used 1 μl of vector onto 50μl of competent cells. Then, placed them on ice for 20-30 min.
- 3.3. Each transformation tube was heat shock performed by incubation at 42°C for 90 sec.
- 3.4. After that, each tube was put on ice for 2 min.
- 3.5. 450 μl of LB media (without antibiotics) was added, then incubated in 37°C shaking incubator for 60 min. before centrifuged at 12,000g for 5 min to pellet and discard supernatant.
- 3.6. The cell pellet was resuspended with 50μl of LB media (without antibiotics) to place all the transformation onto LB agar plate (containing 100μg/ml Amplicilin) by spreading.
- 3.7. Incubate plate at 37°C for 16-18 hours or overnight.

4. Colony PCR

- 4.1. Bacterial clones were cultured on LB agar plates and grown overnight at 37°C.
- 4.2. A maximum of 5-10 colonies were picked from each plated transformation and used for colony PCR with standard M13 primers or interesting gene primers.

5. Plasmid Extraction and Bacterial Plasmid DNA Collection

- 5.1. Bacterial clones were cultivated in 6 ml of LB broth by shaking at 200 rpm, 37°C.
- 5.2. 1 ml of bacterial clones was separated for stock collection by added 200 µl of glycerol.
- 5.3. 5 ml of bacterial clones were harvested for plasmid DNA extraction by GeneJET Plasmid Miniprep Kit (Thermo Scientific, #K0509 Lot 00136306)
- 5.4. 5 ml of Bacterial cells in LB medium were pellet by centrifugation 11,000g, 30 sec.
- 5.5. 250 µl of buffer resuspension solution was added and mixed by vortex or pipetting before transferred to microcentrifuge tube.
- 5.6. 250 µl of lysis solution was added and mixed gently by invert tube 6-8 times until the solution becomes viscous and slightly clear, then incubated only 5 min at room temperature or until clear to avoid denaturation of supercoiled plasmid DNA.
- 5.7. 350 µl of neutralization solution was added and mixed thoroughly by invert tube 6-8 times to avoid localized precipitation of bacterial debris, then the suspension was centrifuged to pellet cell debris and chromosomal DNA for 5 min at 11,000g room temperature.
- 5.8. The column was placed and then 400µl of supernatant was loaded to GeneJET spin column
- 5.9. After that centrifugation for 1 min at 11,000g room temperature to let the supernatant flow-through.

- 5.10. The flow-through was discarded before column was placed back into the same collection tube.
- 5.11. 500 μl of wash solution (diluted with ethanol prior use) was added to GeneJET spin column, centrifuged for 30-60 sec and then the flow-through was discarded before column was placed back into the same collection tube.
- 5.12. The wash procedure was repeated
- 5.13. The GeneJET spin column was transferred into a fresh 1.5 ml microcentrifuge tube. Before 50 μl of elution buffer was added to center of GeneJET spin column membrane, and then centrifuged to get the plasmid.

6. Plasmid DNA Sequencing

- 6.1. The plasmid DNA concentration was measured at A260/280 by NanoDrop1000.
- 6.2. The plasmid DNA was diluted to 100 ng/ μl before sequencing.

